Fast Atom Bombardment Mass Spectrometry Studies of Ruthenium(II) Polypyridyl Coordination Complexes and of Group V Triptycenes and Related Complexes

Jeffrey W. Nye, B.Sc. (Hons.)

A Thesis

submitted to the Department of Chemistry

in partial fulfilment of the requirements

for the degree of

Master of Science

September 1986

Brock University

St. Catharines, Ontario

Abstract

In order to investigate the use of Fast Atom Bombardment Mass Spectrometry (FAB-MS) as a tool for structural characterization, two groups of complexes are analyzed. The first group is a set of ruthenium(II) coordination complexes containing bidentate polypyridyl ligands. The positive and negative ion FAB-MS spectra are found to be sufficient to allow for an almost complete characterization of the central metal atom, the ligands and the counter anions contained in the intact complex. An unusual observation of multiply charged ions in the positive ion FAB-MS spectra (i.e. $[RuL_3]^{2+}$) is explained to be as a result of the oxidative quenching of the excited state of the doubly charged ion by the matrix, 3-nitrobenzyl alcohol. An analysis of a mixture shows that the technique is a good one for identifying components therein.

A group of triptycene and related complexes containing Group V elements is also analyzed by FAB-MS and the results, in terms of relative abundances of fragment ions, are found to be consistent with known metal-carbon bond strengths.

Acknowledgements

The author would like to express his sincere appreciation to Dr. J. Miller for his patience and supervision during the course of this research.

Thanks are also due to Dr. G.B. Deacon and Dr. A.G. Massey for providing the chemical compounds without which this thesis would not have been. Much appreciation is due Dr. K. Balasanmugam for his help in understanding the spectra obtained from the ruthenium(II) coordination complexes.

Finally, the author would like to thank his wife, Faye, for her understanding and encouragement during the writing of this thesis.

Table of Contents

List of Illustrations

List of Tables

List of Schemes

A. Introduction

Structural characterization of organometallic and coordination complexes can often lead to important conclusions concerning their functions and reactivities. To this end, inorganic chemists have utilized a large number of techniques in elucidating structural information. Included among these techniques are: infrared and uv-visible spectroscopy, nuclear magnetic resonance and x-ray crystallography. One of the most useful and informative techniques is mass spectrometry.

A mass spectrometer is a device in which ionized molecules or charged fragments of molecules are created and sorted according to their mass-to-charge ratios. A mass spectrum is a plot of the number or abundance of the ions as a function of the mass-to-charge ratio of these ions. Both positive and negative ions can be analyzed.

It is necessary, however, that the species to be analyzed be presented in a charged form in a high vacuum. Therefore, it is not too surprising that a significant amount of work has been carried out to devise different methods of supplying the ionized species. As a group these methods are called ionization techniques.

Classical techniques are those that have been used the longest. The techniques that are considered to be "classical" now include: electron impact (EI), chemical ionization (CI), and field ionization (FI). A second group of ionization techniques, called desorption techniques, have

been developed in response to the single common disadvantage to the classical techniques, that of the requirement for presenting the sample to the ionizing device in the gas phase. These latter techniques are relatively new and will be discussed after an examination of the classical techniques.

1. Classical Ionization Techniques

i) Electron Impact (EI)

Ionization by electron impact involves subjecting sample molecules, in the gas phase, to a beam of 70-100 eV electrons. An electron, colliding with a molecule, causes an ejection of an electron from the molecule creating an excited radical:

$$AB + e^- \longrightarrow {}^*AB^{+\cdot} + 2e^-$$

In this way molecular ions (ions of mass equal to the formula weight) are often observed. Alternatively, the excited molecule can undergo unimolecular decomposition producing both charged and neutral species

$$^*AB^\cdot \rightarrow A^+ + B^\cdot$$
$$^*AB^\cdot \rightarrow A^\cdot + B^+$$

Ions observed in the mass spectrum are representative of the sample molecule in that they correspond to fragments of it. Intensities of the fragments are proportional to the ease of the bond cleavages that formed them. From chemical

knowledge and the experience gained in observing the mass spectra of other similar complexes, the structure of an unknown molecule can be determined from its mass spectrum.

Unfortunately there are shortcomings to the technique. For some molecules, intramolecular bonding is weak and so subjecting it to the electron beam results in complete decomposition and a mass spectrum that contains only small mass ions that bear little resemblance to the original sample molecule. Negative ions produced by EI (i.e. by electron capture) occur rarely; therefore potentially important information available from a negative ion spectrum is lost. Most importantly, EI requires that the sample molecules be presented to the ionizing beam in the gas phase. This precludes the availability of spectra from compounds that are either thermally labile, polar, ionic or of high molecular weight.

ii) Chemical Ionization (CI)

In chemical ionization, reagent ions such as CH_5^+ and NH_4^+ are formed by electron bombardment of high pressure gases such as methane and ammonia respectively. Interactions between the reagent ions and sample molecules introduced into the source area produce "pseudomolecular" ions. These are ions in which the sample molecule has gained or lost a proton (i.e. $[M+H]^+$ or $[M-H]^-$). By changing the reagent gas and its pressure inside the source, attack at structurally significant sites within the sample

molecule can be induced, resulting in fragmentation.

Therefore, in CI, the problems of uncontrolled fragmentation and the absence of negative ion spectra, problems normally encountered in EI, are overcome. The necessity of sample volatilization, however, remains.

iii) Field Ionization (FI)

Sample molecules, in the gas phase, can be ionized by subjecting them to a very intense electric field. This technique is a very good one for providing a large abundance of the ionized intact sample molecule, but the molecules gain very little internal energy. Therefore fragmentation is minimal and the structurally important information available from fragment ions is lost.

Therefore, because of instability to heat or general non-volatility, compounds that are either thermally labile, polar, ionic or of high molecular weight cannot be analyzed using any of the "classical" techniques. Over the last ten to fifteen years, several new methods have been developed which eliminate the need for heating the sample so that it can be ionized in the gas phase [1]. Collectively these new methods are called "desorption" techniques.

2. Desorption Techniques

Desorption techniques are, as the name implies, a method of desorbing ionic species directly from a surface

into the gas phase. The technique may or may not also be responsible for formation of ionic species within the surface. The major techniques currently in use are: field desorption (FD), electrohydrodynamic desorption (EHD), laser desorption (LD), plasma desorption (PD), secondary ion MS (SIMS) and fast atom bombardment (FAB). The latter technique will be discussed under a separate heading since it is central to this thesis.

i) Field Desorption (FD)

It is known that heats of vaporization of biological molecules deposited on a surface are reduced in the presence of a strong electric field gradient [2].

In a modification of field ionization, suggested initially by Becky [3], carbon microneedles, deposited on a fine tungsten wire, are coated with the analyte in a conducting solution. Resistive heating of the wire causes the solvent to evaporate and the sample to melt, allowing it to flow freely. Application of a strong electric field induces formation of pseudomolecular ions by alkali ion or proton attachment. Due to the electric field, the ions thus formed migrate toward the microneedle tips where they are desorbed, or field evaporated.

The major disadvantage to this technique is that the desorbed ions have very little internal energy, as in field ionization. Therefore few fragment ions are observed. Increased heating of the wire induces molecular

fragmentation, but again for thermally sensitive compounds this may be undesirable.

Transient spectra and poor reproducibility due to the variability of the carbon microneedle surface are other problems.

ii) Electrohydrodynamic Desorption (EHD)

Electrohydrodynamic desorption is another modification of the field ionization technique. In EHD, a sample beam is produced by the interaction of a conducting liquid meniscus with a strong electric field [4,5]. The electric field causes the meniscus to form a sharp cone. At a sufficiently high field strength, particles at the tip of the cone are both field ionized and field evaporated to form a sample beam. The beam is sustained by forming the meniscus at the end of a capillary tube through which the sample, in a suitable solvent, is drawn.

Like FI and FD, ions are desorbed with very little internal energy, therefore very little fragmentation is observed. The main source of observable fragment ions is from solution phase reaction products [5].

iii) Laser Desorption (LD)

In this technique, conceived by Mumma and Vastola [6], the sample is applied as a thin layer onto a glass or metal support which is then subjected to a pulse of laser energy. The very high and localized heat of the laser pulse

is absorbed into the sample lattice disrupting intermolecular bonds at the lattice surface. Both ionic and neutral species are ejected. The technique has recently been reviewed [7,8].

Due to the single shot nature of the experiment, ions are detected with a time-of-flight (TOF). Therefore mass range and resolution are limited. The ions can also be detected with an FT analyzer, however operation of these instruments are not as simple. Reproducilbilty is also poor due to the many factors associated with the laser pulse. Sample matrix effects are also common.

iv) ^{252}Cf Plasma Desorption (PD)

The technique, introduced by Macfarlane and Torgensen [2], involves placing the sample in a suitable solvent on a thin metal foil which is placed in front of a fission source. Spontaneous fission of the ^{252}Cf nucleus produces an ion with energy in excess of 100 MeV. The fission fragments pass through the foil and are deposited into the sample matrix. Pseudomolecular ions as well as bond cleavages and losses of small neutral molecules result. Ions desorbed from the surface are accelerated into a TOF analyzer.

Disadvantages of the technique include the mass range and resolution problems associated with TOF analyzers and of course the special precautions required when handling radioactive isotopes.

The main advantages of the technique are that very large molecules can be desorbed and that very little sample is used in a single analysis so the method is practically non-destructive.

v) Secondary Ion Mass Spectrometry (SIMS)

The first successful utilization of SIMS to analyze polar and involatile organic substances was by Benninghoven [9]. Previous attempts yielded very short-lived ion currents followed by sample surface charging and thermal degradation. Benninghoven found that by reducing the bombarding ion flux, much longer lasting ion currents could be obtained. Also, by angling the incident ion beam, so that only about a monolayer of sample was bombarded, radiation damage was minimized. The bombarding ions normally used in SIMS are Ar^+ or Xe^+.

For some types of compounds, though, informative spectra were unobtainable. Problems involved with the SIMS technique include: low ion currents due to the lowered incident beam flux, surface charging of insulating compounds, and difficulties in steering a charged ion beam (the bombarding ions) onto a surface that is so close to the accelerating field.

3. Fast Atom Bombardment (FAB)

i) Introduction

Fast atom bombardment is a relatively new technique (as are all of the desorption techniques). It was introduced by Barber and co-workers in 1981 [10,11]. Their motivation was to be able to have an ion source that could be fitted to a large double-focussing mass spectrometer and so utilize the wide range of special techniques available with these instruments. These include accurate mass measurement and metastable ion scanning.

For a while SIMS seemed to be such a source; however, because of the problems associated with it (see above), it seemed that there would be some types of compounds for which the mass spectra could not be obtained. A more universal technique was needed.

It seemed simple then to substitute a neutral atom beam for the charged one used in SIMS. Atom guns producing a neutral beam of fast-moving particles were available so this was not a problem. For example the saddle field gun [12a] and the capillaritron [12b] are two of the most often used atom guns.

The second innovation by Barber et al., and what clearly distinguishes FAB from SIMS, was the introduction of the sample as a solution in a liquid "matrix" material. The matrix, in which the sample is dissolved, serves to prolong the lifetime of the spectrum by constantly regenerating (via

diffusion) the surface that is exposed to the bombarding atom beam. That the matrix is necessary has been illustrated by the observation that only transient spectra were obtained when solid organic samples were exposed to the atom beam [13]. The first matrix to be used by Barber's group was glycerol [14]. This matrix was chosen because of its low vapour pressure, high viscosity and its wide ranging solvation properties.

A schematic of the typical FAB ion source is shown in Figure 1. The analyte, as a solution in a suitable liquid matrix, is applied as a thin layer (a) on the surface of a small metallic probe tip (b). The probe tip, in turn, is inserted into the end of the probe (c) which is inserted through vacuum locks into the source area. The atom gun (d) provides a beam of fast moving neutral particles (e) which are incident upon the sample surface. Interactions between the atom beam and the sample surface produce sputtered ionic species (f) which are directed toward the mass analyzer (g) by means of an extraction field (h).

There are several factors involved in the FAB technique that make it advantageous over the classical techniques and over the desorption techniques discussed above. These are:

a) analyzable species are sputtered from the solution surface, therefore no heating is required to bring the analyte into the gas phase. Therefore many compounds that are thermally sensitive may be examined by FAB,

Figure 1. Schematic Diagram of the Typical Fast Atom Bombardment Ion Source

a) sample in a liquid matrix; b) metallic probe tip; c) probe; d) fast atom gun; e) neutral particle beam; f) sputtered ionic species; g) mass analyzer; h) extraction plates (taken from ref. [14]).

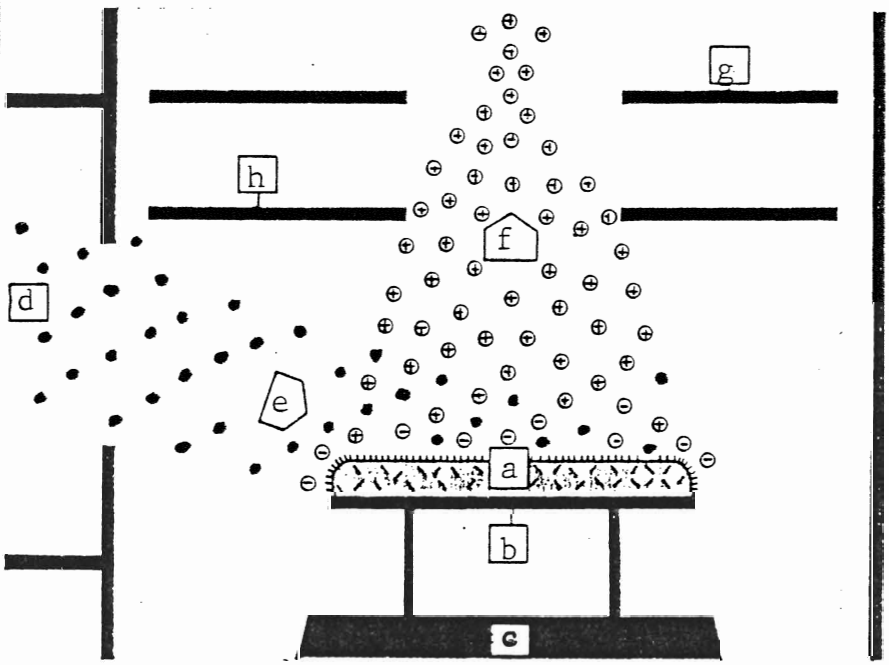
g
h
f
d
e
a
b
c

b) the bombarding atom beam is neutral so the problems of surface charging and beam steering that accompany the SIMS experiment are avoided,

c) sputtering allows for analysis of both positive and negative ionic species,

d) presentation of the analyte as a solution in a liquid matrix allows for longer lived spectra. Sputtered or radiation damaged species are replaced by diffusion from the bulk solution. Therefore the incident atom beam flux can be increased compared to SIMS, resulting in higher ion currents. Longer lived spectra also allow for accurate mass measurement and metastable scanning as well as repeated analyses for reproducibility checks,

e) a large mass range is available due to the use of double-focussing mass spectrometers,

f) sample preparation is relatively simple,

g) the strength of the neutral atom beam-sample interaction is intermediate between EI, where total sample degradation may be observed, and FD, where almost no fragmentation is observed. The energy of the atom beam can be varied somewhat so some degree of control over the extent of fragmentation is available.

Therefore, based on these advantages, FAB is the favoured technique for the analysis of organic and organic-containing compounds. This includes many coordination and all organometallic complexes.

ii) The Nature of the Interaction

It might be useful at this point to consider the nature of the interaction between the incident neutral atom beam and the analyte/matrix solution. This interaction contains two elements for which much experimentation has been performed. These are the source of the ionic species and the mechanisms involved in their formation.

It is unclear whether ions are sputtered solely from a thin layer near the surface [16,17] or whether there is a contribution from the bulk solution [15]. Wong et al. [18] have proposed a surface self-cleaning mechanism in which radiation damaged species are sputtered along with the relevant ionic species leaving a clean surface after each sputtering event. Several studies have shown that the information obtained by FAB correlates well with known solution physical properties of the bulk solution such as dissociation equilibria [19-21], solution concentrations of metal cation-crown ether complexes [22] and solution dynamics [23].

The mechanisms of ion formation are equally uncertain. However several mechanisms have been proposed.

Preionized compounds such as salts and strong acids and bases dissociate in solution yielding cationic and anionic species:

$$n[(M^+)(X^-)] \longrightarrow nM^+ + nX^-$$

Ion clustering produces species of higher molecular weight:

$$\longrightarrow [(M^+)nX^{n-1}]^+ \quad + \quad X^-$$

$$\longrightarrow M^+ \quad + \quad [(M^+)^{n-1}X^{-n}]^-$$

These species are then sputtered and analyzed.

Electrons formed by collisions with incoming neutral atoms and analyte or matrix molecules can be ejected from (or captured by) analyte molecules giving molecular ions [24]:

$$M \longrightarrow M^{+\cdot} \quad + \quad e^-$$

and $$M \quad + \quad e^- \longrightarrow M^{-\cdot}$$

The kinetic energy contained in the incoming atoms is dissipated through vibrational motion of the analyte/matrix lattice. Quite often, especially so in protic matrices such as glycerol, the vibrational energy imparted is sufficient to produce homolytic bond cleavages leaving hydrogen and other free radicals [24]. Combinations of these radicals with analyte or matrix molecules can produce a variety of ions including pseudomolecular ions:

$$M \longrightarrow (M-H)^{\cdot} \quad + \quad H^{\cdot}$$

$$(M-H)^{\cdot} \xrightarrow{+e^-} (M-H)^-$$

$$M^{+\cdot} \quad + \quad G \longrightarrow (M+H)^+ \quad + \quad (G-H)^{\cdot}$$

$$M^{-\cdot} \quad + \quad G \longrightarrow (M+H)^- \quad + \quad (G-H)^{\cdot}$$

$$M^{+\cdot} \quad + \quad (G-H)^{\cdot} \longrightarrow (M-H)^+ \quad + \quad G$$

where G represents a matrix molecule. Since almost all matrices commonly in use contain relatively weak bonds to hydrogen, pseudomolecular ions of these types are the most

often found ions in the FAB mass spectrum.

Therefore three types of ions may be found in the FAB mass spectrum: intact cations and/or anions, molecular ions, and pseudomolecular ions. The types and amount of each of these ions will depend to a large extent on the nature of the matrix. Therefore it is important that careful consideration be taken in choosing the matrix and in light of the spectrum obtained, interpretation should take into account the possibility of all of the above mechanisms occuring to varying degrees.

iii) Applications to Organometallic and Coordination Complexes

While the motivation for the discovery of the technique was to provide a method for analyzing thermally unstable and biologically important molecules, the technique of FAB-MS soon found applications to many organometallic and coordination complexes for which other techniques had proved intractable. Several papers reviewing these applications have appeared [26-28] and as expected for any new technique, more and more are found with time. In this section will be discussed some of the results obtained by other workers, especially where these results are relevant to the work presented in this thesis.

Barber et al. were among the first to publish a complete study of a group of organometallic compounds [29].

They obtained the FAB spectra of a series of cobalamines (see Figure 2) including the methyl-, hydroxy- and cyano- (vitamin B_{12}) derivatives and of the coenzyme of vitamin B_{12}. The matrix used in the experiment was glycerol.

Both positive and negative ion spectra were obtained, with the negative ion spectrum giving less fragmentation information overall. A pseudomolecular ion of good intensity was observed in both operating modes (i.e. $[M+H]^+$ and $[M-H]^-$).

In the positive ion spectrum, an intense peak at m/z 1329 corresponded to loss of the axial ligand (CH_3, OH or CN). Major fragments occurring from the m/z 1329 fragment were due to losses of acetamide and cobalt, but mostly due to losses from the other axial chain including, initially, loss of the dimethyl benzimidazole group followed by the sugar and then the phosphate to give the base peak in the spectrum at m/z 971.

Application of the technique to neutral and relatively non-polar substances was demonstrated by the same group [10] with the spectrum of the thermally labile and moisture sensitive mixed silicon-rhodium organometallic complex shown below:

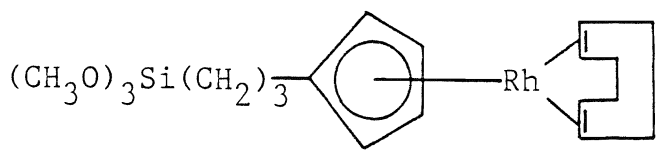

Figure 2. Structure of Cobalamine Derivatives Analyzed by Fast Atom Bombardment (taken from ref. [27]).

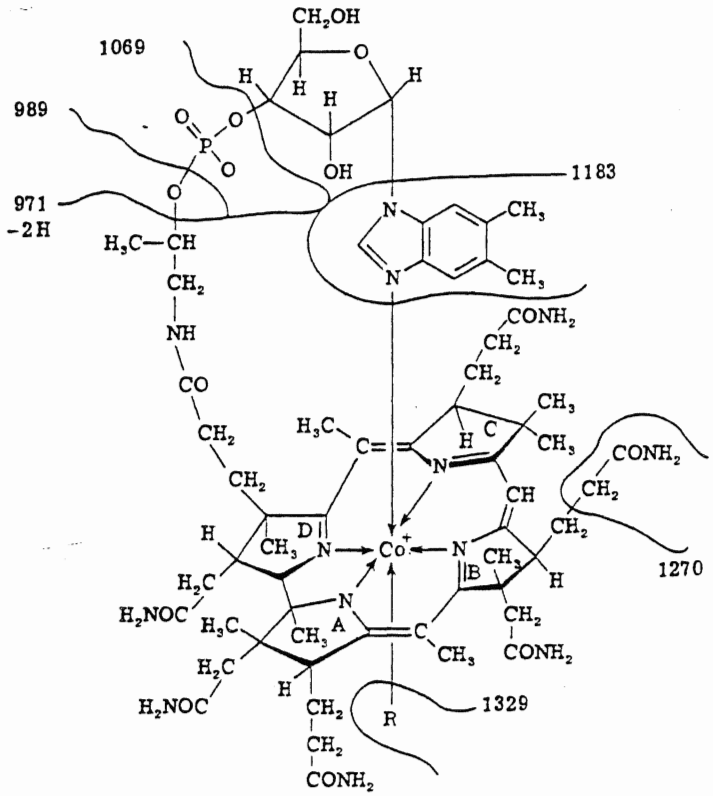

	R	Mol. wt.
Cyanocobalamin	CN	1354 + 1
Methylcobalamin	CH_3	1343 + 1
Hydroxocobalamin	OH	1345 + 1

Coenzyme B_{12}

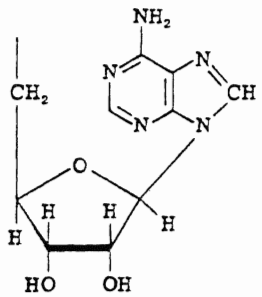

1578 + 1

The molecular ion was observed in the spectrum with good intensity as well as fragments resulting from the loss of the neutrals C_8H_4, $(CH_3O)_3Si$ and $(CH_3O)_3Si(CH_2)_2$, and $(CH_3O)_3Si(CH_2)_3$. The rhodium-cyclopentadiene portion was the last to fragment giving the Rh^+ ion. This study was unique in that no matrix was used since the complex is a liquid at room temperature.

FAB and FD spectra of organoarsenicals in foodstuffs were obtained by van der Greef and de Brauw [30]. Their high resolution FAB mass spectrum of actual marine extracts (crab) in glycerol showed a peak identified as the protonated arsenobetaine, $[(CH_3)_3AsCH_2OO]H^+$. High resolution was required since the arsenic containing molecular species were present in low concentrations. The FD spectra showed, in some cases, no or very weak $[M+H]^+$ ions as well as less fragmentation.

Miller and Fulcher [31] have compared the EI and FAB mass spectra of some Group IV organometallic halides of the type $(phenyl)_3MCl$ where M= Ge, Sn, and Pb, $(phenyl)_3PbX$ where X= Cl, Br and I, and $Sn(phenyl)_nCl_{4-n}$. They found that FAB gave a lower intensity molecular ion than did EI and that in FAB halide loss was preferred over loss of a phenyl group while in EI the opposite was true. Fragmentation pathways in both ionization methods were similar with the exception of the presence of matrix adducts in FAB. For example, in a sulfolane matrix, peaks

corresponding to $M(phenyl)_3sulf_2^+$ and $M(phenyl)_3sulf^+$ were observed.

Another study by Miller et al. [32] compared the EI and FAB mass spectra of hexamethylphosphoramide (HMPA) adducts of phenyl tin(IV) and phenyl lead(IV) halides. As was observed above, the major difference in the spectra obtained was a preferential loss of halide as compared to phenyl in FAB while the opposite was found in EI. Parent ions were not observed using either technique; however, in FAB there were more metal-containing ions containing an HMPA molecule. It was suggested that this was a result of the softer ionization obtained with FAB.

Dalietos et al. have compared the FAB, FD and desorption chemical ionization (DCI) mass spectra of cis-dichloroplatinum amino acid and peptide complexes [33]. They found that FD gave very little fragmentation information and so was of very little use in structural characterization. FAB spectra, on the other hand, contained many fragment ions. With respect to the platinum complexes, the negative ion spectra contained abundant $[M-K]^-$ and $[M-H]^-$ ions as well as considerable fragmentation and ions due to adducts with water and glycerol. The positive ion spectra were dominated by the alkali ion.

Johnstone and Lewis [22] have examined the crown ether complexes of alkali and alkaline earth cations. Their results suggest that it may be possible to use the FAB mass spectral fragmentation data as a measure of the stability

constants of crown ethers with cations since, for their system, the ion intensities correlated with the known solution behaviour of the complexes.

Davis et al. [34] have obtained the FAB mass spectra of a large number of mono- and poly-nuclear transition metal complexes that did not give EI mass spectra. They found that all of the compounds gave spectra that were structurally informative, but that not all of the compounds gave molecular or pseudomolecular ions. However, the highest mass ion observed in every case was in agreement with the known solution behaviour of that compound. For example, complexes of the type $[M(PPh_3)_4]$ (where M= Pd and Pt) are known to dissociate in solution to give $[M(PPh_3)_3]$. The spectrum for M= Pd did indeed show as the highest mass ion, $[Pd(PPh_3)_3]^{+\cdot}$. Glycerol was used as the matrix.

Blumenthal et al. [35] have used FAB to characterize high molecular weight ruthenium-gold complexes. The compounds, all analyzed using thioglycerol as matrix, gave molecular or pseudomolecular ions and enough fragment ions to be structurally informative. As an example, the complex $Ru_3Au_2(\mu^3\text{-}S)(CO)_9(PPh_3)_2$ gave the molecular ion, $M^{+\cdot}$, at m/z 1504 followed by a series of peaks corresponding to successive losses of the nine carbonyl groups. Finally a peak at m/z 1176 is due to the loss of 9 CO and a phenyl group.

A comparison of the FAB and FD mass spectra of selected η^3-allylic complexes of Pd and Ni by Tkatchenko et

al. [36] showed that while FD gave a more intense molecular cation, FAB gave more fragment ions from which a structural identification could be made. They found that the principal fragmentations occurred between metal-ligand bonds. In a mixture of two complexes, they observed peaks due to the exchange of ligands.

Sharp et al. [37] have studied some organometallic complexes of Rh, Ir and Pt in which a cumulene ligand is attached to the metal in either a σ- or π-bonded manner. They found that principal fragmentations occurred via loss of intact ligands (in this case a cumulene) and that the observed fragmentations were consistent with the known solution chemistry of the complexes. They concluded that the most readily lost ligands are those that are anionic followed by unsaturated organics. The most difficult ligands to lose, compared to the other ligands, were the π-acids such as CO and PPh_3.

Cationic technetium(III) complex salts were examined using FAB by Cohen et al. [38]. The mass spectra of the compounds (see Figure 3 for the general structure of the complexes) showed intense complex cations ($[C^+]$) as well as distinctive fragmentation information. The principal loss from the $[C^+]$ ion was an intact ligand, D to give the ion $[W^+]$. A correlation was observed between known metal-ligand bond strengths and the ease of ligand loss as measured by the ratio $[C^+]/[W^+]$. It was found that alkyl phosphine ligands form more stable chelate bonds than do phenyl arsine

Figure 3. Structure of Cationic Complex Salts of Tc or Fe Containing Phosphine and/or Arsine Ligands.

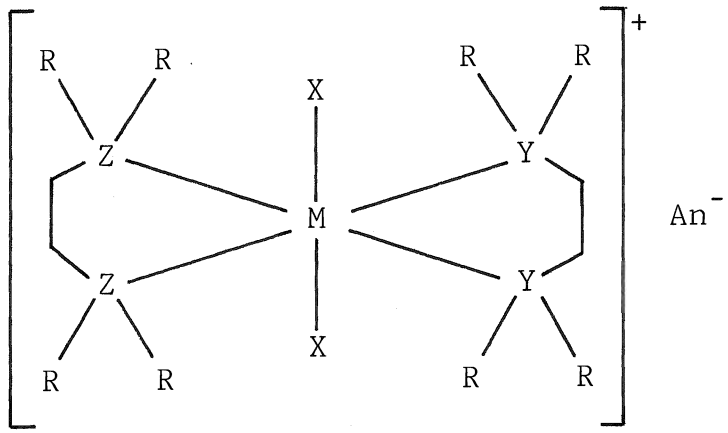

M = Tc or Fe

X = Cl or Br

Y = P or As

Z = P or As

R = Me, Et, Pr, Bu or Ph

D = $R_2ZC_2H_4YR_2$

W = $[C^+]$ - D

An = Cl^-, ClO_4^-, or PF_6^-

and/or phosphine ligands.

The authors also found that changing the counter anion, An^-, had no effect on the spectra. This, as we shall see, is in contradiction with the results presented in this thesis.

Divisia-Blohorn et al. [39] have also examined cationic transition metal complexes using the FAB technique. The complexes of interest were Ir(III) and Rh(III) coordination complexes containing bidentate nitrogen-donor ligands. Two matrix-analyte reactions were observed, presumably initiated by particle bombardment. First, in thioglycerol as matrix, one or two Cl atoms were replaced by TGL radicals. This substitution occurred more rapidly for the Rh complexes. Secondly, when a ligand contained the diazo functional group, it was hydrogenated once or twice depending on the ability of the matrix to generate hydrogen radicals. Only in glycerol was the diazo group observed to be hydrogenated, since hydroxy protons are more reactive than the equivalent protons in thioglycerol. The hydrogen radicals must originate from the matrix since on using deuteroglycerol, the diazo group was deuterated.

Unger [40] has combined the technique of MS/MS with FAB in a study of a series of cationic technetium and iron coordination complexes as shown in Figure 3. Structural characteristics such as site of oxidation and relative stability to ligand dissociation were obtained from the MS/MS spectra. The advantage of using multiple MS is that

peaks due to the matrix and background, which clutter a normal mass spectrum, are absent. From his results, Unger has determined that the major factors controlling ligand dissociation for these complexes are the steric requirements of the alkyl group attached to the coordinating As or P atoms (Y in Figure 3) and the nature of the central metal atom. Identity of X, whether it was Cl or Br, seemed to have no effect on the mass spectra.

Hacksell et al. [45] have used FAB to help characterize two stable glycopyranosyl palladium complexes (spectra Figure 4). The highest mass ion in either spectrum corresponded to loss of chloride from the parent molecule, giving the intact complex cation. While the authors do not mention it in the text, relative binding strengths of triphenyl phosphine and triphenyl arsine groups correspond to the relative intensities of the ions resulting from the loss of each group. From solution studies, we expect arsine groups to be more weakly bound than the corresponding phosphine group. The spectra do indeed show that the ratio of the ions $[M\text{-}Ph_3XCl]^+/[M\text{-}Cl]^+$ is much greater when X = As than when X = P. The authors do not state which matrix they have used for the study.

Bojesen [41] has examined a large number of coordination complexes containing polypyridyl ligands. As matrix he used either glycerol or sulfolane, however, only one matrix was used for each complex. The highest mass ions found in the mass spectra were of the form $[ML_nX]^+$ or

Figure 4. Positive Ion FAB Mass Spectra of Triphenyl Phosphine (top) and Triphenyl Arsine (bottom) Derivatives of a Glucopyranosyl Palladium Complex (taken from ref. [45]).

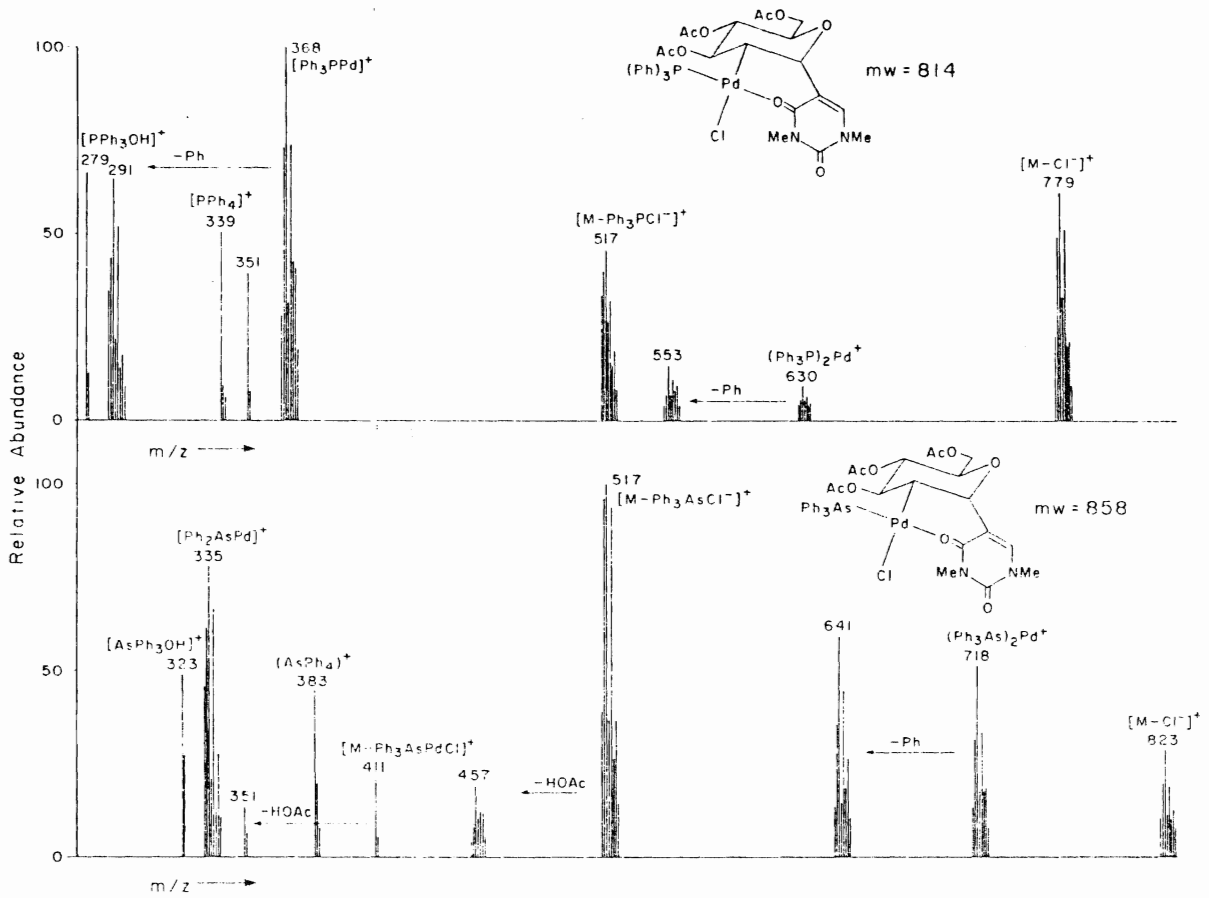
Relative Abundance
100
50
0
m/z
[PPh3OH]+
279
291
-Ph
368
[Ph3PPd]+
[PPh4]+
339
351
[M-Ph3PCl]+
517
553
(Ph3P)2Pd+
630
-Ph
[M-Cl]+
779
AcO
AcO
AcO
(Ph)3P
Pd
Cl
MeN
NMe
mw = 814
[Ph2AsPd]+
335
[AsPh3OH]+
323
(AsPh4)+
383
351
-HOAc
[M-Ph3AsPdCl]+
411
457
-HOAc
517
[M-Ph3AsCl]+
641
-Ph
(Ph3As)2Pd+
718
[M-Cl]+
823
Ph3As
mw = 858

$[ML_n]^+$. Since all of the transition metals used in his study were in the +2 or +3 oxidation state, then there must be a reduction of the complexes in some cases to give the $[ML_n]^+$ ions. Bojesen does not account for this observation. Some ligand fragmentation was observed. No matrix adduct ions were observed and the FAB spectrum of a mixture of two different complexes showed that ligand exchange did not occur.

Although many of the complexes studied by Bojesen contained multiply charged transition metals, only one multiply charged complex cation was observed, the $[Ru(bpy)_3]^{2+}$ cation from the complex $[Ru(bpy)_3](ClO_4)_2$. The matrix used was sulfolane. Unfortunately he did not analyze the same complex in the other matrix nor did he analyze the other Ru containing complex ($[Ru(tpen)](ClO_4)_2$) in the matrix sulfolane. Therefore no conclusions can be drawn about the effect of the matrix on the production of multiply charged ions. The results presented in this thesis show that the matrix does have an effect on the appearance of multiply charged ions. Bojesen concludes that FAB is well suited as a technique for the structural characterization of coordination complexes.

A series of three papers by Cerny et al. [42-44] describe the FAB mass spectra of some coordination complexes. The probable mechanisms of fragmentation were determined. These papers are important to this thesis in that the coordination complexes studied by Cerny et al. are

very similar to those studied in the first part of this thesis.

The first study [42] compared the FAB and FD mass spectra of some cationic transition metal complexes in which the metal was in a neutral, +1 or +2 oxidation state. It was concluded that for neutral complexes, FD gave more information about the parent molecule while FAB gave more fragmentation information. Therefore the methods should be complementary. For +1 complexes FAB is the preferred method giving both molecular ion and fragment information. For +2 complexes, there did not seem to be a preferred method since both FAB and FD gave poor spectra.

Several generalizations were made concerning the fragment ions found in the FAB mass spectra of these complexes:

a) monodentate ligands were lost in preference to bidentate ligands. Bidentate ligand loss occurred only from fragment ions.

b) redox processes produce many fragment ions. Fragment ions were produced by a reduction of the formal oxidation state of the metal center,

c) where data were available, there was a parallel between ligand loss and ease of reduction in FAB and ground state solution substitutional and redox chemistry of the complexes.

In another study [43] a series of bis(alkyl imidazole) Cu(I) and Cu(II) chelates were analyzed using

FAB. The spectra were obtained using glycerol as matrix. The overall charge of the complexes was either neutral, +1 or greater than +1. Complexes with +1 charge gave the intact complex cation as the highest mass ion in the positive mass spectrum. Neutral complexes were protonated, presumably by the matrix. Of most interest were complexes with overall charge greater than +1. In no case were multiply charged ions observed. Three processes to explain their absence were proposed: reduction of Cu(II) to Cu(I) by loss of an anionic ligand as a radical, reduction of Cu(II) by addition of an electron and, in the case of the dinuclear complexes, by clustering with anions. Therefore, for this system, some mechanism is in effect in which multiply charged ions are disfavoured.

In the most recent study by this group [44] a series of organometallic derivatives of Ru(II) as Os(II) were analyzed by FAB and FD. All compounds contained two 2,2'-bipyridyl (bpy) ligands, with the remaining coordination sites occupied by either η^2-alkene, η^2-alkyne, carbonyl, alkyl or hydrido ligands. They found, as expected, that while FD gave a more intense molecular ion, FAB gave more fragment ions on which a structural identification could be based.

From an analysis of the mass spectra (an example of which is shown in Figure 5) the fragmentation pathways were shown to be of four types:

a) redox fragmentation of metal-ligand bonds (i.e.

Figure 5. Positive Ion FAB and FD Mass Spectra of $[Os(bpy)_2(3\text{-hexyne})Cl]PF_6$ (taken from ref. [44]).

FD

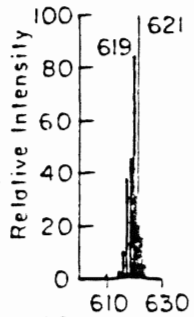
Relative Intensity
100
80
60
40
20
0
619
621
610
630

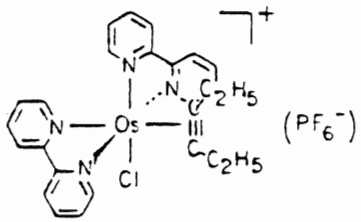
+
N
N
C2H5
Os
III
C
C2H5
N
Cl
(PF6−)

FAB

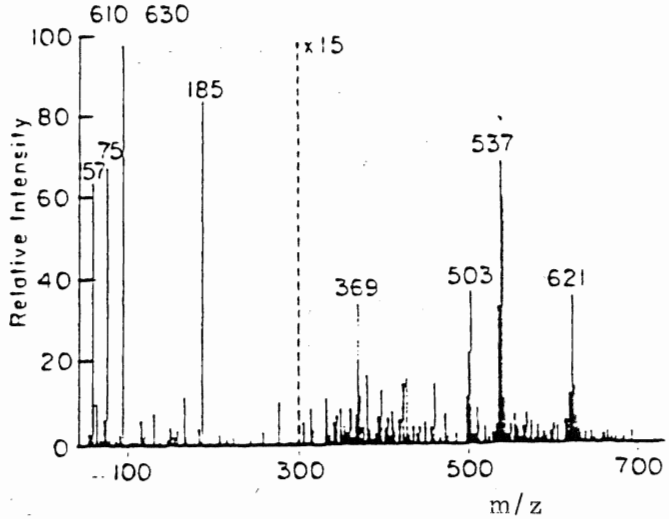
Relative Intensity
100
80
60
40
20
0
x15
185
75
57
537
369
503
621
100
300
500
700
m/z

homolytic dissociation),

b) simple loss of neutral ligands,

c) oxidative addition of coordinated bpy, and

d) reductive elimination of HX (where X= Cl, H or alkyl).

Again for this system, no multiply charged ions were observed. As we shall see, for the first group of the complexes studied in this thesis, some of these mechanisms are followed. However, there are some important differences that will be expanded upon in the discussion.

In summary then the following features are expected to be found in the FAB mass spectra of organometallic and coordination complexes. Compared to field desorption, more structurally relevant information is contained in the FAB mass spectrum. Major fragmentations occur via losses of intact ligands. In studies in which a counter anion is present in the parent molecule, there may or may not be an effect on the spectrum. Multiply charged ions are, almost without exception, not found, even if an intact polycation is present in the parent molecule.

The general tendency in all of the reports described above is for the information contained in the FAB mass spectrum to correlate well with the known solution chemistry of the analyte and the matrix being studied.

4. Scope of the Thesis

The objective of this thesis is to show that mass spectrometry and in particular the technique of Fast Atom

Bombardment (FAB) for providing mass analyzable species is useful for the structural characterization of organometallic and coordination complexes. In order to achieve this objective, two large but quite different groups of compounds were obtained.

i) Ruthenium(II) Polypyridyl Coordination Complexes

Growing interest in the use of ruthenium(II) polypyridyl complexes to photochemically catalyze the photoreduction of water has prompted many research groups to synthesize and characterize many new types of these complexes. Interest lies mainly in making the complexes with different numbers and types of polypyridyl ligands, the simplest of which is bipyridine. One of the most useful isomers of this molecule is 2,2'-bipyridine:

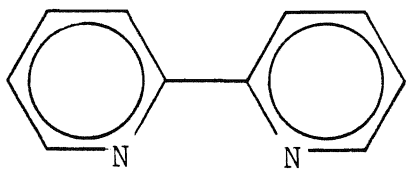

The polypyridyl ligands can be thought of as being Lewis bases which coordinate via electron donation to the central metal atom which can be thought of as being the Lewis acid.

Substitution in the pyridine rings and/or further linking of the rings as in 1,10-phenanthroline:

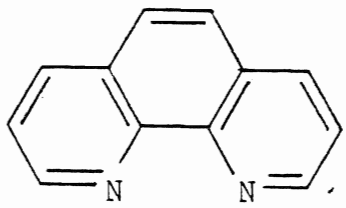

has, as expected, a profound effect on the reactivity of the ligand toward the metal as well as on the complex itself. The solution physical properties of many of these ligands and the complexes formed by them have been thoroughly investigated and tabulated [46-49].

We have obtained a large number of the ruthenium(II) polypyridyl derivatives and we have recorded the FAB mass spectra of all of them. Examination of the spectra will allow us to confirm the observations noted by other workers on similar type systems, especially the studies reported by Bojesen and Cerny, et al. [41-44]. The fragmentations observed will be explained in terms of the solution basicities of the ligands as well as in terms of stereochemical and electronic effects caused by coordination of the ligands to the central metal atom. Aspects of the fragmentation mechanism that have not been fully explained by other workers will also be investigated. A mechanism will be proposed that will explain the role of the matrix in the production of doubly charged ions. The FAB technique

will be used to examine its application to the analyis of unknown mixtures.

ii) Group V Triptycenes and Related Complexes

The second group of complexes are true organometallic complexes and therefore quite distinct from the preceding coordination complexes. These are complexes containing the main group elements from Group V: P, As, Sb and Bi. The structures of the complexes are as shown in Figure 6.

Both EI and FAB spectra were obtained for the complexes. Therefore a comparison will be made of the two techniques and of the spectra obtained by both methods. Figure 6 shows the general structure of the complexes.

A comparison will also be made based on the identity of the central metal atom. It is expected that as one goes down Group V (i.e. from P to Bi), that bonding to carbon would change significantly. Therefore this change should be noticed in the abundance of fragment ions formed by cleaving metal-carbon bonds. This will be investigated and, if found to be true, then the FAB technique will have been shown to be useful in structural characterization for these complexes too.

Figure 6. General Structure of Group V Triptycenes And Related Complexes.

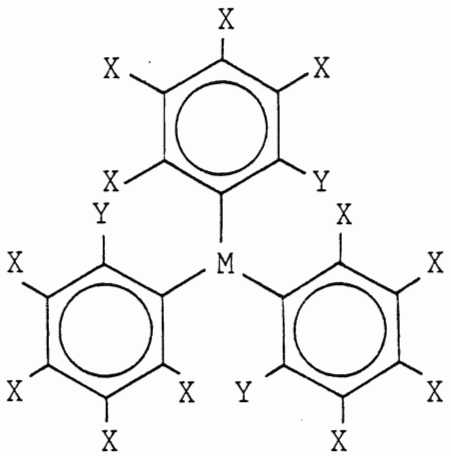

X = H, Y = Cl, M = P, As, Sb, Bi

X = F, Y = Br, M = P, As, Sb, CH_3Si

X = F, Y = H, M = As

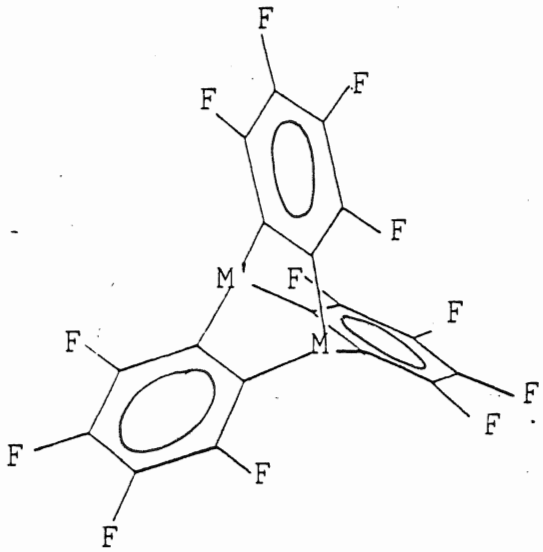

M = M' = P, As, Sb, Bi, CH_3Si

M = Sb, M' = P, As

B. Experimental

1. Instrumentation

Positive ion FAB and EI mass spectra were recorded on a Kratos (AEI) MS-30 double beam mass spectrometer. The instrument has been modified to include a Kratos FAB source in beam one and an MS-80 magnet that increases the available mass range to about m/z 1000 at 4kV accelerating voltage. A schematic of the system is shown in Figure 7.

Samples for EI analysis were admitted via a direct insertion probe into the beam two source area which was heated to 180° C. 70 eV electrons were used for bombardment.

Fast atom bombardment was provided by an Ion Tech Ltd. saddle-field type fast atom gun. Argon or xenon were used as the bombarding atoms. The gun was operated at approximately 1.0 mA providing 6-8 keV fast atoms.

Data were collected as peak time centroids and then converted to masses, offline, using an interfaced Kratos DS-55 datasystem. Resolution was approximately 1000 and the magnet was scanned at 10 seconds/decade. Calibration of the magnet scan was performed using tris-(perfluoroheptyl)-S-triazine (HPT) for FAB spectra and perfluorokerosene (PFK) or an HPT/PFK mixture for EI spectra.

Some of the important DS-55 data system programs are: PLOT for obtaining pictorial representations of the mass spectra, QUAN for quantitative reports with respect to

Figure 7. Schematic Diagram of Kratos (AEI) MS-30 System

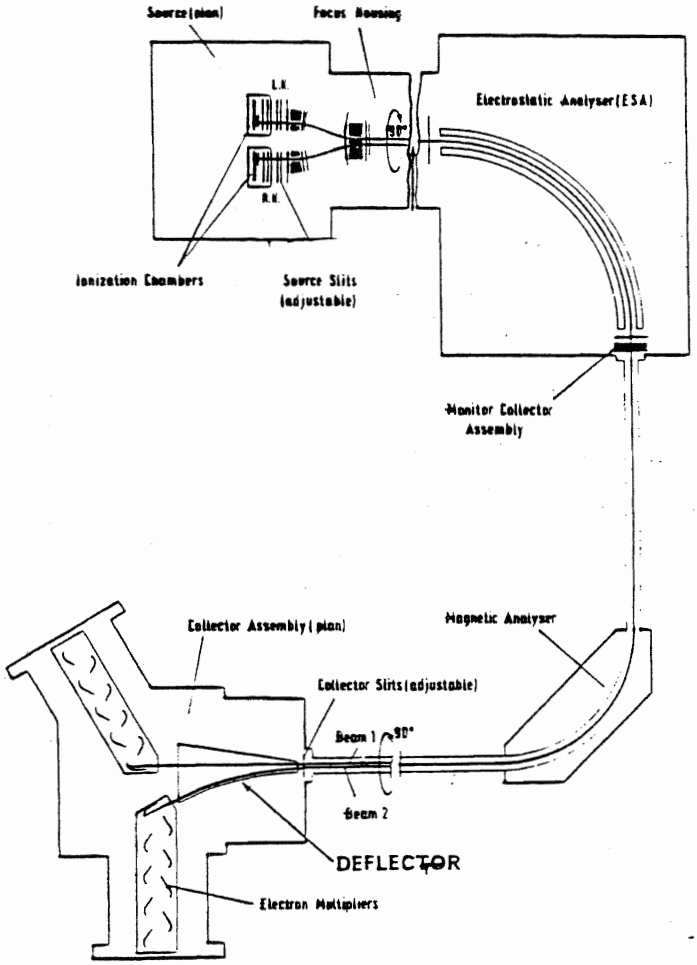
Source (ion)
Focus Housing
L.H.
R.H.
90°
Electrostatic Analyser (E.S.A.)
Ionization Chambers
Source Slits
(adjustable)
Monitor Collector
Assembly
Collector Assembly (ion)
Magnetic Analyser
Collector Slits (adjustable)
Beam 1
90°
Beam 2
DEFLECTOR
Electron Multipliers

peak masses and intensities, PKAVG for averaging individual scans and SUBTR for removing matrix and/or background peaks.

Theoretical isotopic cluster patterns were obtained using either of the computer programs BMASROS or DMASCAL.

The program BMASABD used a least squares approach to deconvolute overlapping peak clusters. Given a cluster of peaks containing a number of different species, and the expected contribution from each of the species, the program calculates the percent composition due to each of the different species.

The single negative ion FAB mass spectrum was recorded on a VG Analytical ZAB-E mass spectrometer. Figure 8 is a schematic of this system.

This instrument uses the same FAB gun and operating conditions as did the Kratos spectrometer. Calibration was achieved by matching cesium iodide cluster peaks.

2. Source of the Compounds Analyzed

i) The ruthenium(II) coordination complexes were obtained from Dr. G.B. Deacon of Monash University, Australia. They are the result of the PhD thesis work of Dr. N.C. Thomas. Preparations of most of the complexes have appeared elsewhere [50]. Most of them have been characterized by other methods such as HPLC, x-ray crystallography and elemental analysis.

Figure 8. Schematic Diagram of VG Analytical ZAB-E System (taken from sales literature)

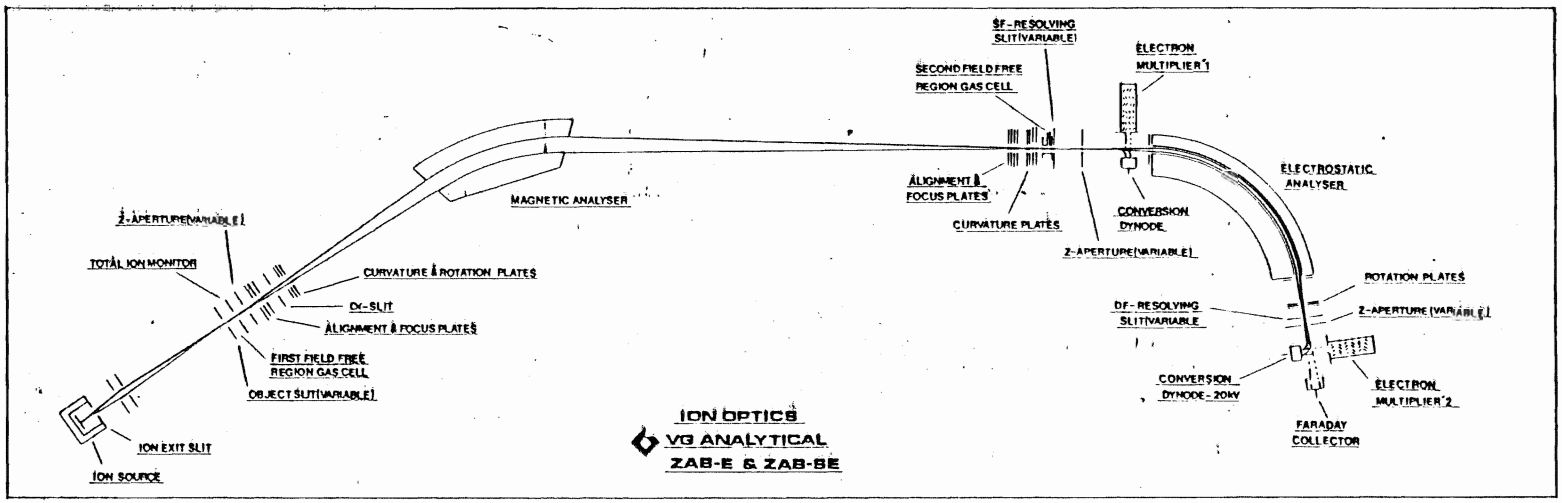
ION OPTICS
VG ANALYTICAL
ZAB-E & ZAB-SE
ION SOURCE
ION EXIT SLIT
OBJECT SLIT(VARIABLE)
FIRST FIELD FREE REGION GAS CELL
ALIGNMENT & FOCUS PLATES
DY-SLIT
CURVATURE & ROTATION PLATES
TOTAL ION MONITOR
Z-APERTURE(VARIABLE)
MAGNETIC ANALYSER
SECOND FIELD FREE REGION GAS CELL
ALIGNMENT & FOCUS PLATES
CURVATURE PLATES
CONVERSION DYNODE
Z-APERTURE(VARIABLE)
DF-RESOLVING SLIT(VARIABLE)
ELECTRON MULTIPLIER 1
ELECTROSTATIC ANALYSER
ROTATION PLATES
Z-APERTURE(VARIABLE)
DF-RESOLVING SLIT(VARIABLE)
CONVERSION DYNODE-20KV
ELECTRON MULTIPLIER 2
FARADAY COLLECTOR

Ion Optics

A list of the complexes analyzed for this thesis is given in Table 1. Diagrams of the ligands contained in the complexes, as well as the abbreviations used for them in this report, are shown in Figure 9.

ii) The Group V organometallic complexes were obtained from Dr. A.G. Massey of Loughborough University, U.K. Preparations of these complexes have appeared elsewhere [51]. Table 2 is a list of the complexes analyzed.

3. FAB Sample Preparation and Analysis

The ruthenium(II) complexes were prepared for analysis by premixing 1-5 μg of the solid complex with 10 μl of the solvent. For the Group V complexes, a saturated solution in the chosen matrix was prepared. Table 3 is a list of the various matrix materials used in this study and the sources of each.

The appropriate solution was then applied to the surface of a bevelled stainless steel probe tip of 2mm diameter until the entire surface was covered. This required about 2 μl. The probe tip was next inserted into the end of the probe which was then inserted through a series of vacuum locks into the source area.

Table 1. Ruthenium(II) Polypyridyl Coordination Complexes

$[RuL_3]X_2$ series

- $[Ru\ (bpy)_3\ ](PF_6)_2$
- $[Ru\ (bpy)_3\ ](CF_3SO_3)_2$
- $[Ru\ (bpy)_3\ ]Cl_2$
- $[Ru\ (phen)_3\ ](PF_6)_2$
- $[Ru\ (phen)_3\ ](CF_3CO_2)_2$
- $[Ru\ (dpa)_3\ ](PF_6)_2$
- $[Ru\ (dmb)_3\ ](PF_6)_2$

$[RuL_2L']X_2$ series

- $[Ru\ (bpy)_2\ (phen)\ ](PF_6)_2$
- $[Ru\ (phen)_2\ (bpy)\ ](PF_6)_2$
- $[Ru\ (dmb)_2\ (bpy)\ ](PF_6)_2$
- $[Ru\ (dmb)_2\ (phen)\ ](PF_6)_2$
- $[Ru\ (bpy)_2\ (dpa)\ ](PF_6)_2$

$[RuLL'L'']X_2$ series

- $[Ru\ (phen)\ (dmb)\ (bqy)\ ](PF_6)_2$
- $[Ru\ (bpy)\ (dmb)\ (bqy)\ ](PF_6)_2$
- $[Ru\ (bpy)\ (phen)\ (bqy)\ ](PF_6)_2$
- $[Ru\ (bpy)\ (phen)\ (dmb)\ ](PF_6)_2$
- $[Ru\ (bpy)\ (phen)\ (dpk)\ ](PF_6)_2$
- $[Ru\ (bpy)\ (phen)\ (tmp)\ ](PF_6)_2$
- $[Ru\ (bpy)\ (dmb)\ (dib)\ ](PF_6)_2$
- $[Ru\ (bpy)\ (phen)\ (dzf)\ ](PF_6)_2$
- $[Ru\ (bpy)\ (phen)\ (dpa)\ ](PF_6)_2$
- $[Ru\ (dmb)\ (phen)\ (dpa)\ ](PF_6)_2$

$[RuLL'(CO)Cl]X$ series

- $[Ru\ (bpy)\ (phen)\ (CO)\ Cl\ ](PF_6)$
- $[Ru\ (bpy)\ (dmb)\ (CO)\ Cl\ ](PF_6)$
- $[Ru\ (bpy)\ (Bq)\ (CO)\ ]Cl$
- $[Ru\ (bpy)\ (tpy)\ Cl\ ](PF_6)$

Figure 9. Structures of Polypyridyl Ligands and the Abbreviations Used for them.

2,2'-bipyridine (bpy)

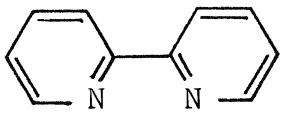

1,10-phenanthroline (phen)

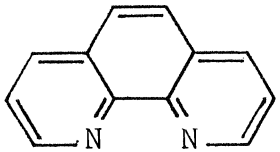

di-(2-pyridyl)amine (dpa)

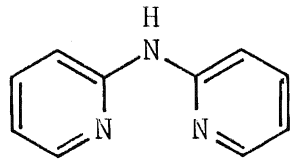

4,4'-dimethyl-2,2'-bipyridine (dmb)

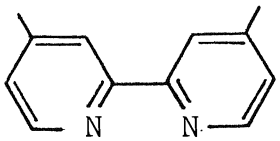

2,2'-biquinoline (bqy)

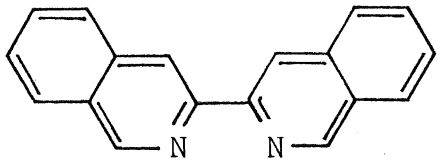

di-(2-pyridyl)ketone (dpk)

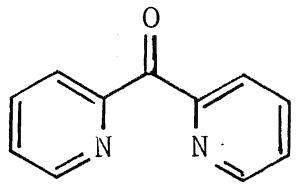

4,4'-diisopropyl-2,2'-bipyridine (dib)

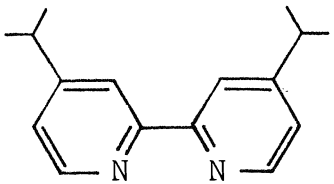

4,5-diazofluorenone (dzf)

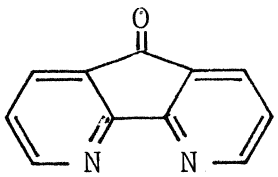

2,2'-6',2''-terpyridine (tpy)

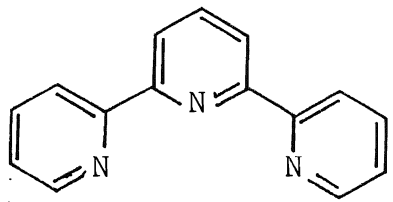

3,4,7,8-tetramethyl-1,10-phenanthroline (tmp)

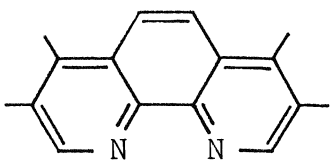

benzo(H)quinolin-10-yl (Bq)

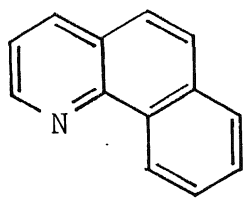

Table 2. Group V Triptycenes and Related Complexes

Tris(2-chlorophenyl) Derivatives

$P(C_6H_4Cl)_3$

$As(C_6H_4Cl)_3$

$Sb(C_6H_4Cl)_3$

$Bi(C_6H_4Cl)_3$

Tris(2-bromotetrafluorophenyl) Derivatives

$P(C_6F_4Br)_3$

$As(C_6F_4Br)_3$

$Sb(C_6F_4Br)_3$

$CH_3Si(C_6F_4Br)_3$

Tris(tetrafluorophenyl) Derivative

$As(C_6F_4H)_3$

Triptycenes

$P_2(C_6F_4)_3$

$As_2(C_6F_4)_3$

$Sb_2(C_6F_4)_3$

$Bi_2(C_6F_4)_3$

$(CH_3Si)_2(C_6F_4)_3$

$PSb(C_6F_4)_3$

$AsSb(C_6F_4)_3$

Table 3. Matrices Used in the Analyses and Their Sources

Matrix	Source
glycerol	Aldrich Chemical Co., Milwaukee, Wisconsin.
sulfolane	BDH Chemicals Ltd., Parle, England.
monothioglycerol	Sigma Chemical Co., St. Louis, Missouri.
3-nitrobenzyl alcohol	Aldrich Chemical Co., Milwaukee, Wisconsin.
2-nitrophenyl octyl ether	Fluka AG, Switzerland.
dimethylformamide	J.T. Baker Chemical Co., Phillipsburg, N.J.
diethylformamide	J.T. Baker Chemical Co., Phillipsburg, N.J.

C. Results and Discussion

1. Ruthenium(II) Polypyridyl Coordination Complexes

i) Introduction

The ruthenium(II) complexes that were analyzed are listed in Table 1. These are coordination complexes in which there are from one to three different polypyridyl ligands. These may include one or more of the following bidentate ligands: 2,2'-bipyridine (bpy), 1,10-phenanthroline (phen), 4,4'-dimethyl-2,2'-bipyridine (dmb), 4,4'-diisopropyl-2,2'-bipyridine (dib), di-(2-pyridyl) amine (dpa), di-(2-pyridyl) ketone (dpk), 2,2'-biquinoline (bqy), 4,5-diazofluorenone (dzf), 3,4,7,8-tetramethyl-1,10-phenanthroline (tmp), and benzo(H) biquinolin-10-yl (Bq). Diagrams of the ligands as well as the abbreviations used for them in this report are as shown in Figure 9.

Some of the complexes were coordinatively unsaturated with respect to the polypyridyl ligands and contained one or two of the monodentate ligands CO or Cl. One complex contained the tridentate ligand 2,2'-6',2''-tripyridine (tpy).

The complexes, as shown in Table 1, were divided into four groups or series. Grouping was based on the

number and type of the ligands present in the molecule. The complexes of the series $[RuL_3]X_2$ contain three of one type of ligand. The positive ion FAB mass spectra for these complexes are shown as Figures A.1 to A.7 in Appendix A. Table 4 is a summary of the spectra for these complexes. The complexes of the $[RuL_2L']X_2$ series contain two different ligands, however, one is present in the complex twice. The spectra for these are shown as Figures A.8 to A.12 and are summarized in Table 5. The series $[RuLL'L"]X_2$ are complexes containing three different bidentate ligands. The spectra are shown as Figures A.13 to A.22 in Appendix A, and are summarized in Table 6. Finally, the series of complexes [RuLL'(CO)Cl)]X are those containing different types of ligands (i.e. mono-, bi- and tridentate). The spectra are shown in Appendix A as Figures A.23 to A.26. Table 7 is the summary of the spectra.

The positive ion FAB mass spectra are averages of at least three consecutive scans. Each has had the matrix spectrum (Figure 10) subtracted. Important ions appearing in each spectrum are labelled with respect to the ligands contained in each ion. The notations L, L' and L" correspond to the ligands as shown in the spectrum title from left to right. The numerical label is that of the nominal mass of the peak of highest intensity in the cluster, which, for reasons that will be explained below, may not be the formula weight of the labelled ion.

Figure 10. Positive Ion FAB Mass Spectrum of 3-Nitrobenzyl Alcohol, the Matrix.

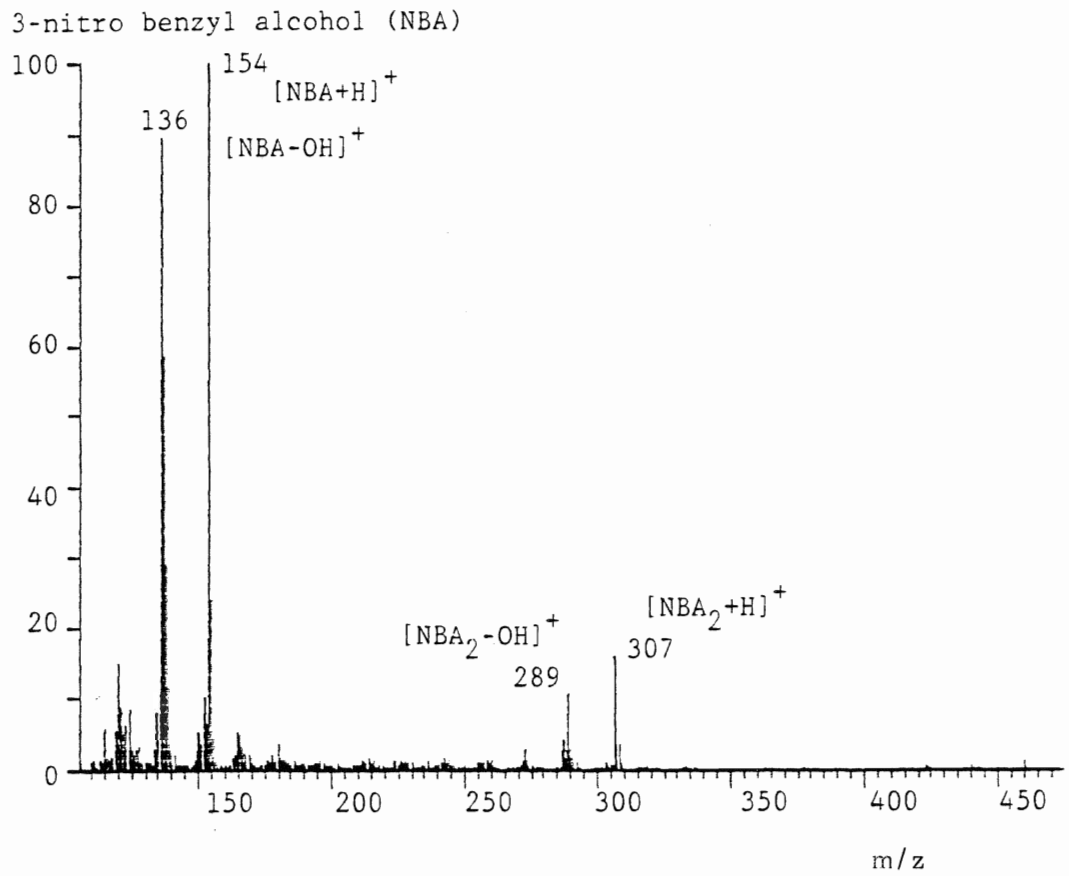
3-nitro benzyl alcohol (NBA)
100
80
60
40
20
0
154
[NBA+H]+
136
[NBA-OH]+
[NBA2-OH]+
289
[NBA2+H]+
307
150
200
250
300
350
400
450
m/z

Only ions above m/z 100 were included in the spectra when averaging. There were several reasons for doing this. First, the spectra below m/z 100 were dominated by ions such as K^+, Na^+ and fragment ions from the matrix. Secondly, and most importantly, there should be no ions relevant to the ruthenium complexes below m/z 100 since all ligands have formula weights well above 100 (the smallest is bpy at 156 amu). Also, the isotopes of a ruthenium atom alone range from 96 to 104 amu, therefore combinations of almost any elements with ruthenium will give ions in the mass spectrum above m/z 100 (assuming they have unit charge).

Tables 4 to 7 summarize the positive ion FAB mass spectra of each series of complexes, giving relative percent intensities of major ions appearing in the spectra. For the most part, these are ruthenium containing ions, however, one important non-metal containing ion, the protonated ligand, is included. The values shown in a Table are given as a % of the total ion current for the ions listed in the Table.

Isotope cluster peak intensities of the same elemental composition were summed for consistency in comparisons. This is important, especially for ruthenium containing ions since ruthenium has isotopes with significant natural abundance (>15%) from 96 to 104 amu (Figure 11a). When in combination with other polyisotopic elements such as are found with these complexes (i.e. C, H, N, and O) the isotope cluster can stretch over twelve to

Figure 11. Isotopic Cluster Patterns

a) top: Ru atom

b) bottom: $[Ru(bpy)(phen)(dpk)](PF_6)^+$ ion.

a)

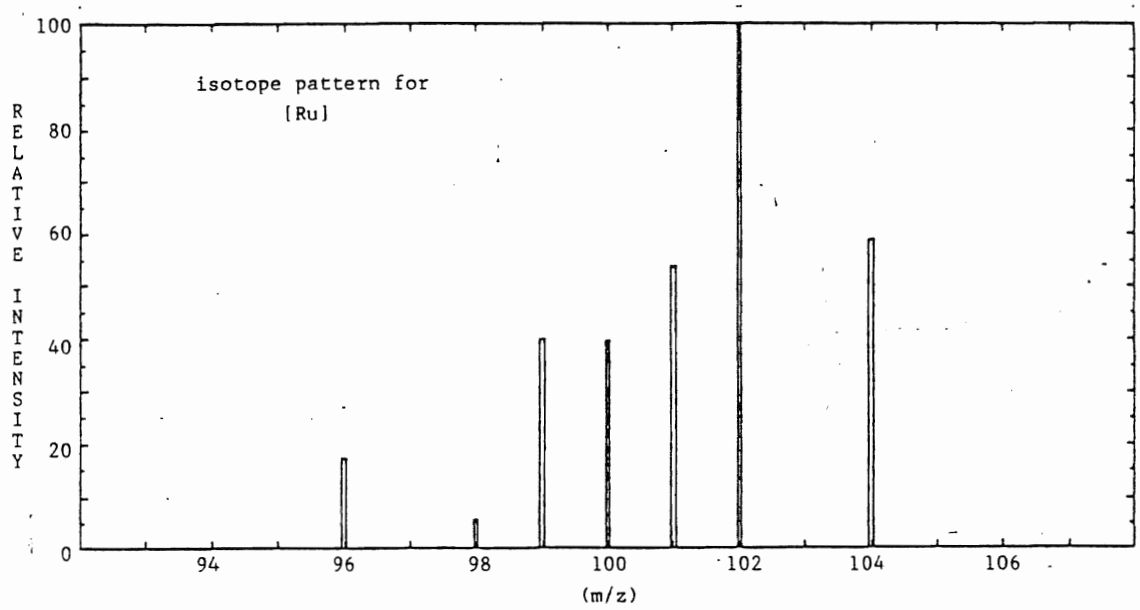
isotope pattern for
[Ru]
RELATIVE INTENSITY
100
80
60
40
20
0
94
96
98
100
102
104
106
(m/z)

b)

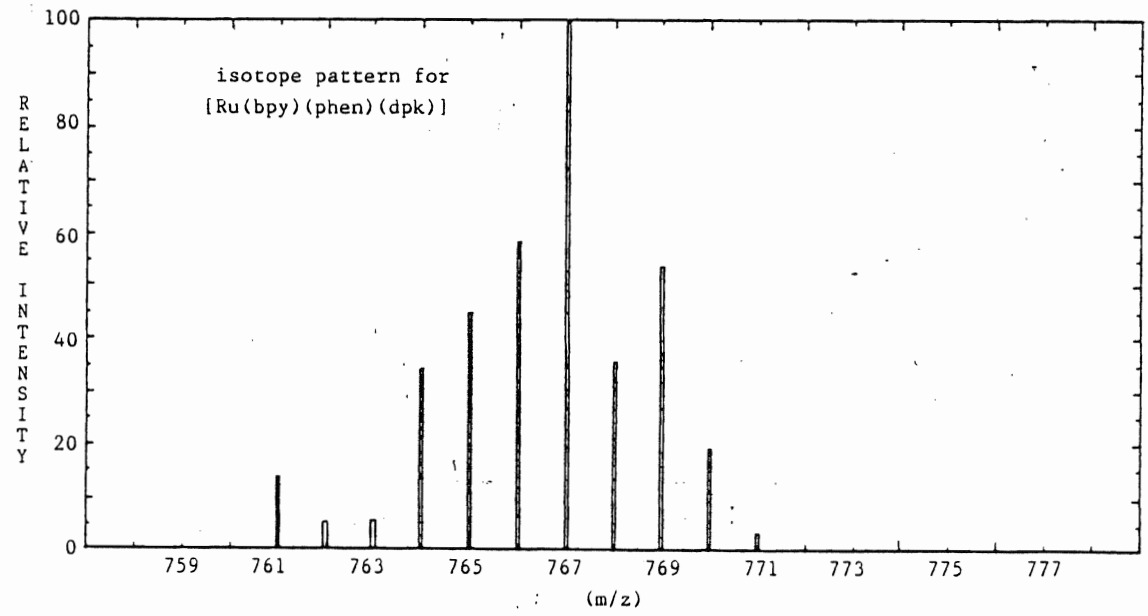
isotope pattern for
[Ru(bpy)(phen)(dpk)]
RELATIVE INTENSITY
100
80
60
40
20
0
759
761
763
765
767
769
771
773
775
777
(m/z)

thirteen mass units (Figure 11b). There are advantages and disadvantages to this. An advantage is that ruthenium containing peaks are easy to spot in the spectrum and from the highest intensity peak, the mass of the ion can be accurately assigned. One disadvantage is that species that have different molecular structure but that coincidentally have formula weights within 12 to 13 amu of each other, overlap in the mass spectrum. In such cases, many of which occur with these complexes, it is possible to deconvolute the clusters using the computer program BMASABD as described earlier.

There are many factors to consider in examining the FAB mass spectra of the coordination complexes. These include: optimization of the matrix, the fragmentation mechanism, anion effects, observation of multiply charged ions, competitive ligand losses and mixture analysis. Therefore, the discussion will be organized in such a manner that each of these are discussed separately.

ii) Matrix Optimization

The matrix is one of the most important variables in the FAB experiment. Therefore, to obtain optimum results from the experiment, a pre-experiment should be performed to determine the best matrix material. The identity of this matrix will change with the particular type of analyte being studied.

The general matrix requirements as outlined by Gower [52] and DePauw [53] are:

a) the analyte should be soluble in the matrix,

b) the vapour pressure of the matrix should be low enough to ensure a relatively long sample lifetime in the high vacuum of the mass spectrometer,

c) the matrix should be viscous but not so viscous as to prevent diffusion of the analyte molecules to the surface,

d) ions from the matrix itself should be in low abundance or should be easily identifiable, and

e) the matrix should not be destructively reactive with the analyte.

Several commonly used matrices were available in the laboratory for a comparative study of the FAB mass spectra obtained for the ruthenium complexes. These were: glycerol (GLY), sulfolane (SUL), thioglycerol (TGL), 2-nitrophenyl octyl ether (NOP) [54], and 3-nitrobenzyl alcohol (NBA) [55]. These are generally recognized as the best matrices to be used for obtaining FAB mass spectra of transition-metal containing complexes [53]. Also used were three matrix mixtures: 30% glycerol in sulfolane (SGL), 50% dimethylformamide in glycerol (DMG) and 50% diethyl-formamide in glycerol (DEG). For the comparison the complex $[Ru(bpy)_3](PF_6)_2$ was chosen. The reasons for this choice were sample availability and simplicity of the spectrum

obtained. The samples were made up in approximately the same concentrations (approximately 10 μg of the analyte was dissolved in 10 μl of the matrix). All samples were analyzed at the same time to maintain similar machine operating conditions over the comparison.

Following the matrix requirements above, several of the matrices were quickly eliminated. Both glycerol and 2-nitrophenyl octyl ether suffered from poor solubility. Sulfolane, while dissolving the complex well, had a very high vapour pressure allowing only one or two scans before the ion current disappeared.

The remaining matrices all satisfied the general requirements. Therefore, only a visual examination of the spectra obtained using each matrix would allow a final choice to be made. The spectra are shown as Figures 12a through 12e. Important peaks in the spectra are: $[RuL_3]X^+$ (m/z 715), $[RuL_3]^+$ (m/z 570), $[RuL_3]^{2+}$ (m/z 285), $[RuL_2]^+$ (m/z 413), $[RuL]^+$ (m/z 257) and LH^+ (m/z 157). The spectra are shown only for the mass range 156-723. This range covers all of the ions of interest but none of the matrix monomer peaks. These are usually the most intense in the spectra and can dwarf peaks due to the analyte, therefore they were purposefully omitted so that analyte peaks could more clearly be seen.

It was obvious that the matrices DMG and DEG gave the poorest results (Figures 12d and 12e). Ions from the

Figure 12. Positive Ion FAB Mass Spectra of $[Ru(bpy)_3](PF_6)_2$ in the Matrices:

a) thioglycerol (TGL)

b) 30% glycerol in sulfolane (SGL)

c) 3-nitrobenzyl alcohol (NBA)

d) 50% dimethylformamide in glycerol (DMG)

e) 50% diethylformamide in glycerol (DEG).

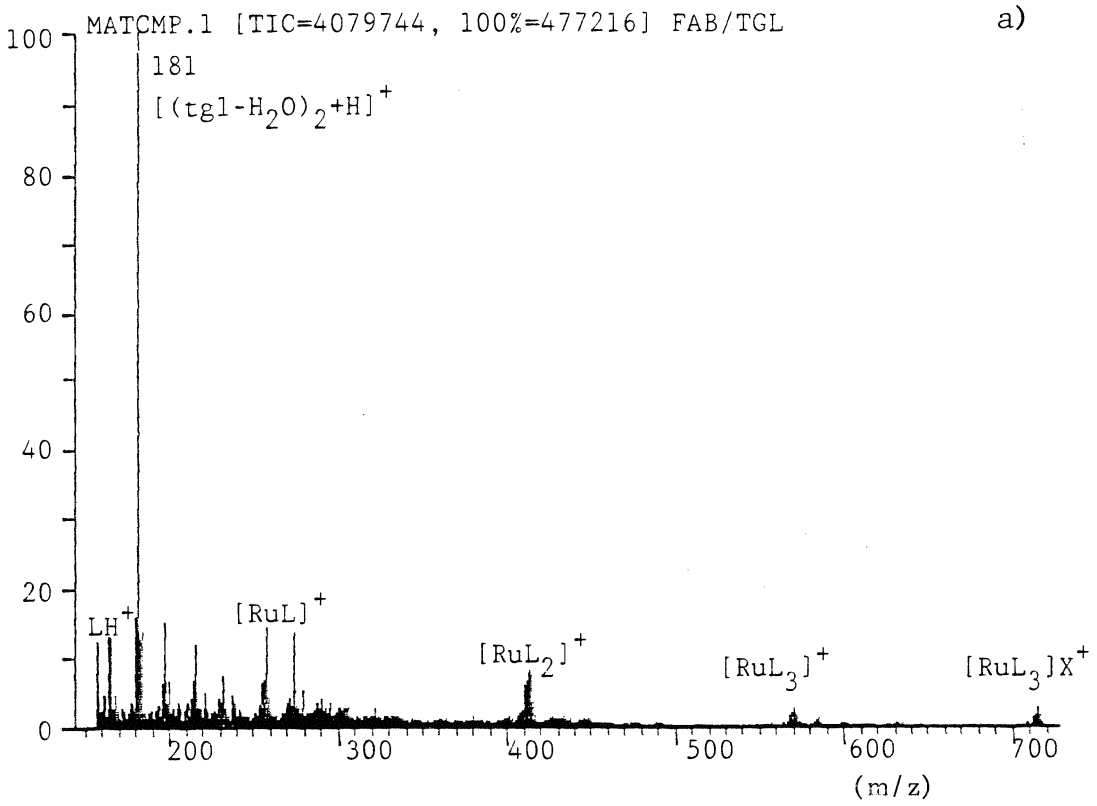
MATCMP.1 [TIC=4079744, 100%=477216] FAB/TGL
a)
181
[(tgl-H2O)2+H]+
LH+
[RuL]+
[RuL2]+
[RuL3]+
[RuL3]X+
100
80
60
40
20
0
200
300
400
500
600
700
(m/z)

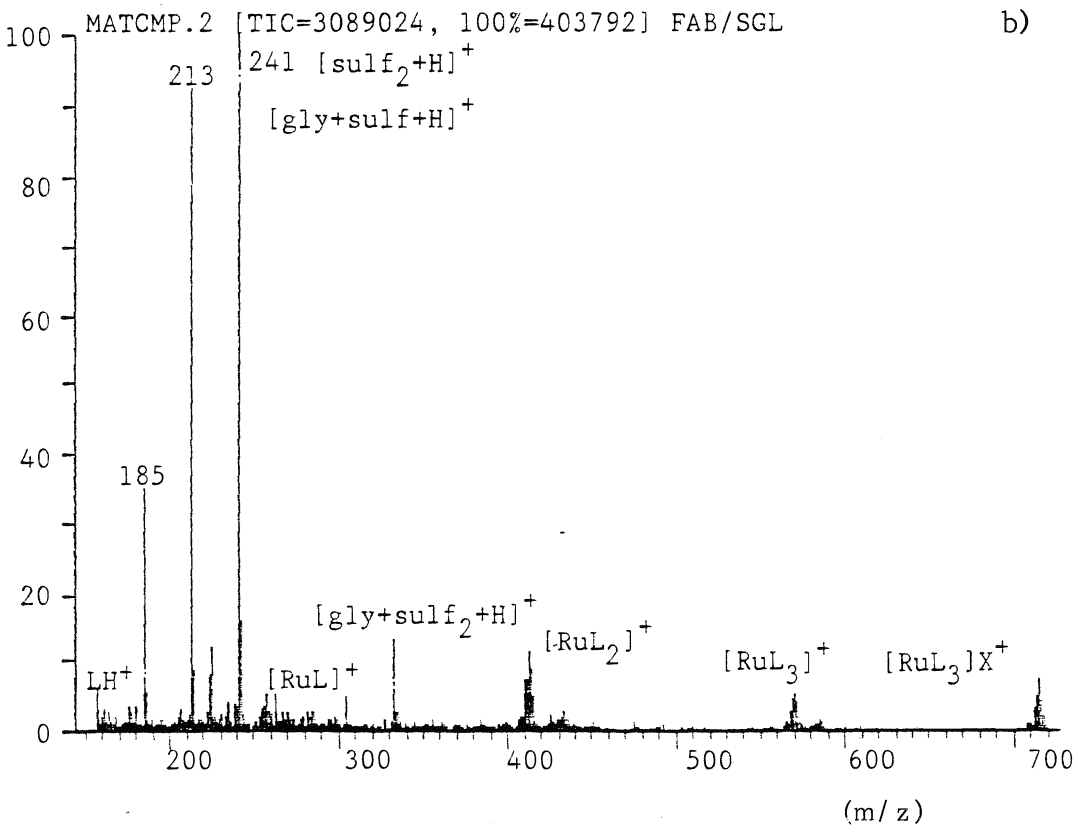
MATCMP.2 [TIC=3089024, 100%=403792] FAB/SGL
b)
241 [sulf2+H]+
213
[gly+sulf+H]+
185
[gly+sulf2+H]+
LH+
[RuL]+
[RuL2]+
[RuL3]+
[RuL3]X+
100
80
60
40
20
0
200
300
400
500
600
700
(m/z)

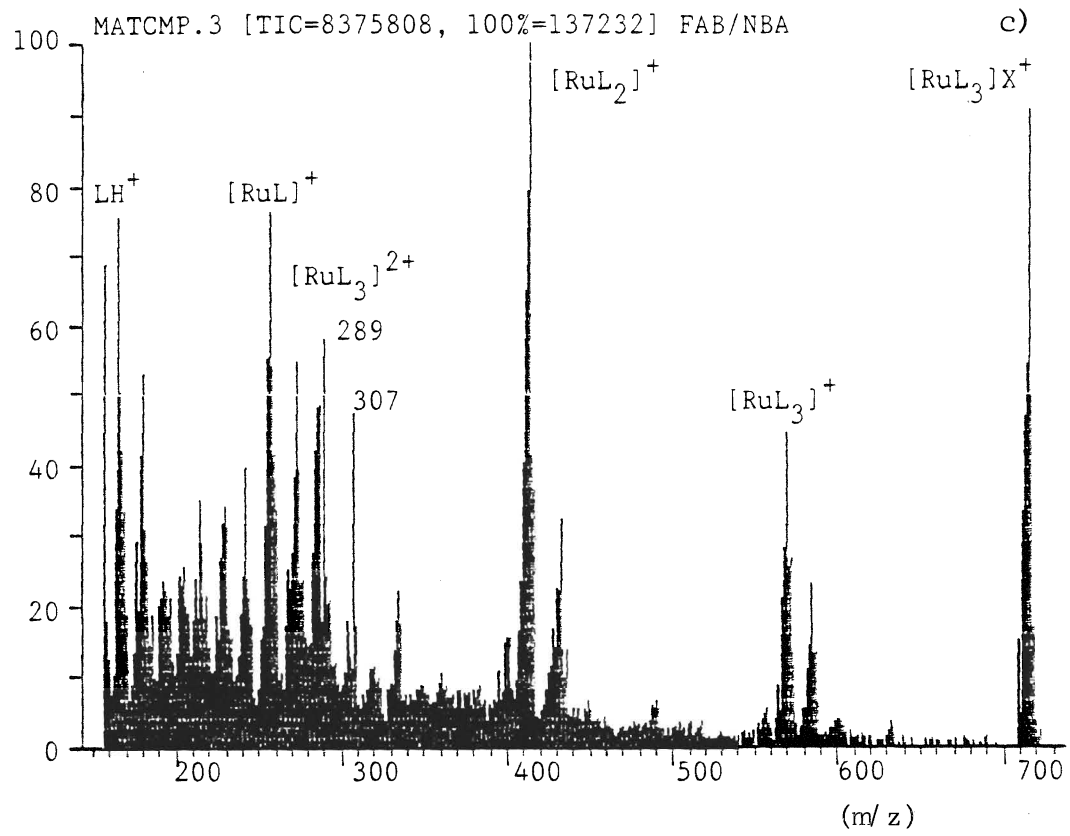
MATCMP.3 [TIC=8375808, 100%=137232] FAB/NBA
c)
100
80
60
40
20
0
LH+
[RuL]+
[RuL3]2+
289
307
[RuL2]+
[RuL3]+
[RuL3]X+
200
300
400
500
600
700
(m/z)

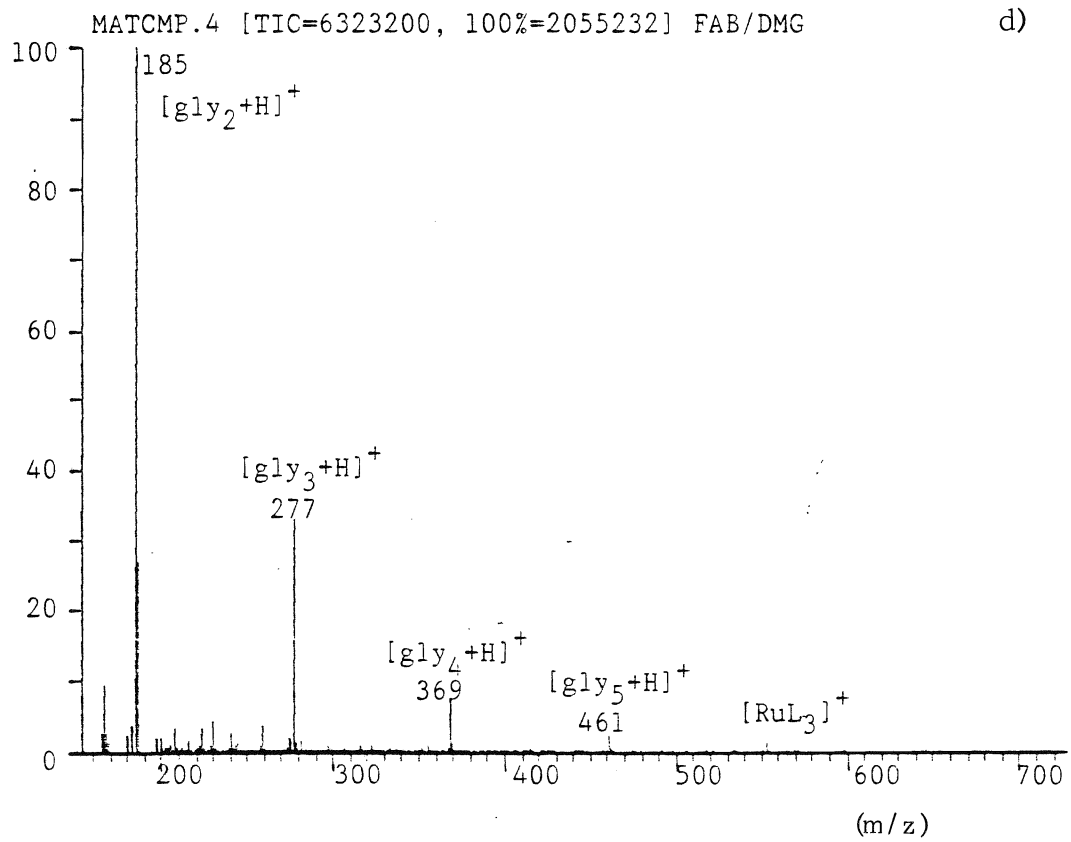
MATCMP.4 [TIC=6323200, 100%=2055232] FAB/DMG
d)
100
80
60
40
20
0
185
[gly2+H]+
[gly3+H]+
277
[gly4+H]+
369
[gly5+H]+
461
[RuL3]+
200
300
400
500
600
700
(m/z)

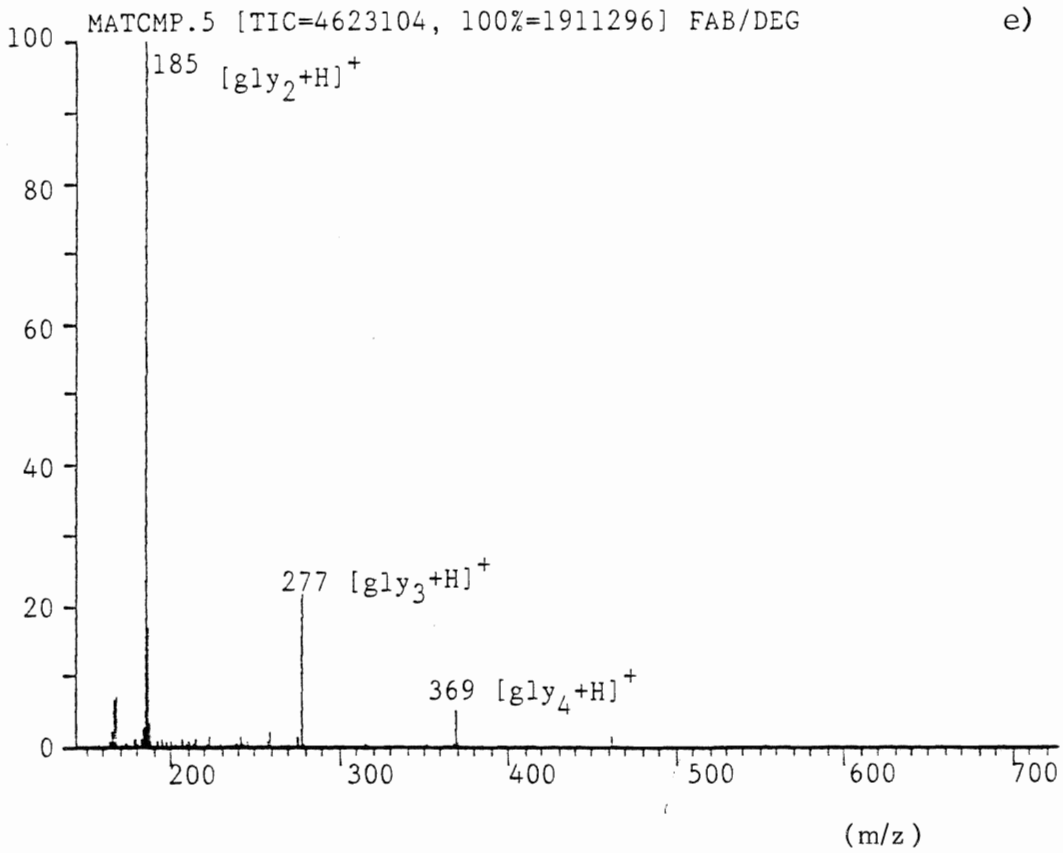
MATCMP.5 [TIC=4623104, 100%=1911296] FAB/DEG
e)
100
80
60
40
20
0
185 [gly2+H]+
277 [gly3+H]+
369 [gly4+H]+
200
300
400
500
600
700
(m/z)

analyte are barely visible and matrix cluster peaks are of high intensity. The purpose of mixing DMF or DEF with the glycerol was to increase the solubility of the analyte in the matrix glycerol. However, once inside the source area of the spectrometer, fractional distillation of the more volatile DMF or DEF may result in a sample that contains mostly glycerol. Since, as was observed, the solubility of the analyte in glycerol was poor, then a poor FAB spectrum was obtained.

The three remaining matrices, TGL, SGL and NBA all gave FAB spectra that contained useful information, in the form of readily recognizable ruthenium containing peaks. However, the spectrum obtained using NBA was by far the best of the three. In the NBA spectrum, while the noise level was quite high, especially at the low mass end, most of the ion current was carried by peaks due to the analyte. In the TGL and SGL spectra, matrix cluster peaks account for a large proportion of the total ion current. Over the mass range chosen, NBA has only two matrix cluster peaks (see NBA spectrum Figure 10). These are: $[NBA_2\text{-}H]^+$ (m/z 307) and $[NBA_2\text{-}OH]^+$ (m/z 289). The intensity of these ions compared to the intensity of analyte ions is very low.

Therefore, based on the general matrix requirements and on the quality of the spectra obtained from each of the matrices, 3-nitrobenzyl alcohol was chosen as the optimum matrix for FAB analysis of the ruthenium(II) complexes.

One disadvantage to the use of NBA is the high level of noise or background present in the spectra. Most of this is due to the matrix (see Figure 10). Subtraction of the pure matrix spectrum from the spectrum with analyte present is efficient and removes much of the background. Fortunately, the high background that remains is at the low end of the spectrum where few peaks of interest appear.

iii) Fragmentation Mechanism of the Tris-bidentate Complexes

To determine a fragmentation mechanism, one must first identify all of the peaks appearing in the mass spectrum. Then through the consideration of known physical properties and previous observations made by other workers studying similar systems, relationships between the observed ions can be established. Observations of metastable ions to confirm the proposed mechanisms are also of use, unfortunately they could not be detected with our MS-30.

In the spectra of the ruthenium complexes, identification of ions is fairly simple, both because, as has been explained, the ruthenium isotopic pattern clearly identifies ruthenium containing ions, but also because there are few relevant ions in the spectrum. Only six important ions appear in each spectrum, although there may be more than one kind of each of these ions due to the presence of different kinds of ligands in the analyte. For simplicity,

only the spectra of the tris-ligand complexes, as shown in Table 4, will be considered in determining the fragmentation mechanism. The ions appearing in the spectra of these complexes are of the form: $[RuL_3]X^+$, $[RuL_3]^{2+}$, $[RuL_3]^+$, $[RuL_2]^+$, $[RuL]^+$ and $(L+H)^+$.

Complexes such as the ruthenium complexes never give the parent ion in the mass spectrum, neither as the molecular ion ($[M^{+\cdot}]$) nor as a pseudomolecular ion ($[M+H]^+$) [38-44]. This is attributed to pre-formation of ions in the polar matrix material due to a simple ionic dissociation. Therefore, the ion of highest mass observed in the spectrum is the complex cation $[RuL_3]X^+$. The negative ion FAB mass spectrum of the complex $[Ru(bpy)_3](PF_6)_2$ (Figure 13, top) is dominated by a peak corresponding to the intact counter anion, i.e. PF_6^- (m/z 145). No ruthenium containing peaks appear in the negative ion spectrum. Other peaks are due to the matrix: $[NBA]^{-\cdot}$ (m/z 153), $[NBA_2-H]^-$ (m/z 305) and others. The positive ion FAB mass spectrum for the same complex on the same instrument is shown for comparison.

Therefore, present in the matrix/analyte solution are X^- and $[RuL_3]X^+$ ions and it is from the latter that initial fragmentation must occur.

Since one anion can be dissociated relatively easily then it seems reasonable to expect that the second anion might also dissociate yielding $[RuL_3]^{2+}$. Since this is a doubly charged ion and ionic species are analyzed via a

Table 4. Positive Ion FAB Mass Spectra of $[RuL_3]X_2$ Complexes[a]

	L = bpy X = PF_6	bpy CF_3SO_3	bpy Cl	phen PF_6	phen CF_3CO_2	dpa PF_6	dmb PF_6
Fragment			Relative Intensity				
$[RuL_3]X^+$	18.7	18.8	5.8	22.9	6.5	4.2	10.9
$[RuL_3]^{2+}$	12.1	7.3	8.6	9.3	12.6	3.8	16.0
$[RuL_3]^+$	8.8	8.3	12.4	10.0	15.9	3.3	4.5
$[RuL_3\text{-}H]^+$	3.2	2.8	3.6	7.0	5.7	39.7	6.4
$[RuL_2]^+$	13.2	14.8	20.6	18.8	20.5	5.8	12.5
$[RuL_2\text{-}H]^+$	14.2	11.6	17.1	11.5	11.5	22.4	19.2
$[RuL]^+$	7.4	6.8	5.9	10.7	11.8	7.2	8.0
$[RuL\text{-}H]^+$	10.7	9.1	9.9	4.0	4.7	6.3	14.6
$[LH]^+$	3.8	3.5	3.5	5.7	5.6	7.3	8.0
$[RuL_2]X^+$	2.5	12.3	12.5	-	2.3	-	-
$[RuL_2]^{2+}$	5.5	4.7	0.0	-	2.8	-	-

[a] Relative intensities are calculated based only on the ions listed in this table. Isotope cluster peak intensities of the same elemental composition are summed.

Figure 13. FAB Mass Spectra of $[Ru(bpy)_3](PF_6)_2$ in 3-NBA Recorded on the VG ZAB-E

top: Negative Ion Mass Spectrum

bottom: Positive Ion Mass Spectrum.

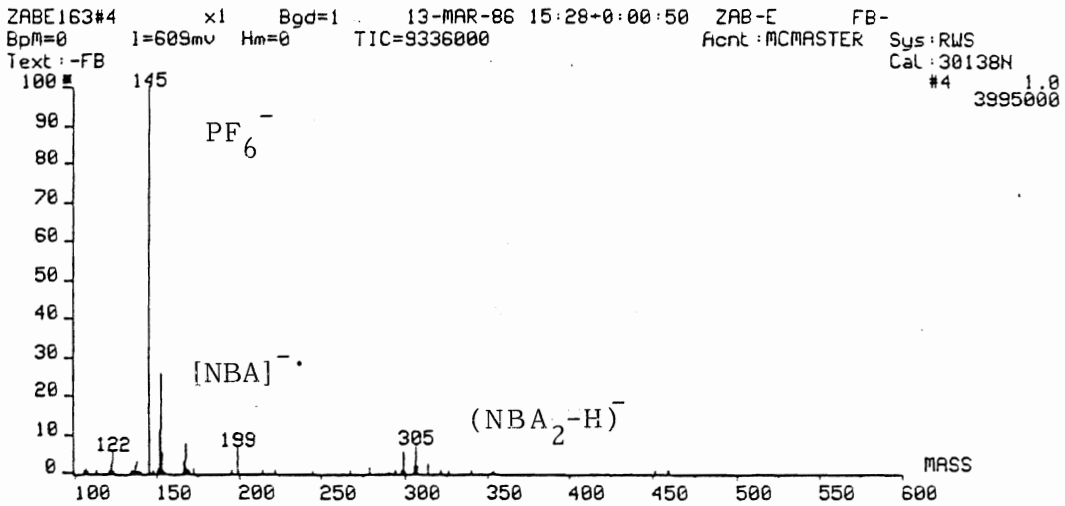
ZABE163#4 x1 Bgd=1 13-MAR-86 15:28+0:00:50 ZAB-E FB-
BpM=0 I=609mv Hm=0 TIC=9336000 Acnt:MCMASTER Sys:RWS
Text:-FB Cal:30138N
#4 1.0
3995000
145
PF6-
[NBA]-·
(NBA2-H)-
122
199
305
MASS

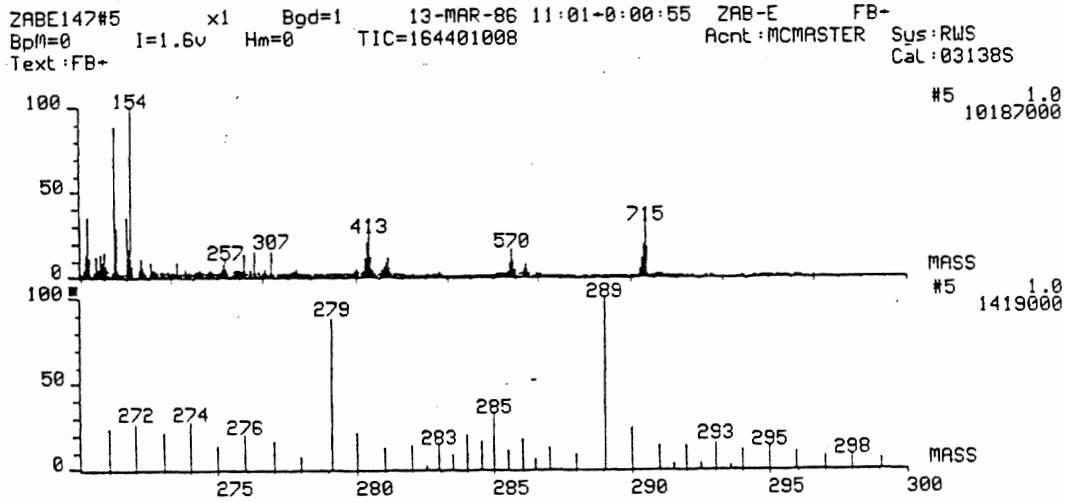
ZABE147#5 x1 Bgd=1 13-MAR-86 11:01+0:00:55 ZAB-E FB+
BpM=0 I=1.6v Hm=0 TIC=164401008 Acnt:MCMASTER Sys:RWS
Text:FB+ Cal:03138S
#5 1.0
10187000
154
257
307
413
570
715
MASS
#5 1.0
1419000
279
289
272
274
276
283
285
293
295
298
MASS

mass-to-charge ratio, then this ion is observed at half its nominal mass. From Table 4, it appears that this is a favourable process since this particular ion carries from 3.8% to 16.0% of the total positive ion current. However, a cluster of peaks also appears in the spectrum at a mass-to-charge ratio that is correct for the singly charged analogue of $[RuL_3]^{2+}$. Cerny [42-44] and Bojesen [41] have also reported observing the singly charged ion, i.e. $[RuL_3]^{+}$. They suggest that it may be formed due to a ligand localized reduction of the doubly charged complex. Since there are free electrons present in the matrix/analyte solution, formed under bombarding conditions [24,25], then this is entirely reasonable.

The ligand di-(2-pyridyl)amine (dpa) presents a special case of fragmentation. The intensity of the doubly charged ion is very low, only 3.8% of the total ion current compared to around 10% for all other ligands. Also, the ion $[RuL_3]^{+}$ appears in the mass spectrum at a m/z ratio that is one unit too low. Therefore the ion is actually of the form $[RuL_3\text{-}H]^{+}$. This will be termed the deprotonated analogue of $[RuL_3]^{+}$. Deconvolution of this cluster of peaks shows that it is mostly of the deprotonated form. From Table 4 $[RuL_3\text{-}H]^{+}$ is 39.7% of the ion current while $[RuL_3]^{+}$ is only 3.3%.

Dpa is non-planar in the free state and forms six-membered rings on coordination [57]. When coordinated,

the amine proton becomes more acidic. Loss of the acidic proton is believed to result in a planar and more sterically stable configuration for the ligand. Therefore, reaction with the matrix, the free counter anion, or perhaps free ligand molecules, can remove the acidic proton resulting in a more stable anionic form for the ligand:

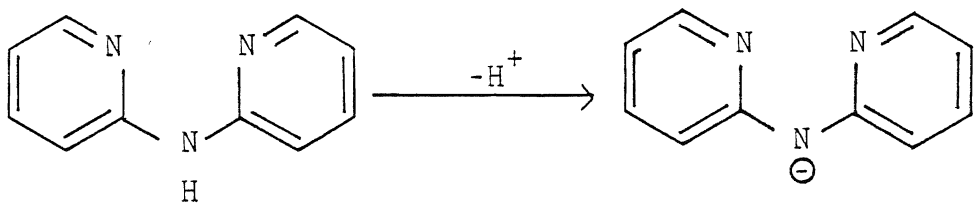

As a result of this the $[RuL_3]X^+$ ion is destabilized. When the ligand dpa is present in a complex, the intensity of this ion is always decreased relative to the same ion when other ligands are present. From Table 4 the ratio $[RuL_3]X^+/[RuL_3\text{-}H]^+$ for L=dpa is 0.1 while for other ligands: L=bpy, 5.8; L=phen, 3.3; L=dmb, 1.7 (all for $X=PF_6^-$).

When L=bpy, phen or dmb there is no easily lost acidic proton as for dpa. All available hydrogens are aromatic or alkyl and therefore more strongly bonded. Therefore the intensity ratio of the deprotonated to non-deprotonated tris-ligand species is small. From Table 4, the $[RuL_3\text{-}H]^+/[RuL_3]^+$ relative intensity ratios are: L=dpa, 10.4; L=bpy, 0.3; L=phen, 0.8; L=dmb, 0.4.

All remaining peaks are formed via loss of intact ligands, from either $[RuL_3]^{2+}$, $[RuL_3]^+$ or $[RuL_2]^+$. This is

a common observation in FAB studies of coordination complexes [36-38, 40, 42] and reflects the differences in relative bond strengths, coordinate bonds being weaker compared to the covalent bonds within ligands.

Loss of one or two ligands from the tris-ligand fragment would result in ions containing two or one ligand respectively. When L=dpa, successive losses of L from $[RuL_3\text{-}H]^+$ yields the ions $[RuL_2\text{-}H]^+$ and $[RuL\text{-}H]^+$.

If ligand loss occurs from the doubly charged tris-ligand fragment then a coordinatively unsaturated (and highly reactive) ion is formed, i.e. $[RuL_2]^{2+}$. Cerny suggests [44] that this ion could undergo an intramolecular oxidative addition yielding a cyclometallated form of the ion. This reaction is well established for ruthenium(II) phenylphosphites [58]:

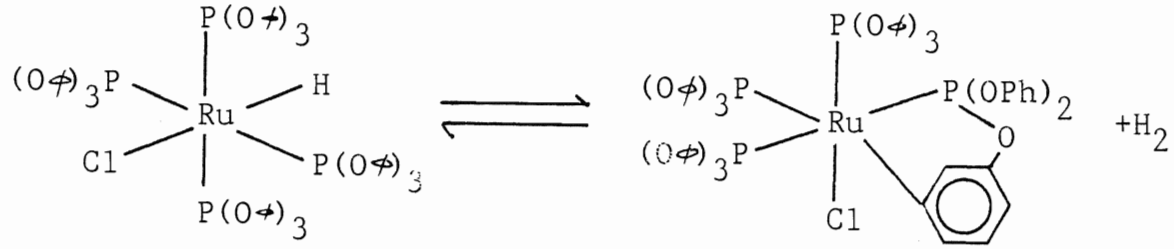

In an analogous reaction with a polypyridyl ligand, a ruthenium-carbon bond is formed accompanied by the loss of a hydrogen radical:

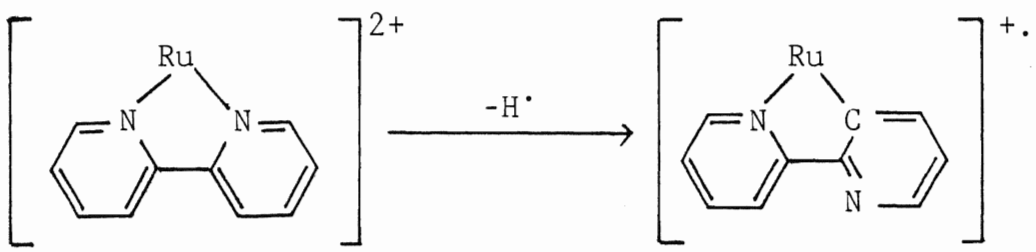

Precedent for the cyclometallated structure has been found in the observation of a similar iridium-bpy complex that has been characterized by x-ray crystallography [59].

Cyclometallation requires rotation of one pyridine ring about the C_2-$C_{2'}$ bond axis. When L=phen this rotation cannot take place since the two pyridine rings are joined:

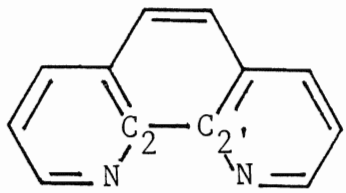

Therefore, formation of the cyclometallate is prevented and abundances of the $[RuL_2\text{-}H]^+$ ion should be low. In fact, the relative intensity ratios for $[RuL_2\text{-}H]^+/[RuL_2]^+$ are: L=bpy, 1.1; L=dmb, 1.5; L=phen, 0.6. The data are from Table 4 and includes only those complexes where $X=PF_6^-$.

Relative intensity ratios for the ions containing a single ligand also reflect the degree of cyclometallation. From Table 4, $[RuL\text{-}H]^+/[RuL]^+$ ratios are: L=bpy, 1.4; L=dmb, 1.8; L=phen, 0.4. Again only those complexes where $X=PF_6^-$ are included for comparison.

No further fragmentation occurs as shown by the

absence of other important ruthenium containing ions in the spectra. The fragmentation mechanisms described above are illustrated in Scheme 1. There are three major pathways that have been shown to be ligand dependent. However, due to the complex nature of the matrix/analyte solution under bombardment conditions, including the possibility of the presence of free electrons and radicals [24,25], a particular ligand is not restricted to a particular mechanistic pathway. The data collected and presented in this thesis show, though, that some ligands will tend to favour one pathway over the others available to it. In general these tendencies are: bipyridine type ligands (i.e. those that are flexible and can rotate about one bond such as bpy and dmb) will favour a cyclometallation, inflexible ligands such as 1,10-phenanthroline favour a simple reduction and finally unusually acidic ligands (or those with easily removable protons) such as di-(2-pyridyl) amine will lose a proton.

iv) Anion Effects and Miscellaneous Comments

In a report by Cohen et al. [38] detailing the FAB mass spectra of a series of coordination complexes containing cationic technetium(III) and phosphine and/or arsine ligands, no effect was observed on the mass spectra on changing the counter anion from Cl^- to ClO_4^- or PF_6^-.

Two complexes were available as salts of different

Scheme 1. Fragmentation of Ruthenium(II) Tris-Bidentate Complexes

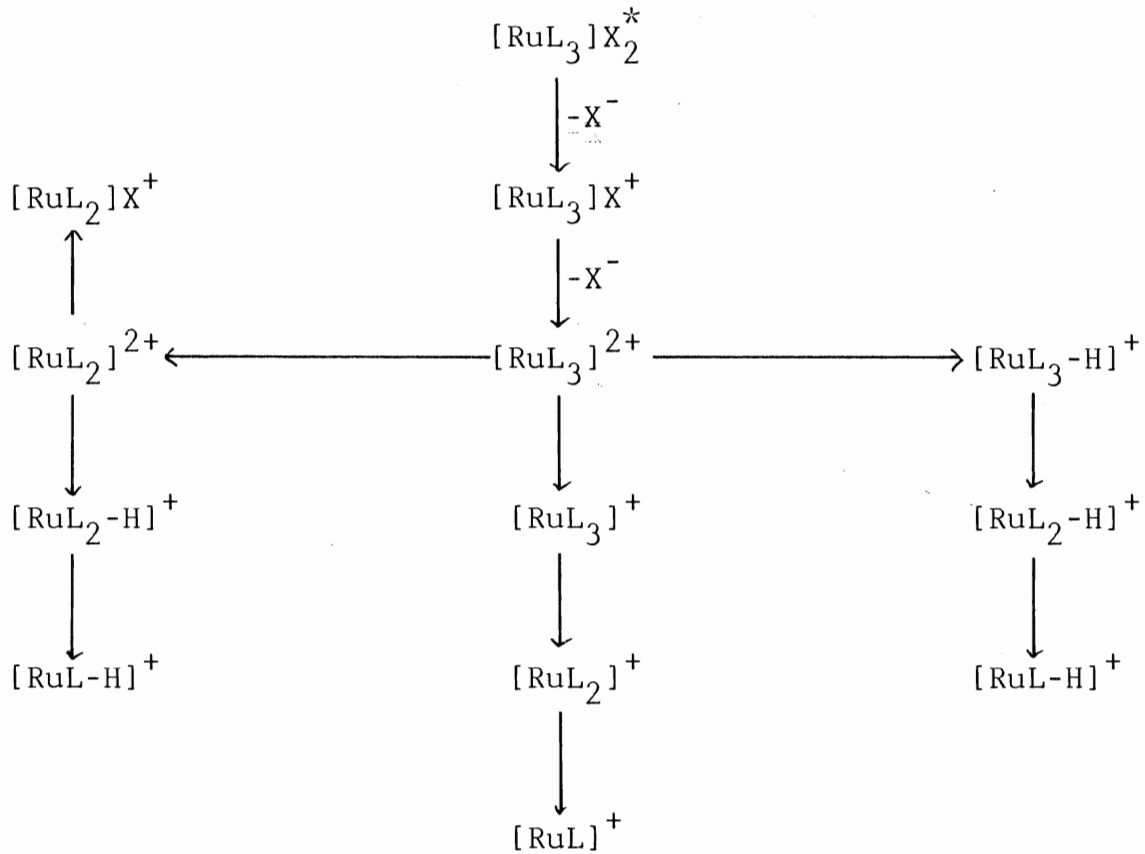

* not observed

anions. These were: $[Ru(bpy)_3]X_2$ where X= Cl^-, PF_6^- and $CF_3SO_3^-$, and $[Ru(phen)_3]X_2$ where X=PF_6^- and $CF_3CO_2^-$. In contrast to the results of Cohen et al., a significant effect on the mass spectra was observed both in the appearance of additional ruthenium-containing peaks and in changing relatives abundances of some ions.

The most noticeable difference in the spectra is the appearance of two ions in addition to those already described. These can be assigned as $[RuL_2]X^+$ and $[RuL_2]^{2+}$. The appearance is most noticeable for the phen complex since they are completely absent when X=PF_6^-.

Two explanations for the observation of these ions are proposed. The first is the possibility of chelation of the anion to the metal center. This is certainly possible for the ligands $CF_3SO_3^-$ and $CF_3CO_2^-$:

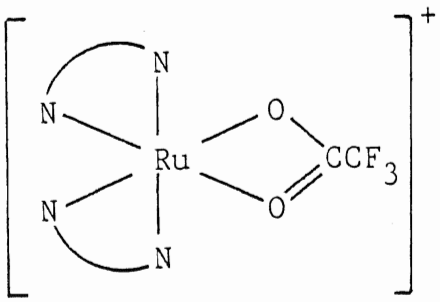

and

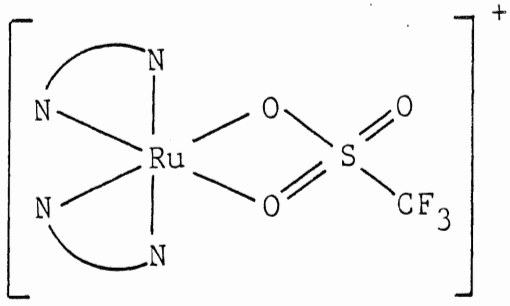

but not for Cl^-; nevertheless a significant abundance of the two new ions is observed when X= Cl^-. Therefore, some additional factor must be involved.

The simplest explanation is that since Cl^- is a smaller anion then PF_6-, then the electrostatic attraction

between the $[RuL_2]^{2+}$ ion and the anion will be greater for Cl^- than for PF_6^-. Therefore it should be expected that intensities of the ion $[RuL_2]X^+$ will be greater for Cl^- than for PF_6^-. From Table 4, the relative intensity of the $[RuL_2]X^+$ ion (for L=bpy) increases from 2.5% of the total ion current when X= PF_6^- to 12.5% when X= Cl^-.

The second important difference noted in the spectra is a decrease in the abundance of the complex cation when X= Cl^- for L=bpy and when X= $CF_3CO_2^-$ for L=phen, as compared to when X= PF_6^- for both complexes. This suggests that the complex cation dissociates more readily, i.e. that bonding to the tris-ligand doubly charged ion is weakened for these anions and therefore they are lost more easily.

Miscellaneous Comments

The spectrum of the complex $[Ru(dmb)_3](PF_6)_2$ contains several peaks that cannot be attributed to this compound. These are due to an impurity in the sample that was identified as $[Ru(dmb)_2(CO)Cl](PF_6)$. This compound is an intermediate in the synthesis of the intended complex. Of course, the presence of the impurity probably affects the abundance of some of the ions in the spectrum since they may be formed from this complex instead. Therefore, the data obtained for this complex have not been used to establish any of the conclusions drawn in the discussion.

All of the spectra show ruthenium containing ions

that appear at approximately sixteen units above both the tris- and bis-ligand fragments. Since these ions are of quite low intensity, it was not possible to determine their correct identities. However, it is thought that they may be oxidation products due to a reaction in the matrix NBA, which is known to be oxidizing in nature. The site of the oxidation is unknown, though it could be on a ligand or, in the case of the bis-ligand fragment, on the central metal atom.

v) Information Available from the Spectra

a) $[RuL_3]X_2$ Series

An example of the spectra obtained for this series of complexes is shown for $[Ru(phen)_3](CF_3CO_2)_2$ in Figure 14. The results for the complete series are summarized in Table 4. Major ruthenium containing ions were identified from their characteristic isotopic pattern (an example is shown in Figure 11). The ion of highest mass in Figure 14 is $[Ru(phen)_3](CF_3CO_2)^+$ (m/z 755). The ions $[Ru(phen)_3]^{2+}$ (m/z 321) and its singly charged analogue $[Ru(phen)_3]^+$ (m/z 642) help in the identification of the anion which can be confirmed by examining the negative ion FAB mass spectrum.

Observation of the multiply charged ions allows for the identification of the oxidation state of the central metal atom. In this case it is +2 since the doubly charged

Figure 14. Positive Ion FAB Mass Spectrum of $[Ru(phen)_3](CF_3CO_2)_2$.

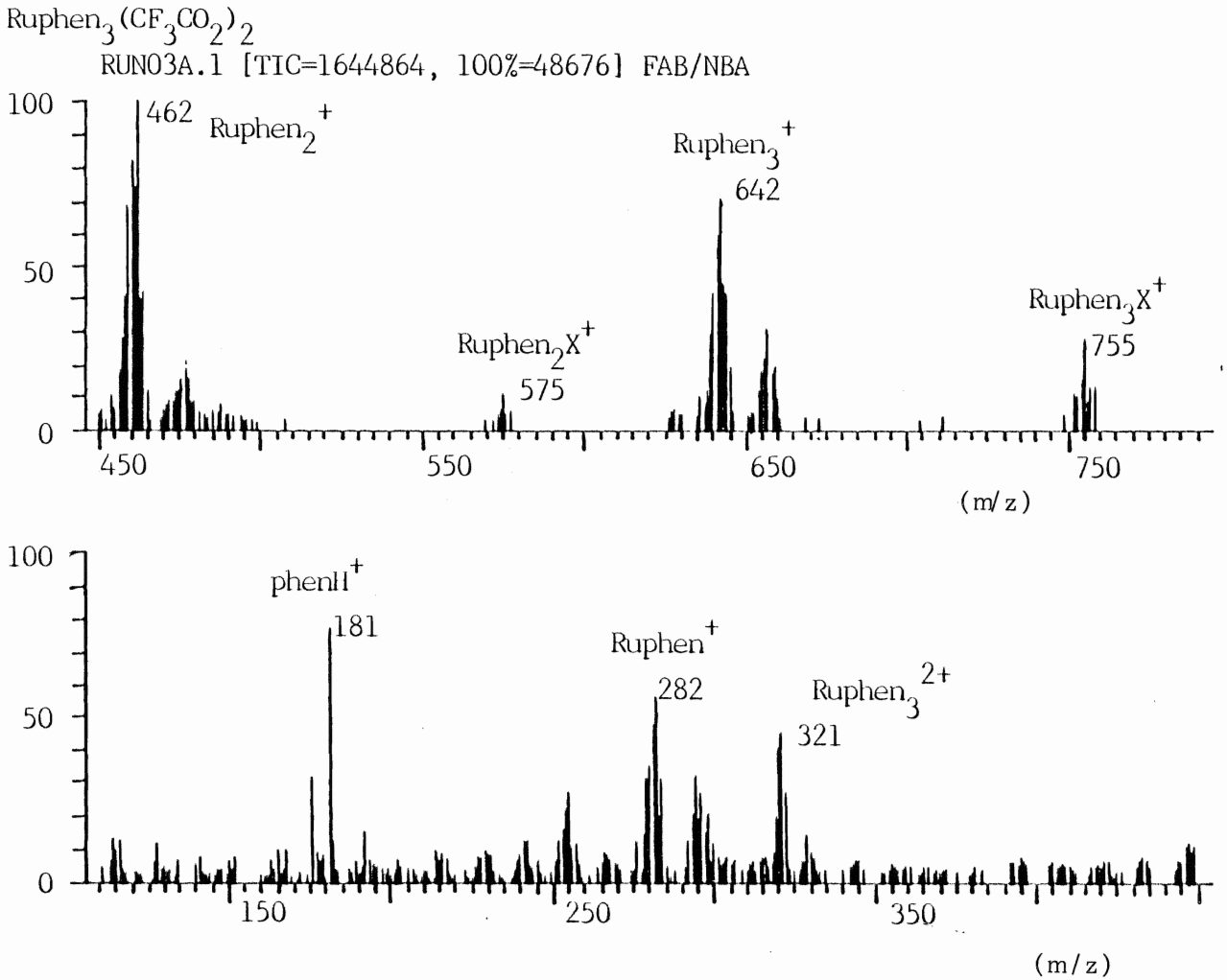
Ruphen3(CF3CO2)2
RUN03A.1 [TIC=1644864, 100%=48676] FAB/NBA
100
50
0
462
Ruphen2+
Ruphen3+
642
Ruphen2X+
575
Ruphen3X+
755
450
550
650
750
(m/z)
100
50
0
phenH+
181
Ruphen+
282
Ruphen3 2+
321
150
250
350
(m/z)

ion is observed. Reduction processes that may or may not occur in the matrix/analyte solution can mask the true charge on the metal atom, so this method may not be reliable.

Other ions arising from intact ligand losses are: $[Ru(phen)_2]^+$ (m/z 462) and $[Ru(phen)]^+$ (m/z 282). These ions along with the protonated ligand ion, $(phen+H)^+$ (m/z 181) enable us to deduce the number and type of ligands present in the parent molecule.

Therefore from the positive and negative FAB mass spectra and the ions contained therein, a nearly complete structural characterization can be made concerning: the identity and oxidation state of the central metal atom, the number and type of ligands, and the number and type of anions contained in the intact analyte molecule.

Deductions concerning the chemical nature of the ligands can also be made. As explained in a previous section, the ligand dpa contains an acidic proton, unlike the other ligands. Loss of the proton produces the preferred and more stable anionic form of the ligand. Therefore, the deprotonated analogues of the ions described above for the complex $[Ru(phen)_3](CF_3CO_2)_2$ are more stable and appear in greater abundance in the mass spectrum (see Table 4).

In every spectrum (except when L=dpa) the bis-ligand containing ion $[RuL_2]^+$ is in greater abundance than either

of the tris- ($[RuL_3]^+$) or single-ligand ($[RuL]^+$) containing ions, suggesting that the solution stability constant, k_2, for the formation of $[RuL_2]^+$ is greater than either k_1 for $[RuL]^+$ or k_3 for $[RuL_3]^+$. This is in agreement with similar reported behaviour of hexacoordinate complexes using laser mass spectrometry [73].

b) $[RuLL'L"]X_2$ series

The positive ion FAB mass spectrum for $[Ru(dmb)(bpy)(bqy)]\ (PF_6)_2$ is shown in Figure 15. A summary of the mass spectra obtained for the complete series is given in Table 5. Peaks corresponding to the ions $[Ru(dmb)(bpy)(bqy)]^{2+}$ (m/z 349), $[Ru(dmb)(bpy)(bqy)]^+$ (m/z 698) and $[Ru(dmb)(bpy)(bqy)](PF_6)^+$ (m/z 843) allow a deduction of the complex formula weight, as well as the number and type of anions present in the intact complex. The isotopic pattern along with the observation of doubly charged ions allows for a complete characterization of the central metal atom. Neutral losses of intact ligands yields the ions $[Ru(bpy)(bqy)]^+$ (m/z 514), $[Ru(dmb)(bqy)]^+$ (m/z 541) and $[Ru(dmb)(bpy)]^+$ (m/z 442). The presence of these ions indicates that there are three different ligands contained in the intact complex. This is confirmed by the presence of the ions $[Ru(dmb)]^+$ (m/z 286), $[Ru(bpy)]^+$ (m/z 257), $[Ru(bqy)]^+$ (m/z 357), $(dmb+H)^+$ (m/z 185), $(bpy+H)^+$ (m/z 157) and finally $(bqy+H)^+$ (m/z 257).

Figure 15. Positive Ion FAB Mass Spectrum of $[Ru(dmb)(bpy)(bqy)](PF_6)_2$.

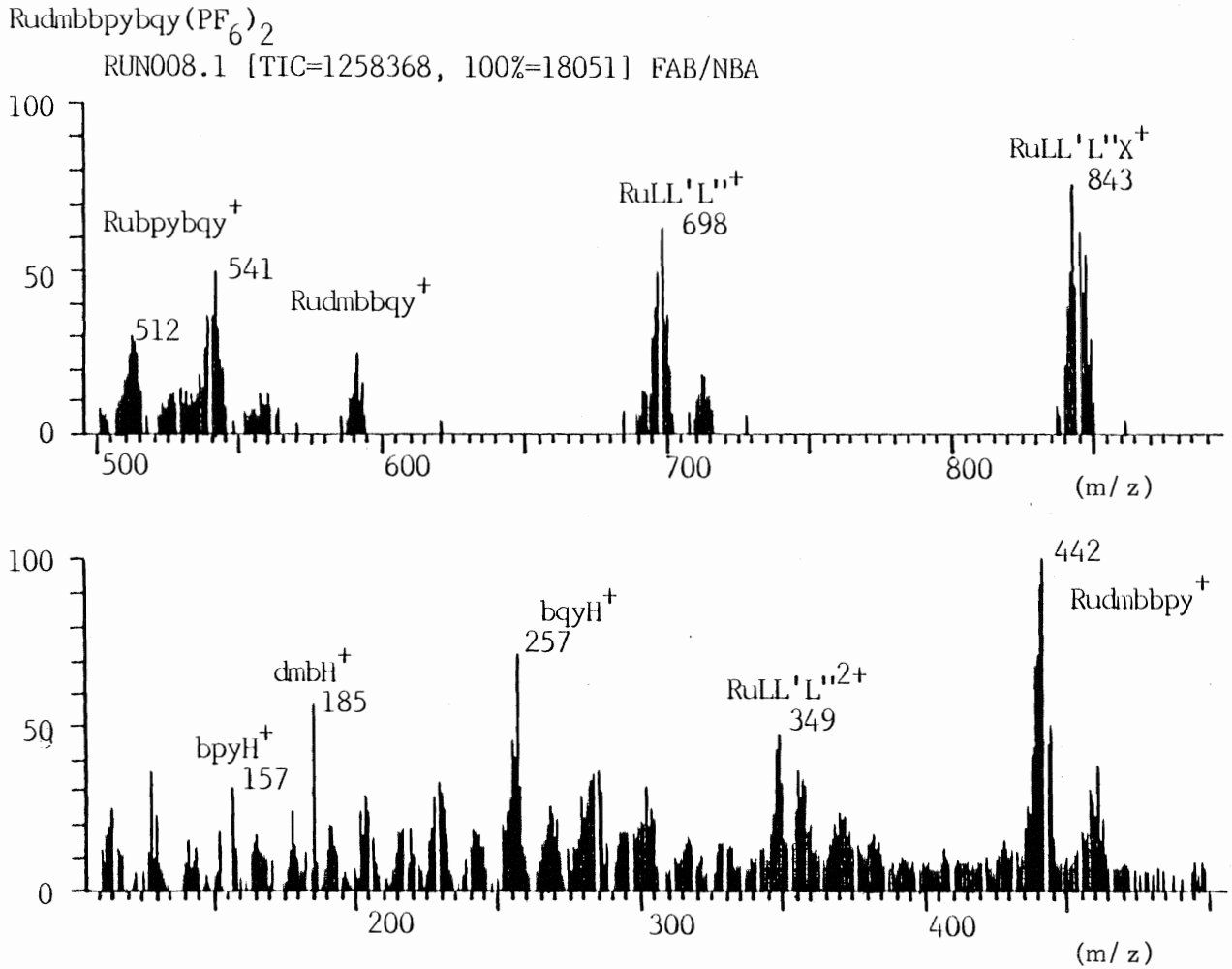
Rudmbbpybqy(PF6)2
RUN008.1 [TIC=1258368, 100%=18051] FAB/NBA
100
50
0
Rubpybqy+
541
512
Rudmbbqy+
RuLL'L''+
698
RuLL'L''X+
843
500
600
700
800
(m/z)
100
50
0
442
Rudmbbpy+
bqyH+
257
dmbH+
185
bpyH+
157
RuLL'L''2+
349
200
300
400
(m/z)

Table 5. Positive Ion FAB Mass Spectra of $[RuLL'L'']X_2$ Complexes[a]

L = phen L' = dmb L'' = bqy	bpy dmb bqy	bpy phen bqy	bpy phen dmb	bpy phen dpk	bpy phen tmp	bpy dmb dib	bpy phen dzf	bpy phen dpa	dmb phen dpa
Fragment				Relative Intensity					
$[RuLL'L'']X^+$	8.9	15.3	16.5	14.6	11.1	20.4	24.3	12.5	1.8	3.2
$[RuLL'L'']^{2+}$	13.3	10.0	8.5	7.7	7.1	13.9	8.1	8.7	7.2	9.7
$[RuLL'L'']^{+b}$	10.9	10.8	10.7	10.9	11.7	13.5	15.1	12.4	27.4	36.9
$[RuLL']^{+b}$	23.5	19.0	18.9	12.4	25.1	5.5	7.1	28.4	8.7	14.4
$[RuLL'']^{+b}$	8.7	6.5	4.9	3.9	0.5	8.1	8.0	0.1	4.4	2.7
$[RuL'L'']^{+b}$	5.4	9.2	10.5	14.9	6.1	15.6	7.7	5.2	8.9	7.8
$[RuL]^{+b}$	7.7	9.9	6.4	11.9	13.6	5.8	4.3	11.2	13.5	5.0
$[RuL']^{+b}$	5.9	9.2	10.8	11.0	15.7	7.2	4.6	13.5	12.7	11.9
$[RuL'']^{+b}$	6.3	6.0	8.1	5.5	1.3	6.0	18.0	1.6	8.3	2.0
$[LH]^+$	3.5	1.5	1.2	1.4	1.8	0.7	0.9	1.5	1.8	2.0
$[L'H]^+$	2.8	2.1	2.4	3.4	4.6	2.1	0.9	3.3	3.9	3.3
$[L''H]^+$	3.2	0.5	0.9	2.6	1.3	1.5	1.2	1.8	1.5	1.0

[a] Relative intensities are calculated based only on the ions listed in this table. Isotope cluster peak intensities of the same elemental composition are summed. $X=PF_6^-$

[b] includes the ion intensity due to the deprotonated analogue of this ion.

The data in Table 5 show that the relative intensities of ions containing only two ligands decreases in the order:

$$[Ru(dmb)(bpy)]^+ > [Ru(dmb)(bqy)]^+ > [Ru(bpy)(bqy)]^+$$

In other words, the ligand bqy is lost more readily to give the ion $[Ru(dmb)(bpy)]^+$ than either of the other two ligands. The relative ordering shown above indicates that the relative ease of losing one of the ligands decreases in the order:

$$bqy > bpy > dmb$$

Another way of stating this is that dmb is a stronger chelating ligand than either bpy or bqy. Confirmation of this observation is provided by the relative intensities of the ions containing only one ligand, which decrease in the order:

$$[Ru(dmb)]^+ > [Ru(bpy)]^+ > [Ru(bqy)]^+$$

Relative intensities of the protonated ligand ions suggest that the chelating power of the ligands toward protons also decreases in the order:

$$(dmb+H)^+ > (bpy+H)^+ > (bqy+H)^+$$

This is in agreement with the observation that, excluding steric and electronic effects, the stability constants of metal chelates are related to the solution basicities of the ligands [49]. The latter observation is in agreement with the measured values of the solution pK_a's of the ligands. The solution basicities of the ligands decrease in the order

[48]:

dmb (5.40) > bpy (4.30) > bqy (3.10)

Similar results were obtained for the complexes; $[Ru(bpy)(phen)(dpk)](PF_6)_2$, $[Ru(bpy)(phen)(dpa)](PF_6)_2$, $[Ru(bpy)(phen)(dzf)](PF_6)_2$ and $[Ru(bpy)(phen)(bqy)](PF_6)_2$.

An apparent anomaly involving the complex $[Ru(bpy)(phen)(dmb)](PF_6)_2$ is easily explained if steric and electronic effects are considered. The relative intensities of the fragment ions containing two ligands decrease in the order:

$$[Ru(phen)(dmb)]^+ > [Ru(bpy)(phen)]^+ > [Ru(bpy)(dmb)]^+$$

Therefore bpy is most readily lost, but the latter part of the observation indicates that the ligand dmb is lost more readily than phen even though it is more basic (pK_a of dmb=5.4 but pK_a of phen=4.9 [48]). This observation is further confirmed by the relative intensities of the other fragment ions, i.e.:

$$[Ru(bpy)]^+ > [Ru(phen)]^+ > [Ru(dmb)]^+$$

and

$$(phen+H)^+ > (dmb+H)^+$$

Similar relationships were found for complexes containing the same ligands but containing the dications Cu(II), Cd(II) and Zn(II) [48]. Solution studies of these complexes showed that the association equilibrium constant (i.e. K_3 for the reaction:

$$ML_2 + L \xrightarrow{K_3} ML_3 \quad)$$

for the complexes is always greater for phen than for dmb.

The apparent disagreement between the equilibrium constants and the ligand basicities is explained as a result of a combination of steric and electronic effects [49]. Ligands containing alkyl groups substituted on the pyridine rings are more basic because of the electron donating nature of these substituents. Therefore, in the above complex, bpy is lost more readily than dmb because the methyl groups increase the basicity of dmb relative to bpy. Ligands that are more sterically bulky and that are more easily distorted from planarity to accommodate multiple-ligand coordination, lose some resonance stabilization by adopting a non-planar configuration [49]. Therefore the ligand dmb is made less basic by coordinating along with other large and bulky ligands such as phen. The ligand phen is not affected in this manner since it is rigid and cannot bend.

Therefore the information obtained by comparing relative intensities of fragment ions in the FAB mass spectrum of $[Ru(bpy)(phen)(dmb)](PF_6)_2$ can be correlated with the known solution chemistry of the complex. Similar behaviour and correlation was found for the complexes $[Ru(phen)(dmb)(bqy)]\ (PF_6)_2$, $[Ru(bpy)(phen)(tmp)](PF_6)_2$, $[Ru(bpy)(dmb)(dib)](PF_6)_2$ and $[Ru(phen)(dmb)(dpa)]\ (PF_6)_2$.

Using the concept of inferring relative chelating powers of various ligands, with respect to ruthenium, by comparing the relative intensities of ions such as $[RuLL']^+$, $[RuLL"]^+$, $[RuL'L"]^+$, $[RuL]^+$, $[RuL']^+$, $[RuL"]^+$ and the

protonated ligand ions, an ordering of the ligands found in the complexes listed in Table 5 can be written as:

tmp > phen > dib > dmb > bpy > bqy, dpa, dpk, dzf

The final four ligands cannot be ordered relative to each other since complexes containing mixtures of these ligands were not available.

Ions corresponding to the deprotonated analogues of the ions $[RuLL'L"]^+$, $[RuLL']^+$, $[RuLL"]^+$, $[RuL'L"]^+$, $[RuL]^+$, $[RuL']^+$ and $[RuL"]^+$ were also observed for all of the complexes shown in Table 5. These were deconvoluted from the non-deprotonated analogues by using the computer program BMASABD as described previously. For simplicity the intensities of the two analogues are not shown separately in the Table, rather the values shown are the sums of the intensities of the deprotonated and non-deprotonated species.

As observed with previous series of complexes, when the ligand dpa is present in the complex, an unusually acidic proton is easily removed leaving the ligand in a more stable anionic form. Therefore the ion $[RuLL'L"]X^+$ is destabilized and the deprotonated analogues of the remaining fragment ions are dominant.

c) $[RuL_2L']X_2$ Series

The positive ion FAB mass spectrum for the complex $[Ru(bpy)_2(phen)](PF_6)_2$ is shown in Figure 16. The spectra

Figure 16. Positive Ion FAB Mass Spectrum of $[Ru(bpy)_2(phen)](PF_6)_2$.

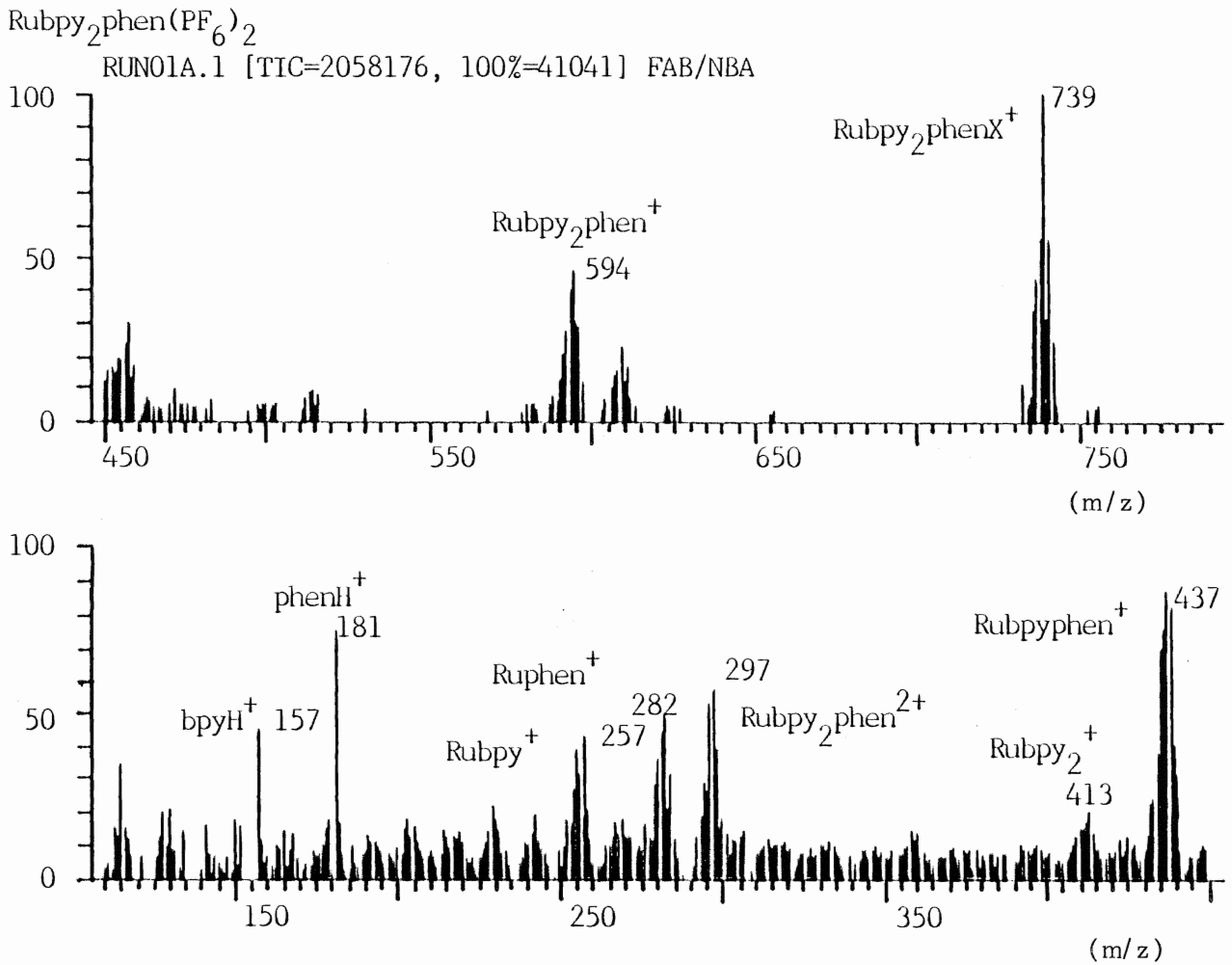
Rubpy2phen(PF6)2
RUN01A.1 [TIC=2058176, 100%=41041] FAB/NBA
100
50
0
739
Rubpy2phenX+
Rubpy2phen+
594
450
550
650
750
(m/z)
100
50
0
phenH+
181
bpyH+
157
Ruphen+
Rubpy+
257
282
297
Rubpy2phen2+
Rubpyphen+
437
Rubpy2+
413
150
250
350
(m/z)

for the complexes in this series are summarized in Table 6. Again, as for the previous series of complexes, ruthenium containing ions were identified by their isotopic patterns. The ions $[Ru(bpy)_2(phen)]^{2+}$ (m/z 297), $[Ru(bpy)_2(phen)]^+$ (m/z 594) and $[Ru[bpy)_2(phen)](PF_6)^+$ (m/z 739) were used to determine the number and type of anions present in the complex as well as its formula weight.

The presence of the ions $[Ru(bpy)(phen)]^+$ (m/z 437) and $[Ru(bpy)_2]^+$ (m/z 413) and the absence of ions such as $[Ru(phen)_2]^+$ (m/z 462) help to establish that the stoichiometry of bpy to phen is 2:1 in the intact complex.

The intensity of the ion $[Ru(bpy)(phen)]^+$ is greater than the intensity of the ion $[Ru(bpy)_2]^+$ even when taking into account the statistical abundance of the bpy ligand (i.e. there are two bpy ligands in the molecule and only one phen). Therefore the ligand bpy is lost more readily than phen. This is in agreement with the results found in the last section for the relative chelating power of the two ligands. The intensities of the fragment ions $[Ru(phen)]^+$ and $[Ru(bpy)]^+$ can also be used to deduce the difference in chelating power since the intensity of $[Ru(phen)]^+$ is greater than that of $[Ru(bpy)]^+$.

Similar behaviour is found for the remaining complexes in this series with the exception of the complex containing the ligand dpa. The effect on the FAB mass spectrum due to this ligand has been described previously.

Table 6. Positive Ion FAB Mass Spectra of $[RuL_2L']X_2$ Complexes[a]

L = bpy L' = phen	phen bpy	dmb bpy	dmb phen	bpy dpa
Fragment	Relative Intensity			
$[RuL_2L']X^+$	17.0	19.2	17.5	25.1	3.5
$[RuL_2L']^{2+}$	13.0	8.5	13.6	11.6	10.0
$[RuL_2L']^{+b}$	10.9	12.9	14.1	15.1	30.4
$[RuL_2]^{+b}$	7.1	17.4	10.9	3.6	14.6
$[RuLL']^{+b}$	22.8	11.7	15.7	26.2	9.8
$[RuL]^{+b}$	10.7	13.9	11.3	5.1	15.4
$[RuL']^{+b}$	12.6	9.2	11.8	9.3	11.3
$[LH]^+$	2.6	6.1	3.6	2.3	2.8
$[L'H]^+$	3.5	1.1	1.5	1.9	2.0

[a] Relative intensities are calculated based only on the ions listed in this table. Isotope cluster peak intensities of the same elemental composition are summed. $X=PF_6^-$

[b] includes the ion intensity due to the deprotonated analogue of this ion.

The same relative ordering of chelating powers of the ligands with respect to ruthenium was found for these complexes as was found in the previous section, i.e.:

phen > dmb > bpy > dpa

Deprotonated analogues of the ions $[RuL_2L']^+$, $[RuLL']^+$, $[RuL_2]^+$, $[RuL]^+$ and $[RuL']^+$ were again observed. As with the last series of complexes, the deprotonated and non-deprotonated species are not shown separately on Table 6.

Protonated ligand ions were observed corresponding to $(L+H)^+$ and $(L'+H)^+$. Their relative intensities correlated with their reported solution basicities and are independent of their stoichiometric occurrance in the intact complex.

d) [RuLL'(CO)Cl]X Series

The positive ion FAB mass spectrum for the complex $[Ru(bpy)(phen)(CO)Cl]PF_6$ is shown in Figure 17. Table 7 is a summary of the mass spectra for the complete series.

No doubly charged ions were observed for these complexes because the formal charge of the complex cation was +1. The highest mass ion observed in the spectrum corresponds to the complex cation $[Ru(bpy)(phen)(CO)Cl]^+$ (m/z 501). Another peak corresponding to loss of 28 mass units is due to the loss of the carbonyl group from the complex cation giving the ion $[Ru(bpy)(phen)Cl]^+$ (m/z 473).

Figure 17. Positive Ion FAB Mass Spectrum of $[Ru(bpy)(phen)(CO)Cl]PF_6$.

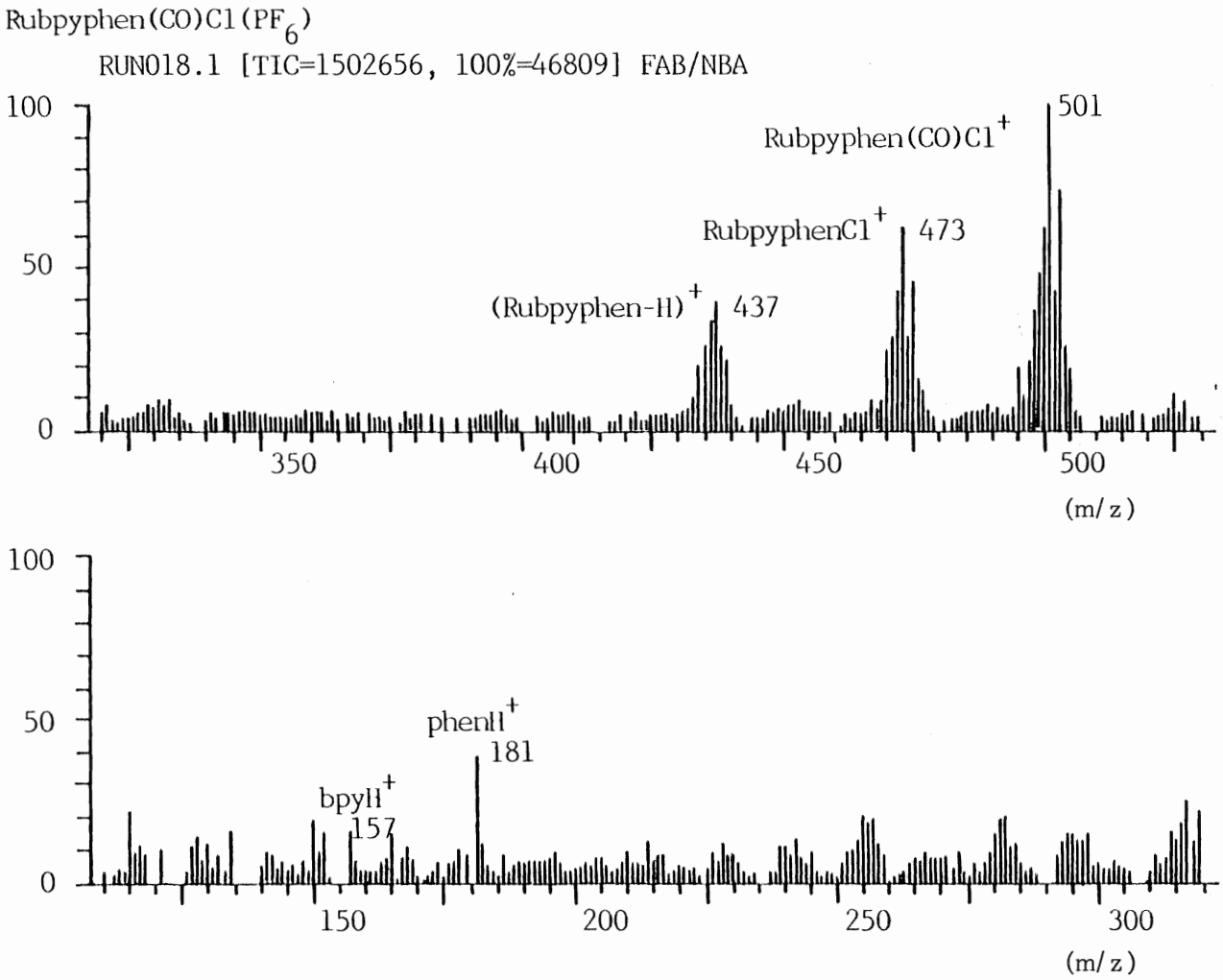
Rubpyphen(CO)Cl(PF6)
RUN018.1 [TIC=1502656, 100%=46809] FAB/NBA
100
50
0
350
400
450
500
(m/z)
(Rubpyphen-H)+
437
RubpyphenCl+
473
Rubpyphen(CO)Cl+
501
100
50
0
150
200
250
300
(m/z)
bpyH+
157
phenH+
181

Table 7. Positive Ion FAB Mass Spectra of [RuLL'(CO)Cl]X Complexes[a]

L = bpy L' = phen	bpy dmb	bpy Bq	bpy tpy
Fragment	Relative Intensity		
$[RuLL'Cl]X^+$			1.1
$[RuLL'(CO)Cl]^+$	29.6	29.9	3.7
$[RuLL'Cl]^+$	19.0	20.2	23.0	34.9
$[RuLL'(CO)-H]^+$	1.9	1.2	8.3	
$[RuLL'-H]^+$	12.7	12.8	24.3	16.6
$[RuL'(CO)Cl]^+$	4.4	3.8	4.0	
$[RuL(CO)Cl]^+$	1.4	3.0	2.5	
$[RuL'Cl]^+$	10.2	3.0	4.8	11.7
$[RuL'(CO)-H]^+$	1.2	2.0	1.9	
$[RuLCl]^+$	2.7	4.3	4.4	5.2
$[RuL(CO)-H]^+$	1.5	4.1	2.2	
$[RuL]^{+b}$	8.0	7.8	8.7	9.7
$[RuL']^{+b}$	3.0	4.1	8.2	19.0
$[LH]^+$	1.4	1.4	2.0	1.5
$[L'H]^+$	3.1	2.2	1.9	0.4

[a] Relative intensities are calculated based only on the ions listed in this table. Isotope cluster peak intensities of the same elemental composition are summed. $X=PF_6^-$

[b] includes the ion intensity due to the deprotonated analogue of this ion.

The isotopic patterns for these two fragment ions are indicative of the presence of a chlorine atom. Loss of the chlorine atom from the latter fragment probably occurs as loss of the neutral HCl accompanied by cyclometallation of the bipyridine ligand as suggested by Cerny et al. [44]. This is confirmed by the resultant fragment ion $[Ru(bpy)(phen)-H]^+$ at m/z 437.

Ions corresponding to $[Ru(bpy)]^+$, $[Ru(phen)]^+$, $(bpy+H)^+$ and $(phen+H)^+$ are useful in deducing the identities of particular ligands present in the complex. As is common for these complexes, the deprotonated forms of the fragment ions $[Ru(bpy)]^+$ and $[Ru(phen)]^+$ were also observed.

Relative chelating power of the different ligands present in each complex could be deduced by comparing relative intensities of peaks such as $[Ru\ LL'Cl]^+$, $[RuLL'(CO)]^+$, $[RuLCl]^+$ and $[RuL'Cl]^+$. It was found that the monodentate ligands were lost more readily than the bidentate ligands and that these were lost more readily than the tridentate ligand. This is related to the number of bonds that must be broken before complete fragmentation.

A full description of the fragmentations observed is shown in Scheme 2.

e) Summary

In summary then it has been shown that the FAB mass spectra are very valuable in terms of structurally

Scheme 2. Fragmentation of [RuLL'(CO)Cl]X Complexes

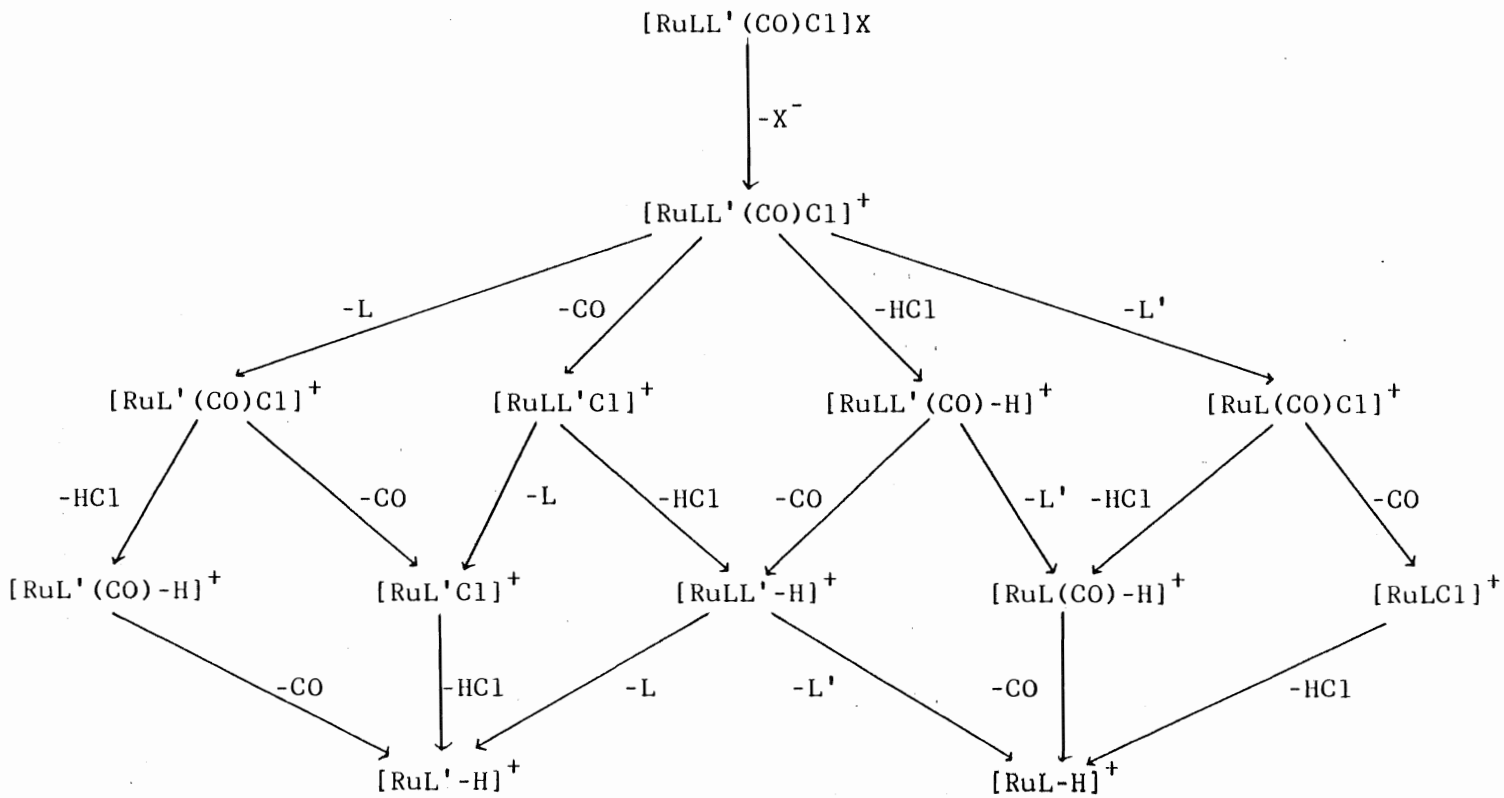

characterizing the ruthenium complexes. From the isotopic pattern and the charge of the multiply charged ion, the central metal atom and its oxidation state can be identified. From ions such as $[RuL_3]X^+$, $[RuL_3]^+$ and $[RuL_3]^{2+}$, and from the negative ion FAB mass spectrum, the number and type of anions can be determined as well as the formula weight of the complex. Ion such as $(L+H)^+$, $[RuL_3]^+$, $[RuL_2]^+$ and $[RuL]^+$ help to establish the identity and stoichiometric ratio of the ligands present in the complex.

The results obtained from the positive ion FAB mass spectrum can be correlated with the known solution chemistry of the analyte.

Relative chelating powers of the ligands can be estimated from the FAB mass spectra of the mixed complexes.

vi) Multiply Charged Ions

Observations of multiply charged ions when using the FAB technique are rare, and in the case of coordination complexes, almost completely unheard of. Only one reported observation of multiply charged ions in the FAB mass spectra of coordination complexes has been found. In a study by Bojesen [41], the ion $[Ru(bpy)_3]^{2+}$ was observed in the positive ion FAB mass spectrum of the complex $[Ru(bpy)_3](ClO_4)_2$ when analyzed using sulfolane as matrix. Another ruthenium containing complex, $[Ru(tpen)](ClO_4)_2$ (where tpen= tetrapyridyl ethylenediamine), did not produce any doubly

charged ions when analyzed as a solution in glycerol. Bojesen states that coordination complexes containing other transition metals gave no multiply charged ions, even when they contained intact polycations.

In none of the extensive studies carried out by Cerny et al. [42-44] are multiply charged ions observed. The authors propose several mechanisms including complex reduction and clustering with anions to explain their absence. Williams et al. [61] suggested that the relatively high heat of formation for polycations in the gas phase could be an explanation. It has subsequently been found that since multiply charged ions are observed in EHD [5] then the heat of formation is probably not an important factor.

This is not say that no multiply charged ions of any kind are found in FAB. Doubly charged ions were observed for some quaternary ammonium salts in FAB [62-63]. They are commonly found using other desorption techniques such as: SIMS [64], FD [65-67], EHD [5] and thermospray MS [68,69]. In general, higher abundances of doubly charged ions were found in FD [65-67] or EHD [5,70,71] than in FAB suggesting that an electric field is necessary for the extraction of ions of charge greater than +1.

In this report, all ruthenium(II) complexes containing complex dications gave spectra containing a doubly charged ion. That these ions were correctly

identified as the doubly charged species was established by the presence of peaks at half-integer mass/charge units and by the fact that they appear in the mass spectrum in a position that is one-half that expected for the singly charged species. The isotopic patterns observed for the doubly charged ions were very similar to those expected by theory. As an example, the mass spectrum of the complex $[Ru(dmb)_2(phen)](PF_6)_2$ is shown in Figure 18. Below this in the Figure is a composite diagram of the expanded mass range, from the top spectrum, where the doubly charged ion was observed, overlaid with the theoretical isotopic pattern for that ion obtained from the program BMASROS. As is clearly shown by this diagram, differences between theoretical and observed are small.

Doubly charged ions were observed only when the analysis was performed using 3-NBA as matrix. Analyses in other matrices including thioglycerol, glycerol and 30% glycerol in sulfolane gave spectra containing no doubly charged ions. Analysis in sulfolane only, while difficult because of the short lived spectrum, did give doubly charged ions; however, they were poorly defined. Therefore, while one might argue that the $[RuL_3]^{2+}$ ions could arise from simple dissociation of the complex in solution, the fact that they are not observed in other matrices is evidence that dissociation is not a major factor in their production. The matrix itself must have some effect.

Figure 18. top: Positive Ion FAB Mass Spectrum of $[Ru(dmb)_2(phen)](PF_6)_2$
bottom: Comparison of Observed and Theoretical Isotopic Patterns for the $[Ru(dmb)_2(phen)]^{2+}$ Ion.

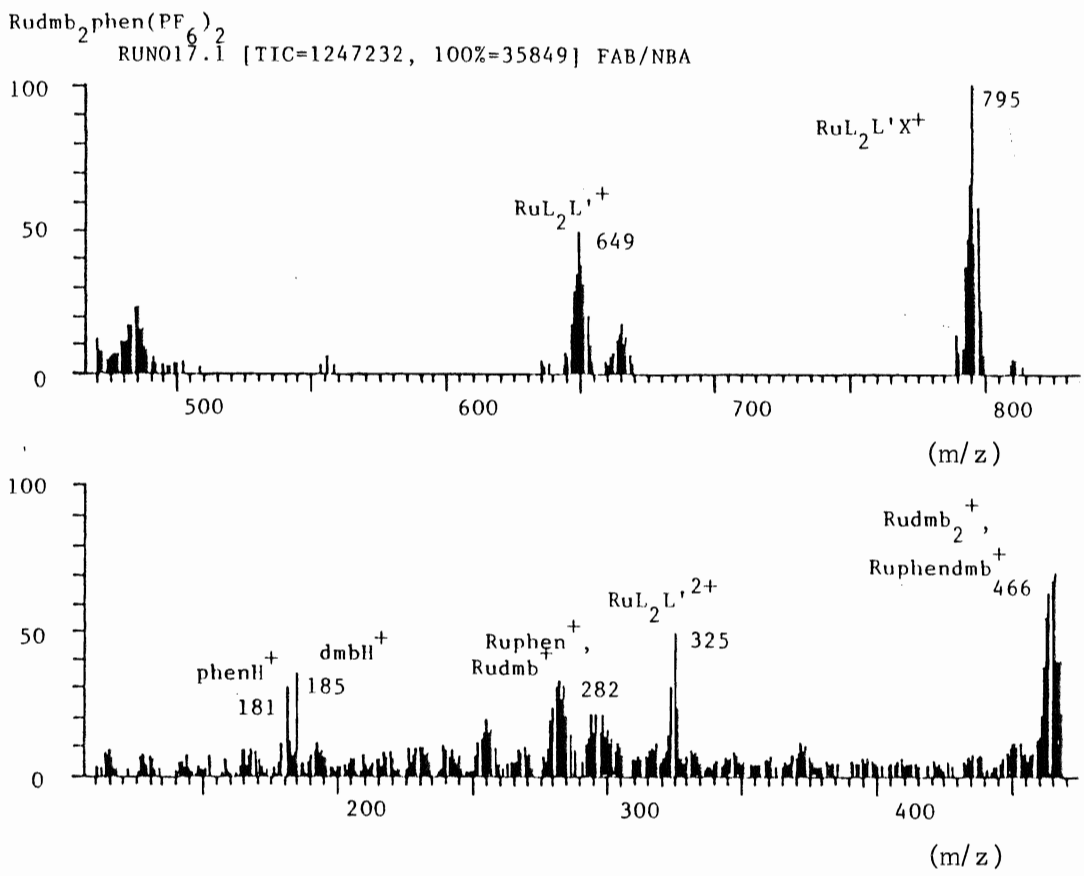
Rudmb2phen(PF6)2
RUN017.1 [TIC=1247232, 100%=35849] FAB/NBA
100
50
0
500
600
700
800
(m/z)
RuL2L'X+
795
RuL2L'+
649
100
50
0
200
300
400
(m/z)
Rudmb2+,
Ruphendmb+
466
RuL2L'2+
325
Ruphen+,
Rudmb+
282
dmbH+
185
phenH+
181

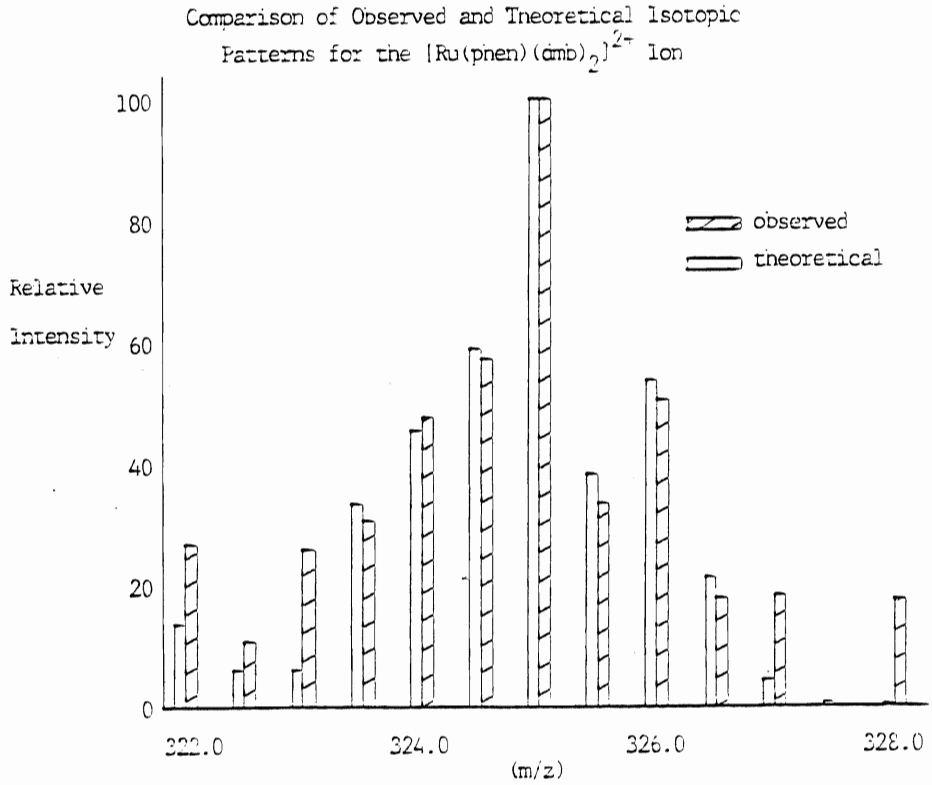
Comparison of Observed and Theoretical Isotopic
Patterns for the [Ru(phen)(dmb)2]2+ Ion
Relative
Intensity
100
80
60
40
20
0
322.0
324.0
326.0
328.0
(m/z)
observed
theoretical

The FAB mass spectra of other transition metal containing complexes do not contain multiply charged ions. The complexes $[Fe(bpy)_3]X_2$, $[Fe(phen)_3]X_2$, $[Co(bpy)_3]X_2$ and $[Ni(bpy)_3]X_2$ (where X= ClO_4^-) gave no indication of the presence of doubly charged ions when analyzed in the matrix 3-NBA. Therefore, a second major factor in the appearance of mutiply charged ions must be the nature of the central metal ion.

To confirm the importance of the matrix, an experiment was conducted in which the intensity ratio of doubly to singly charged $[Ru(bpy)_3]^{n+}$ was monitored as a function of increasing 3-NBA concentration. The complex $[Ru(bpy)_3]Cl_2$ was dissolved in glycerol, a matrix in which it was known that doubly charged ions were not produced. Appropriate dilutions were prepared with 3-NBA and glycerol such that the concentration of the ruthenium complex was always the same. The dilutions were analyzed via FAB and, using the same operating conditions for each dilution, the intensity ratio $[Ru(bpy)_3]^{2+}/[Ru(bpy)_3]^{+}$ was calculated. The results are presented in Figure 19. The plot shows that the amount of doubly charged ion relative to the singly charged analogue, increases from zero when no 3-NBA was present to a maximum when the solution consisted of only 3-NBA as solvent. Therefore 3-NBA is a necessary element in the production of ruthenium containing doubly charged ions.

The absence of multiply charged ions in some

Figure 19. Effect of Addition of 3-NBA to a $[Ru(bpy)_3]Cl_2$ Solution on the Intensity Ratio of Doubly Charged to Singly Charged M = $[Ru(bpy)_3]^{n+}$.

Effect of the Addition of 3-NBA to a $Ru(bpy)_3Cl_2$ Solution on the Intensity Ratio of Doubly Charged to Singly Charged $M = Ru(bpy)_3^{n+}$

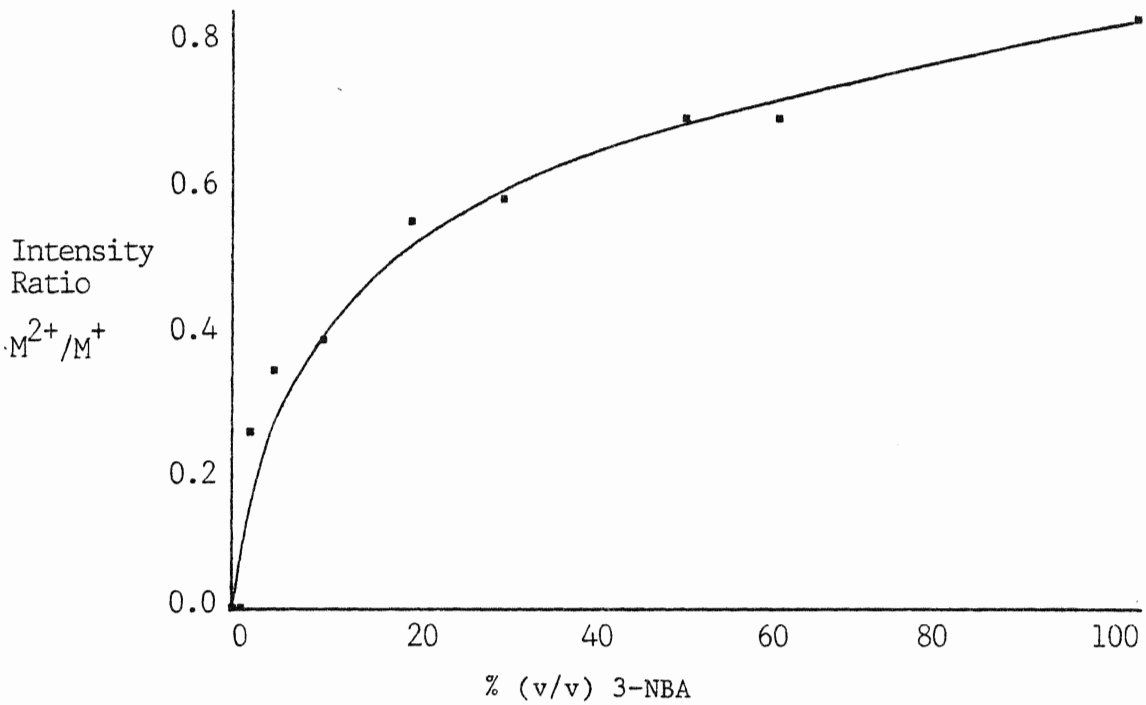

matrices and for some transition metal centers argues for a more complex mechanism of formation. We propose a mechanism that exploits the known photochemical activity of ruthenium complexes and the ability to quench these complexes by some nitroaromatic molecules.

Ruthenium(II) polypyridyl complexes are best known for their ability to photochemically split water into H_2 and O_2. These reactions occur, of course, for the complex in the excited state [47]. In FAB, deposition of large amounts of energy by the incident atom beam into the matrix/analyte solution might perform the same function as light energy on these complexes, that is to convert the complex into its excited state:

$$[RuL_3]^{2+} \longrightarrow {}^*[RuL_3]^{2+} \qquad (A)$$

Nitroaromatic compounds are known to oxidatively quench the excited state of Ru(II) [47]. Therefore 3-nitrobenzyl alcohol, being a nitroaromatic, may also be involved in such a quenching reaction.

The first step in the reaction is the formation of an excited molecule/quencher pair followed by an electron transfer between the pair:

$$ {}^*[RuL_3]^{2+} + A \longrightarrow {}^*[RuL_3]^{2+}\cdot A \longrightarrow [RuL_3]^{3+}\cdot A^- \qquad (B)$$

Where "A" is the quencher, or in this case 3-NBA, the solvent. The ion pair thus formed is caged inside other solvent molecules. In the presence of an electron source such as may exist in FAB [24,25], the caged pair can

separate into two ionic entities:

$$[RuL_3]^{3+}\cdot A^- \xrightarrow{e^-} [RuL_3]^{2+} + A^- \quad (C)$$

A check on the mechanism by monitoring an increase in the A^- ion abundance in the mass spectrum is not expected to be successful. Since A^- is also the molecular ion of the matrix, which is present in a large excess (compared to the ruthenium complex), no significant change will be visible in the spectrum.

Interestingly, reaction (C) may not necessarily proceed as shown. The reaction of $^*[Ru(bpy)_3]^{2+}$ oxidatively quenched with methylviologen (MV^{2+}) does not proceed exclusively as in (C). Excluding the electron source, the reaction is expected to yield $[RuL_3]^{3+}$ and MV^+. However, it has been found that about 80% of the caged pairs undergo a back electron transfer that regenerates the starting ions, i.e. $[RuL_3]^{2+}$ and MV^{2+} [72]. The energy converted in the process is dissipated as heat. Therefore, assuming the same process is in effect for the ruthenium complexes and 3-NBA, the doubly charged ion may be regenerated and when sputtered into the mass spectrometer analysed as such. One electron reductions and back electron transfers that are not successful would yield the singly charged species.

The mechanism proposed above can also be used to explain the observations described above. No doubly charged ions were produced for complexes containing other transition metals because they lack similar photochemical behaviour, or

if they do possess photochemical abilities then they are not quenched in the same manner by nitroaromatic compounds. No doubly charged ions were observed for other matrices because they do not quench the excited state of Ru(II) in the same manner as nitroaromatics. Doubly charged ions were observed using sulfolane because it is an oxidizing matrix, as is 3-nitrobenzyl alcohol. Therefore it might also oxidatively quench the excited state of Ru(II).

vii) Use of the Technique to Identify Components in a Mixture

Bojesen reports [41] that the spectrum obtained from a mixture of the two complexes $[Ru(pic)_4Cl_2]Cl$ and $[Rh(py)_4Cl_2]Cl$, (where pic= 2-methyl pyridine, py= pyridine), contained no ions that could be attributed to a ligand exchange reaction. Ions resulting from such a reaction would contain a mixture of the two ligands along with either transition metal. No ions such as these were observed. Bojesen suggests that the absence of ligand exchange may be due to the relatively high binding constants of nitrogenous ligands.

In a study reported by Tkatchenko et al. [36], ligand exchange between the complexes $[(C_4H_7)Pd(PBu_3)_2]\ PF_6$ and $[(C_4H_7)Pd(tmtu)_2]PF_6$ (where tmtu= tetramethyl thiourea), was observed. Ligand exchange yields the species $[(C_4H_7)Pd(PBu_3)(tmtu)]^+$. These results are not conflicting

with those of Bojesen since the binding constants of ligands such as PBu_3 and perhaps tmtu are expected to be lower. Therefore, complexes containing these ligands fragment more readily and can recombine to produce the exchanged species.

Included in the group of ruthenium(II) coordination complexes were two samples that were mixtures of complexes. One of these was labelled as such and therefore was known to be a mixture. The second sample was labelled as a pure complex. Upon analysis, however, extra peaks were observed in the mass spectrum which were subsequently identified as being due to a second species.

The first sample was labelled as a mixture of the complexes $[Ru(phen)_3](PF_6)_2$ and $[Ru(bpy)_2(dpa)](PF_6)_2$. Both of these complexes were available in relatively pure form, therefore the spectrum of each of these was known. The FAB spectrum obtained for the mixture is shown in Figure 20. Included are the spectra obtained for the pure complexes. As can be seen, all peaks contained in the mixture spectrum (bottom of Figure 20) can be found in either of the two pure complex spectra (top and middle of Figure 20). No peaks due to species formed from ligand exchange were observed. These should be readily visible. For example exchange of one phen in the tris-phen complex for a bpy ligand would give the ion, $[Ru(phen)_2(bpy)]^+$ at m/z 618. This ion is not contained in the mixture spectrum. Since the ligands contained in the ruthenium complexes are of the same type as used in the

Figure 20. $[Ru(phen)_3](PF_6)_2$ and $[Ru(bpy)_2(dpa)](PF_6)_2$

top: Positive Ion FAB Mass Spectrum of Pure $[Ru(phen)_3](PF_6)_2$

middle: Positive Ion FAB Mass Spectrum of Pure $[Ru(bpy)_2(dpa)](PF_6)_2$

bottom: Positive Ion FAB Mass Spectrum of the Mixture.

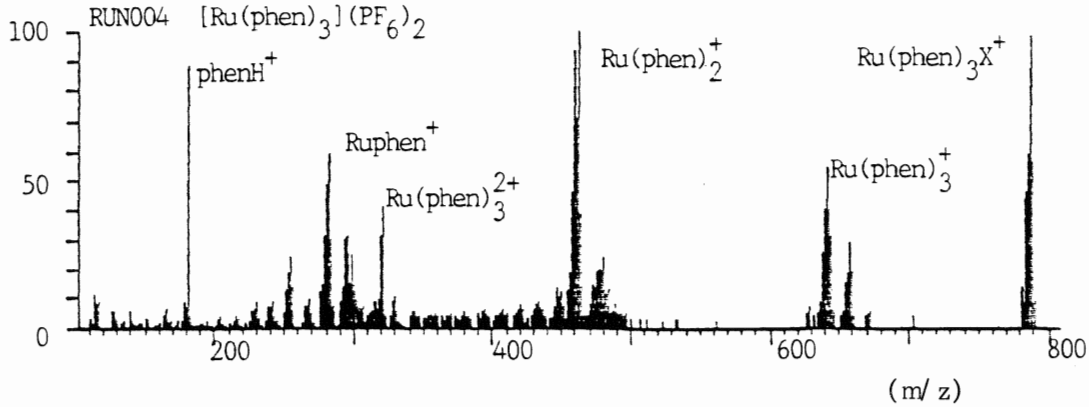
RUN004 [Ru(phen)3](PF6)2
100
50
0
phenH+
Ruphen+
Ru(phen)3 2+
Ru(phen)2+
Ru(phen)3+
Ru(phen)3X+
200
400
600
800
(m/z)

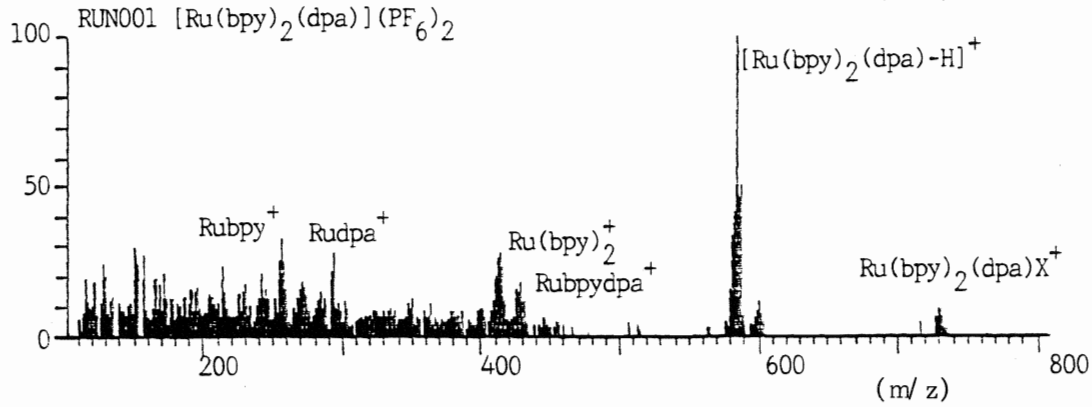
RUN001 [Ru(bpy)2(dpa)](PF6)2
100
50
0
Rubpy+
Rudpa+
Ru(bpy)2+
Rubpydpa+
[Ru(bpy)2(dpa)-H]+
Ru(bpy)2(dpa)X+
200
400
600
800
(m/z)

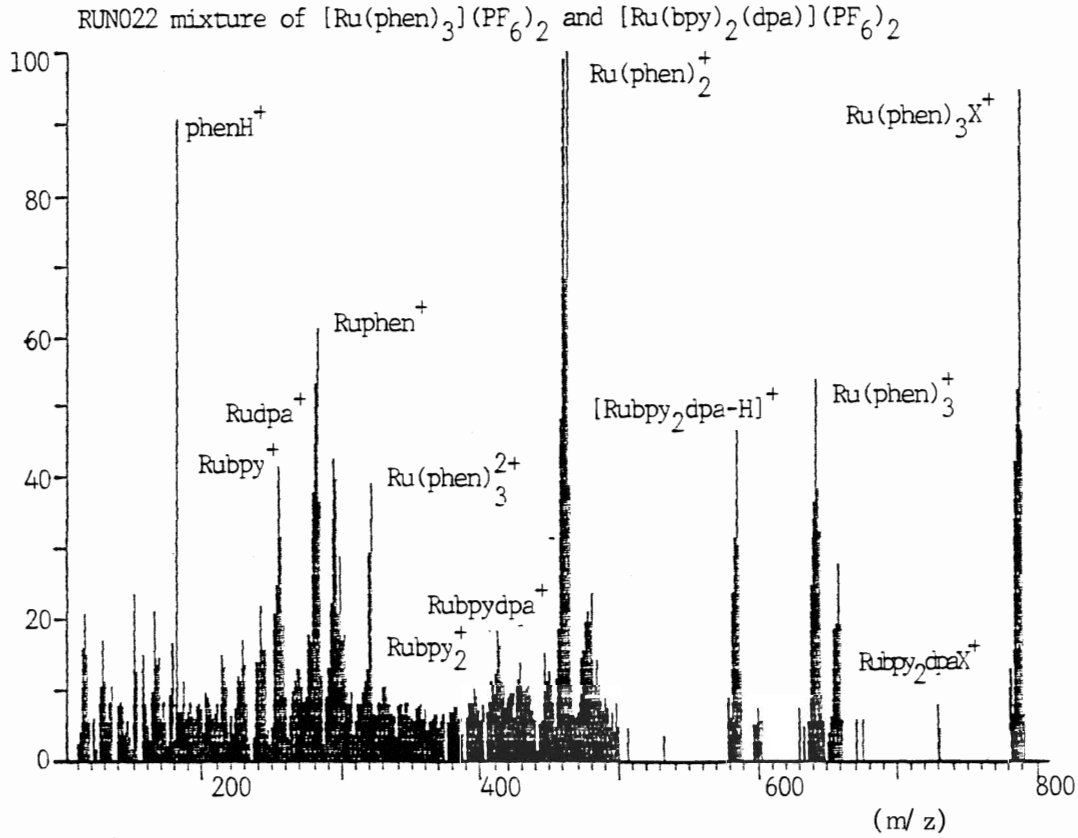
RUN022 mixture of [Ru(phen)3](PF6)2 and [Ru(bpy)2(dpa)](PF6)2
100
80
60
40
20
0
phenH+
Ruphen+
Rudpa+
Rubpy+
Ru(phen)3 2+
Rubpydpa+
Rubpy2+
Ru(phen)2+
[Rubpy2dpa-H]+
Ru(phen)3+
Ru(phen)3X+
Rubpy2dpaX+
200
400
600
800
(m/z)

Bojesen study, then these results confirm his observations.

While it is not possible to determine absolute quantities of each complex in the mixture, it is possible to estimate relative quantities. The ions due to the complex $[Ru(phen)_3](PF_6)_2$ are all of higher abundance than the corresponding ions due to the other complex. Therefore there is more of the tris-phenanthroline complex present in the mixture than of the other complex.

Relative intensities of peaks arising from the same complex in the mixture spectrum are in close agreement with those found in the pure complex spectrum. Table 8 is a summary of the spectra for the complex $[Ru(phen)_3](PF_6)_2$ in both the mixture and in the pure form. Deviations between relative peak intensities (expressed as a % of the total positive ion current for the ions listed in the Table) are very low and average to zero. This suggests that formation of particular ions in the mixture is unaffected by the presence of ions from another complex and reinforces the conclusion that ligand exchange does not occur.

The second sample was labelled as containing only the complex $[Ru(bpy)(dmb)(dib)](PF_6)_2$. Another sample vial was labelled with this designation, yet it gave a very different mass spectrum (Figure 21). Comparison of the two, and consideration of the peaks contained therein, showed that there were peaks in the former sample that could not be described as having come from the labelled complex. These

Table 8. Comparison of Positive Ion FAB Mass Spectrum for $[Ru(phen)_3](PF_6)_2$ as a Pure Complex and as a Mixture

species	Relative Intensity Pure Complex*	Mixture§	Deviation
$[Ru(phen)_3]X^+$	22.9	19.7	-3.2
$[Ru(phen)_3]^{2+}$	9.3	9.7	0.4
$[Ru(phen)_3]^+$	17.0	16.1	-0.9
$[Ru(phen)_2]^+$	30.3	31.1	0.8
$[Ru(phen)]^+$	14.7	17.2	2.5
$(phen+H)^+$	5.7	6.1	0.4
		average deviation	0.0

* data taken from Table 4.

§ extracted from RUN022

Figure 21. $[Ru(bpy)(dmb)(dib)](PF_6)_2$ and $[Ru(dmb)_2(dib)](PF_6)_2$

top: Positive Ion FAB Mass Spectrum of the Mixture

bottom: Positive Ion FAB Mass Spectrum of Pure $[Ru(bpy)(dmb)(dib)](PF_6)_2$.

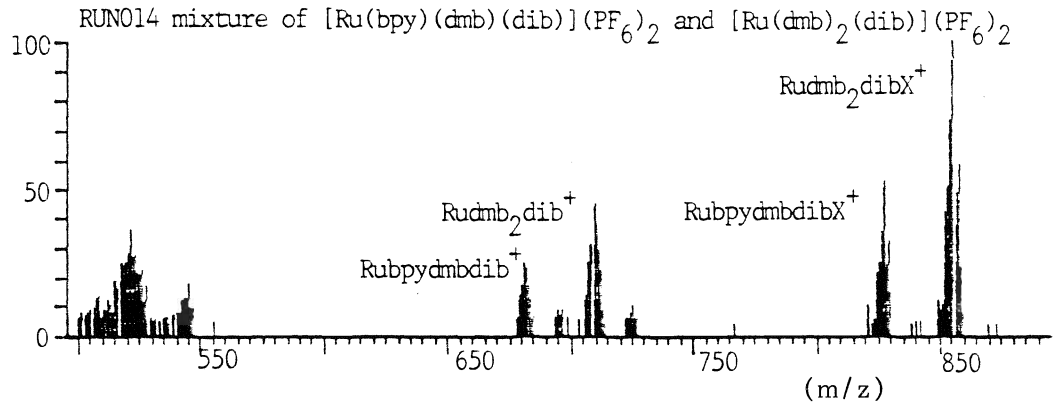
RUN014 mixture of [Ru(bpy)(dmb)(dib)](PF6)2 and [Ru(dmb)2(dib)](PF6)2
100
50
0
Rudmb2dibX+
Rudmb2dib+
RubpydmbdibX+
Rubpydmbdib+
550
650
750
850
(m/z)

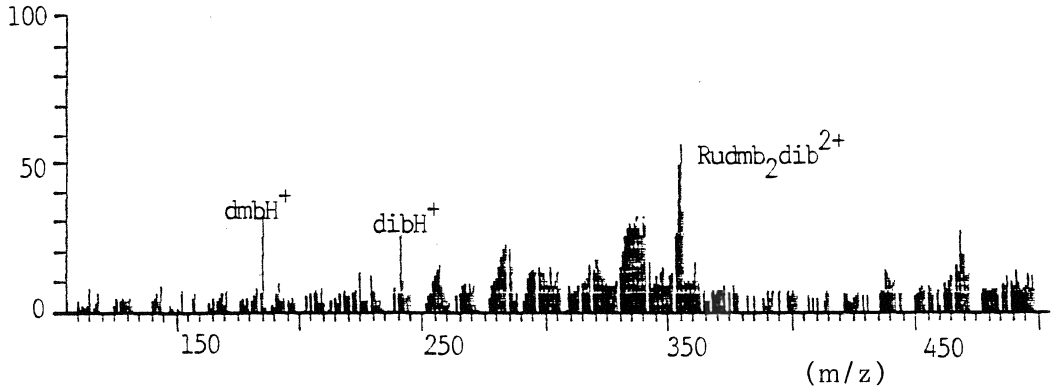
100
50
0
Rudmb2dib2+
dmbH+
dibH+
150
250
350
450
(m/z)

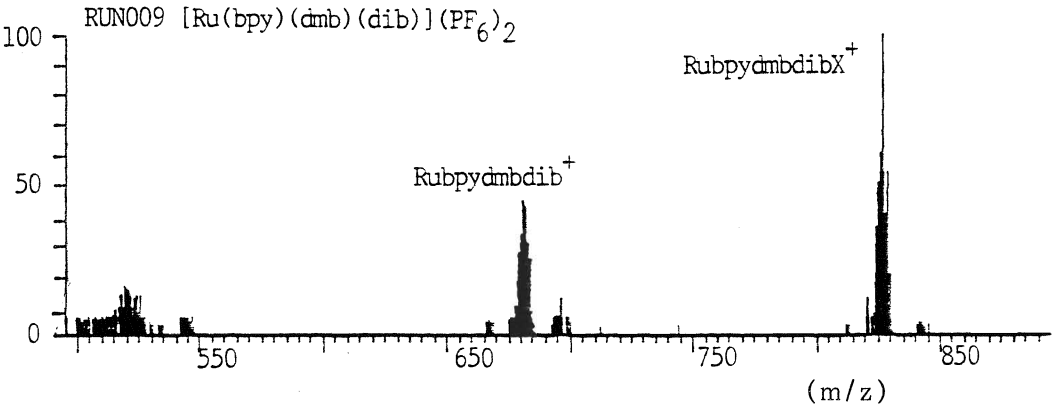
RUN009 [Ru(bpy)(dmb)(dib)](PF6)2
100
50
0
RubpydmbdibX+
Rubpydmbdib+
550
650
750
850
(m/z)

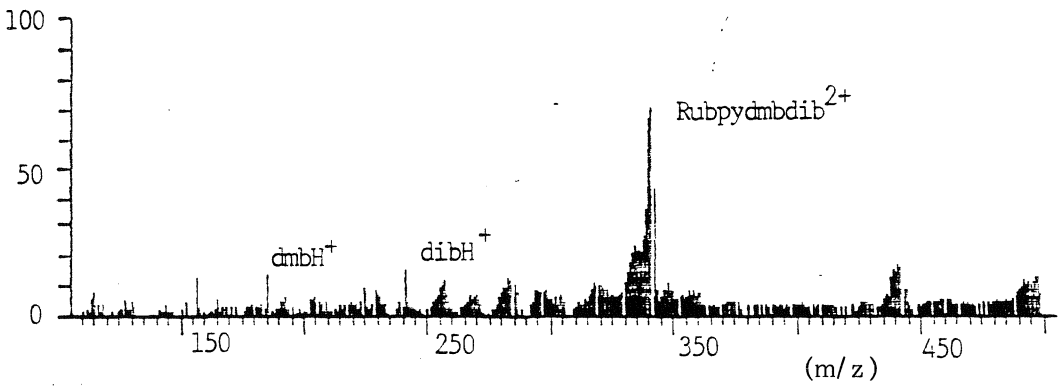
100
50
0
Rubpydmbdib2+
dmbH+
dibH+
150
250
350
450
(m/z)

extra peaks were, however, from their characteristic isotopic pattern, due to ruthenium containing ions. Careful consideration of all logical possibilities arising from the reaction from which these complexes were synthesized, lead to the conclusion that the extra peaks were due to the presence of the complex $[Ru(dmb)_2(dib)](PF_6)_2$. Comparative peak abundances indicated that there was more of this complex in the mixture than of the labelled complex. The possibility of ligand exchange from the labelled complex to form the second complex was discounted by the results found for the first complex.

Therefore, it has been demonstrated that, in agreement with Bojesen [41], complexes containing polypyridyl ligands do not undergo ligand exchange reactions during FAB analysis. The technique is extremely useful, therefore, in separating components in a mixture so that a complete identification can be made.

2. Group V Triptycenes and Related Complexes

i) Introduction

A group of related organometallic derivatives of Group V were analyzed using both electron impact (EI) and fast atom bombardment (FAB) for providing mass analyzable species. The complexes, as listed in Table 2, can be divided into three different series. These are: $M(C_6H_4Cl)_3$ where M=P, As, Sb and Bi; $M(C_6F_4X)_3$ where X=Br for M=P, As and Sb and X=H for M=As; $MM'(C_6F_4)_3$ where M=P for M'=P and Sb, M=As for M'=As and Sb and M=M'=Sb and Bi. Only the last series of complexes are true triptycenes as shown in Figure 6 (bottom). The second series of complexes are intermediates or by-products of the reaction taken to synthesize the triptycenes. The first series is related to the others in that the central metal atom is three coordinate, with the coordinating groups being aromatic rings. Two complexes were included containing a Group IV metal atom. However, the central metal atom is still three coordinate with respect to the aromatic rings. These complexes are: $CH_3Si(C_6F_4Br)_3$ and $(CH_3Si)_2(C_6F_4)_3$. Therefore they fall within the series $M(C_6F_4X)_3$ and $MM'(C_6F_4)_3$ respectively.

The positive ion FAB and EI spectra for the complexes are shown in Appendix B. Acompanying the discussion for each series of complexes is a single

representative example of the FAB and EI spectra for that series. The EI spectra were obtained under the conditions as outlined in the Experimental section as were the FAB spectra. No matrix optimization experiment was performed as only the matrix sulfolane gave useful results.

Included in the discussion for each series is a Table partially summarizing the positive ion mass spectra for all the complexes in that series. Values given in the Tables are expressed as a percentage of the total positive ion current. Only important ions were included, therefore the relative intensities may not sum to 100%. Other ions present in the spectra, but not shown in the Tables, arise from minor decompositions, matrix adducts in FAB and from other background peaks. For comparative purposes, relative intensities were summed over the isotopic peak cluster where appropriate. Metal containing and other non-metal containing ions were separated in the Tables, for clarity. Overlapping peak multiplets were deconvoluted using the computer program BMASABD, as explained in the Experimental section.

ii) Formation Mechanism of the Molecular Ion in FAB

FAB analysis is best suited to complexes that have large dipole moments or that are ionic since these are requirements for good dissolution in the polar matrices normally used in FAB. The ions produced from these

complexes are removed from the matrix/analyte surface into the gas phase via sputtering by bombarding atoms. In general, involatile, neutral molecules, lacking protonation sites and having large molecular weights are analyzed by FAB only with great difficulty. It has been suggested, however, that if a molecule can be presented to the incoming fast atom beam in the gas phase then it may be ionized by colliding with a fast atom in a manner similar to electron impact [74-78]. Therefore a spectrum is obtained that is similar to that obtained by EI.

The organometallic complexes studied in this part of the thesis are relatively involatile under the conditions encountered in FAB. On heating, they do provide good EI mass spectra. The complexes are also relatively non-polar and therefore do not dissolve well in any polar matrix. Therefore they might be expected to give poor FAB mass spectra. In fact, extremely poor results were obtained using most of the available matrices in our laboratory. Very good spectra were obtained, however, when using the matrix sulfolane. Moreover, the molecular ion was observed in all of the spectra with good intensity except for those complexes that were inherently unstable due to weak interatomic bonding.

It is suggested, therefore, that the use of the volatile matrix sulfolane was responsible for the good results obtained by FAB. When using sulfolane as a matrix

it is normally expected that only a few scans can be collected due to rapid evaporation of the matrix. Thus, it is possible that along with evaporating matrix molecules, some analyte molecules can be carried or sputtered into the gas phase. These then could be ionized by collisions with the incoming fast atom beam or perhaps with other species formed from the matrix.

Further evidence of this process is found in the similarity of the EI and FAB mass spectra. Also, the molecular ion is generally in greater abundance in the FAB mass spectrum reflecting the relatively "softer" nature of a bombarding atom as opposed to an electron.

iii) Tris(2-chlorophenyl) Derivatives [$M(C_6H_4Cl)_3$, M=P, As, Sb and Bi]

Figure 22 is an example of the positive ion FAB and EI mass spectra obtained for this series of complexes, shown for the complex $P(C_6H_4Cl)_3$. Table 9 summarizes the results obtained for the remaining complexes. Scheme 3 helps to explain the fragmentations and rearrangements observed.

The molecular ion, ($[P]^{+\cdot}$), was observed as the base peak (m/z 364) in both spectra. This ion is observed for all complexes but decreases in intensity in the order:

P > As > Sb > Bi

This reflects the increasing weakening of the metal-carbon bond as one goes down Group V until bismuth which is

Figure 22. Positive Ion FAB and EI Mass Spectra of 2-chlorophenyl Derivative of Phosphorus $P(C_6H_4Cl)_3$.

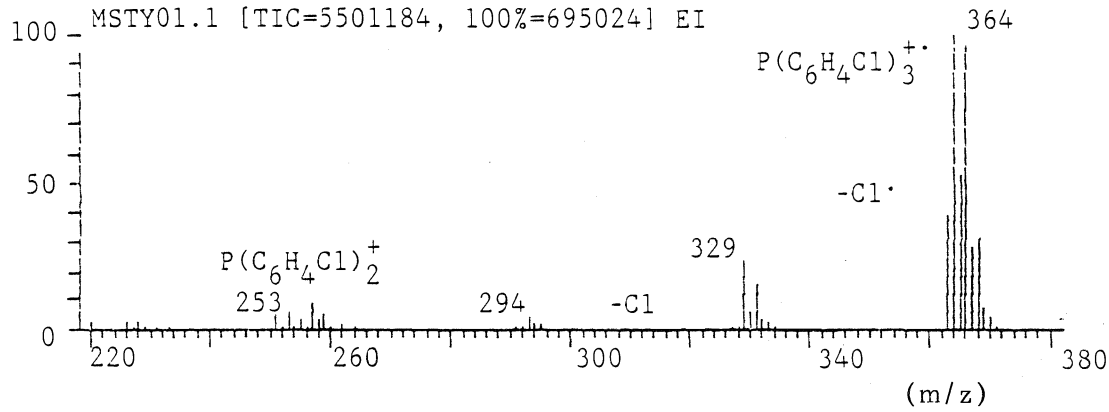
MSTY01.1 [TIC=5501184, 100%=695024] EI
100
50
0
364
$P(C_6H_4Cl)_3^{+\cdot}$
-Cl·
329
$P(C_6H_4Cl)_2^+$
253
294
-Cl
220
260
300
340
380
(m/z)

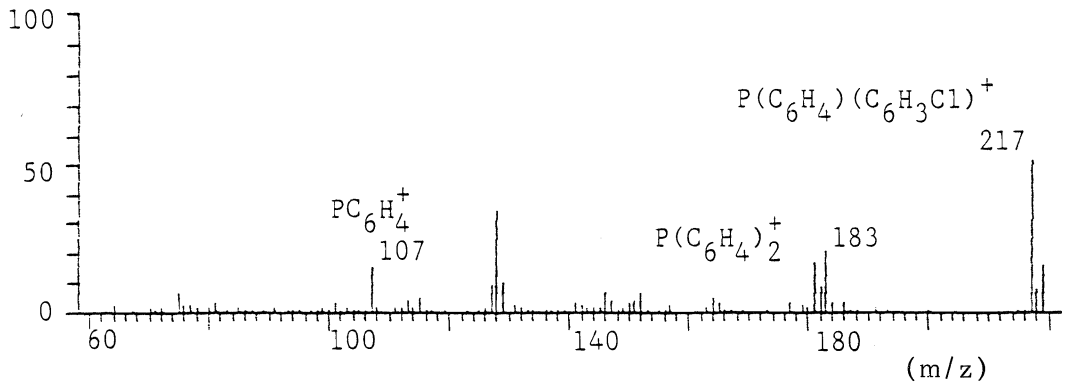
100
50
0
$P(C_6H_4)(C_6H_3Cl)^+$
217
$PC_6H_4^+$
107
$P(C_6H_4)_2^+$
183
60
100
140
180
(m/z)

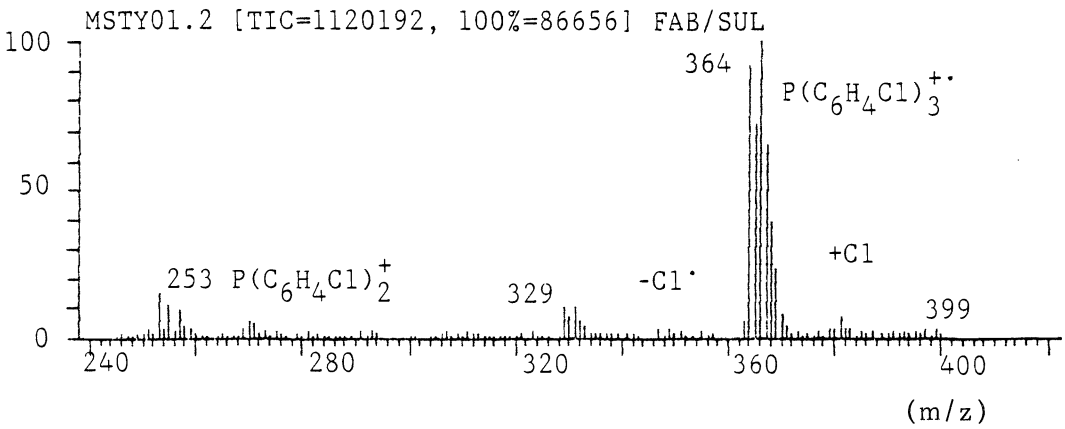
MSTY01.2 [TIC=1120192, 100%=86656] FAB/SUL
100
50
0
364
$P(C_6H_4Cl)_3^{+\cdot}$
+Cl
253 $P(C_6H_4Cl)_2^+$
329
-Cl·
399
240
280
320
360
400
(m/z)

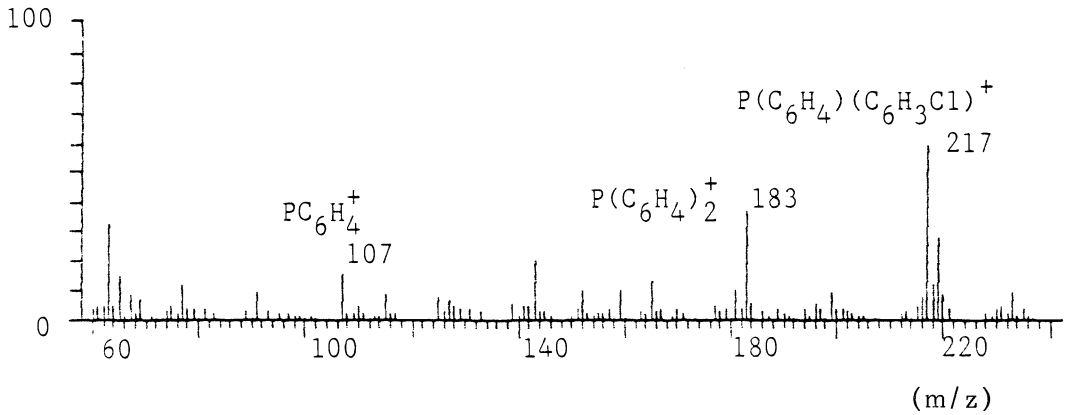
100
0
$P(C_6H_4)(C_6H_3Cl)^+$
217
$PC_6H_4^+$
107
$P(C_6H_4)_2^+$
183
60
100
140
180
220
(m/z)

Table 9. Partial Positive Ion FAB and EI Mass Spectra of $M(C_6H_4Cl)_3$ Complexes

M=	Relative Intensity							
	P		As		Sb		Bi	
	EI	FAB	EI	FAB	EI	FAB	EI	FAB
metal-containing ions								
$P^{+\cdot}$	32.4	23.5	23.5	25.4	15.5	14.7	0.3	2.0
$(P+Cl)^+$		0.3		1.1		1.1		
$(P-Cl)^+$	6.4	3.0	0.6	0.9		0.9		0.8
$(P-H)^+$	13.2	8.1				3.2		
$M(C_6H_4Cl)_2^+$	1.5	3.3	5.0	7.7	8.0	8.1	12.5	34.1
(" $-H)^+$								
(" $-H_2)^+$	1.9	0.5		0.5				
(" $-Cl)^+$		0.7	0.2	0.4		0.4	0.1	0.4
(" $-Cl_2)^+$	3.0	3.3	2.0	2.2	0.9	3.1		
(" $-HCl)^+$	9.9	7.8	20.1	16.9	24.7	19.0	5.6	4.3
$MC_6H_4Cl^+$	0.8	2.3	10.2	1.8	11.6	5.4	20.5	15.6
(" $-Cl)^+$	2.1	1.4	6.1	3.0	0.3	0.2		
M^+	-	-	1.3	0.6	0.3	0.2	22.3	12.6
non-metal containing ions								
$(C_6H_4)_2^+$	0.9	0.9	2.9	1.8	8.0	4.3	17.0	7.1
$(C_6H_4)(C_6H_3Cl)^+$	0.5	0.7	12.2	4.1	6.3	1.7	3.4	0.7
$(C_6H_4)^+$	0.5	1.1	1.0	1.0	1.1	1.2	1.2	0.9

Scheme 3. Fragmentation of $M(C_6H_4Cl)_3$ Complexes

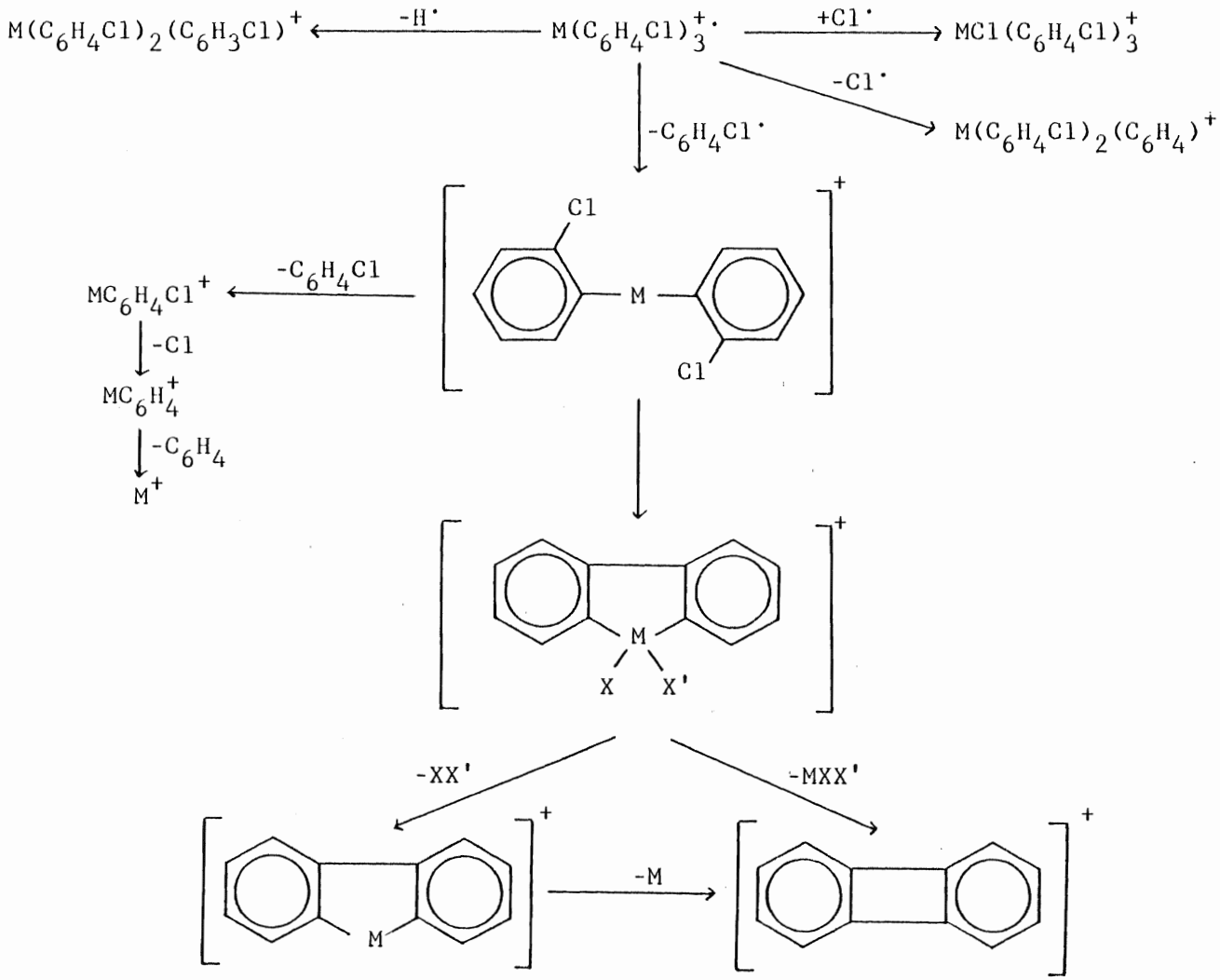

expected to have the weakest metal-carbon bond [58]. This is in fact observed. When M=Bi, the base peak in the spectra is the ionized metal atom, Bi^+.

Chlorine addition to the molecular ion was observed, but only in FAB, suggesting that it is a solution process involving chlorine radicals present due to fragmentations that will be described below. $(P+Cl)^+$ was observed at m/z 399 in Figure 22. This ion is present in very low abundance, therefore it is a minor process.

Fragmentations of the molecular ion involve radical losses such as:

$$M(C_6H_4Cl)_3^{+\cdot} \longrightarrow M(C_6H_4Cl)_2(C_6H_3Cl)^+ + H^\cdot$$

$$M(C_6H_4Cl)_3^{+\cdot} \longrightarrow M(C_6H_4Cl)_2(C_6H_4)^+ + Cl^\cdot$$

Chlorine radical loss is favoured over hydrogen radical loss except when M=P. Multiple chlorine loss was observed only for the phosphorus derivative.

The major mode of radical loss from the molecular ion was loss of an intact ring system, i.e. $(C_6H_4Cl^\cdot)$. This loss yields an ion whose structure is as in (I):

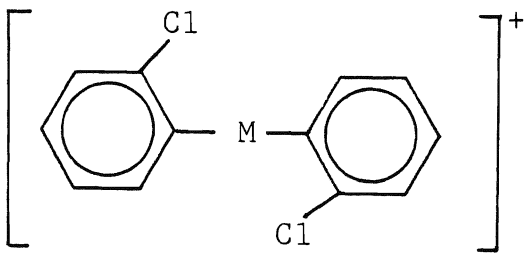

(I)

Steric requirements force the two chlorine substituents to be as far away from each other as possible. Miller and

others [49 and references contained therein] have suggested that a better representation for this ion is as shown in (II):

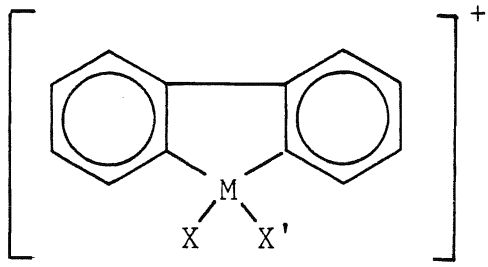

(II)

Formation of (II) involves a rearrangement requiring migration of ring substituents (either halogen or hydrogen in this case) to the central metal atom. The identities of X and X' are not specified in (II) since they can conceivably be one of: X=X'=H, X=X'=Cl or X=H and X'=Cl. The latter combination seems most likely considering that the chlorines are probably situated on opposite sides of the metal atom in (I) which is the precursor. This is confirmed in that loss of HCl from $M(C_6H_4Cl)_2^+$ is the dominant loss as shown by the relatively high intensities of the ion $M(C_6H_3Cl)(C_6H_4)^+$ as listed in Table 9. The other combinations of X and X' are also possible, but to a much smaller extent. Losses of H_2 and Cl_2 were observed, but with much smaller relative intensities.

Appearance of the ion $MC_6H_4Cl^+$ is best explained as originating from fragmentation of the ion of structure (I) rather than (II).

In both FAB and EI, intensities of the ions

$M(C_6H_4Cl)_2^+$ and $M(C_6H_4Cl)^+$ both decrease in the order:

Bi > Sb > As > P

This again is in agreement with the expected metal-carbon bond weakening as one goes down Group V. These two ions are related to each other by structure (I). An analogous bond weakening is observed for structure (II) by an increase in the intensity of the biphenylene ion (i.e. $(C_6H_4)_2^+$) in the same order:

Bi > Sb > As > P

Biphenylene is formed from (II) by consecutive loss of XX' followed by M or simply by loss of MXX'.

Therefore fragmentation of the tris(2-chlorophenyl) derivatives of Group V involves radical losses from the molecular ion. A rearrangement of the ion containing two ring systems might occur but not exclusively so. Fragmentations are related to metal-carbon bond strengths and reflect the weakening bonding expected as one goes down the Group V periodic row. Scheme 3 gives a complete summary.

iv) Tris(2-bromotetrafluorophenyl) Derivatives $[M(C_6F_4Br)_3$, M=P, As, Sb and $CH_3Si]$ and the Tris(3,4,5,6-tetrafluorophenyl) Derivative of As $[As(C_6F_4H)_3]$

The positive ion FAB and EI mass spectra of $Sb(C_6F_4Br)_3$ are shown in Figure 23. These, and the spectra of the remaining complexes are partially summarized in

Figure 23. Positive Ion FAB and EI Mass Spectra of Tris(2-bromotetrafluorophenyl) Derivative of Antimony

$Sb(C_6F_4Br)_3$.

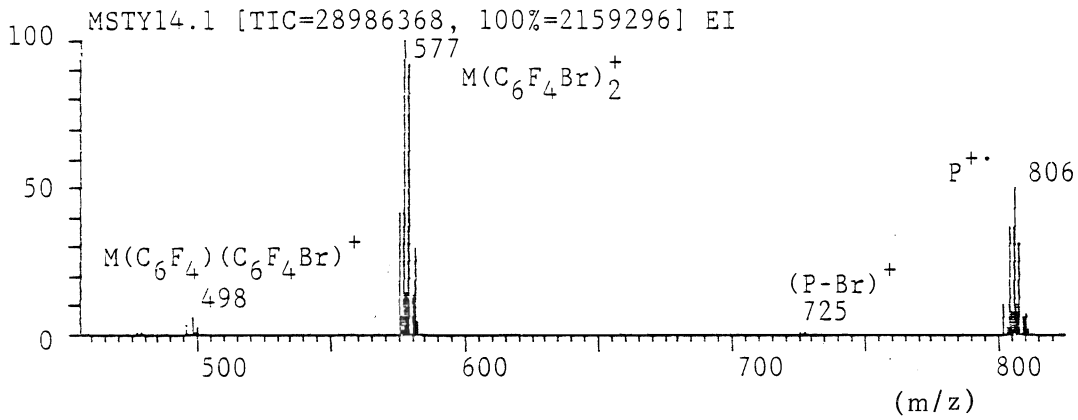
MSTY14.1 [TIC=28986368, 100%=2159296] EI
100
50
0
577
M(C6F4Br)2+
P+·
806
M(C6F4)(C6F4Br)+
498
(P-Br)+
725
500
600
700
800
(m/z)

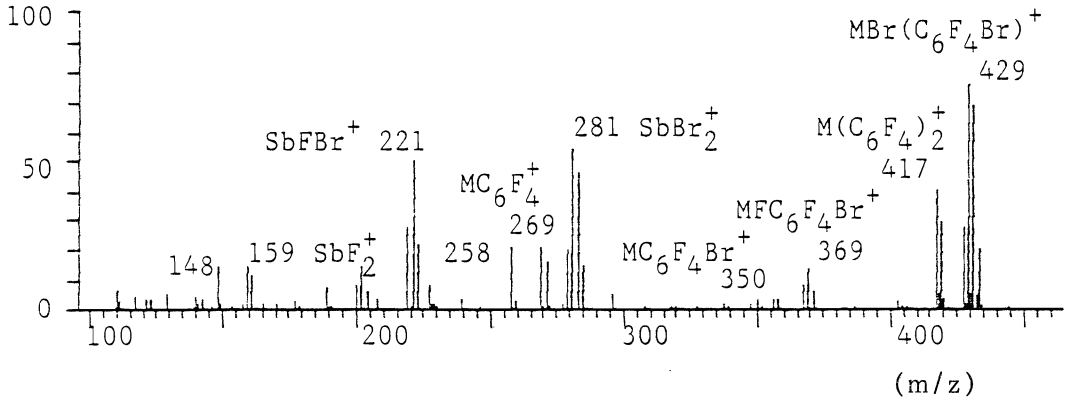
100
50
0
MBr(C6F4Br)+
429
SbFBr+ 221
281 SbBr2+
M(C6F4)2+
417
MC6F4+
269
MFC6F4Br+
369
148
159 SbF2+
258
MC6F4Br+
350
100
200
300
400
(m/z)

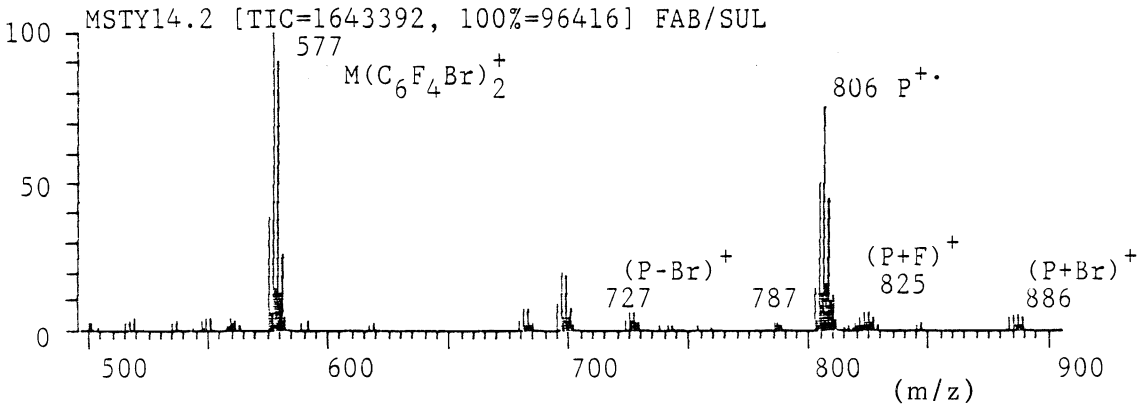
MSTY14.2 [TIC=1643392, 100%=96416] FAB/SUL
100
50
0
577
M(C6F4Br)2+
806 P+·
(P-Br)+
727
787
(P+F)+
825
(P+Br)+
886
500
600
700
800
900
(m/z)

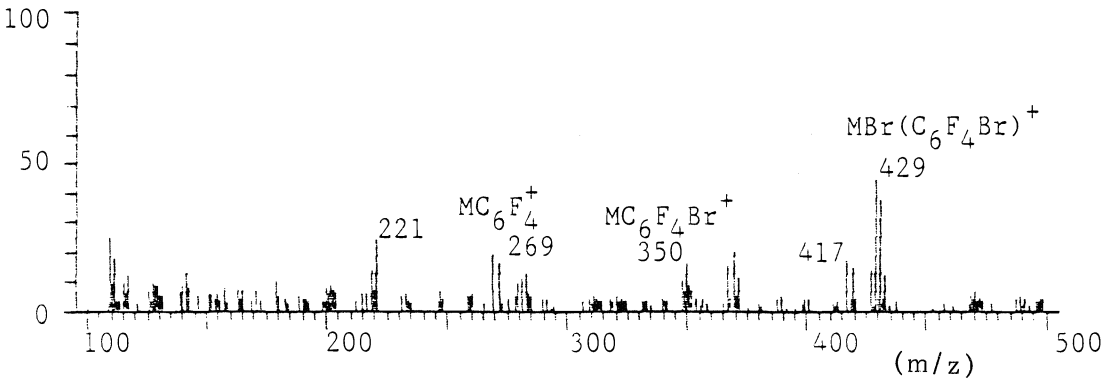
100
50
0
MBr(C6F4Br)+
429
221
MC6F4+
269
MC6F4Br+
350
417
100
200
300
400
500
(m/z)

Table 10a Partial Positive Ion FAB and EI Mass Spectra of $M(C_6F_4X)_3$ Complexes

	Relative Intensity									
M/X=	P/Br		As/Br		Sb/Br		CH_3Si/Br		As/H	
	EI	FAB	EI	FAB	EI	FAB	EI	FAB	EI	FAB
metal containing ions										
$P^{+\cdot}$	18.0	51.0	21.5	40.5	12.1	14.1	9.7	12.2	8.5	35.8
$(P+X)^+$						1.2				
$(P+F)^+$		2.5		0.6		1.6				0.7
$(P-F)^+$	1.1	2.4				0.5			0.1	1.1
$(P-X)^+$	5.5	6.7	0.8	2.0	0.1	1.3	0.4	1.6		
$(P-2X)^+$	0.4	0.9	0.3	0.4	0.1		0.5	1.4		
$(P-3X)^+$	4.2	0.9	0.5				0.1	0.5		
$M(C_6F_4X)_2^+$	0.5	2.5	18.2	16.0	22.5	17.0	1.3	1.2	5.8	14.6
(" $+F)^+$	0.8	0.4					0.1	0.3		0.9
(" $+X)^+$	0.1	0.3								
(" $-F)^+$	0.2	0.1				0.8	0.1			0.4
(" $-X)^+$	1.8	0.9	2.8	1.9	1.0	1.0	2.3	3.9	0.1	
(" $-F_2)^+$						0.2		0.2	0.1	0.8
(" $-X_2)^+$	11.5	5.5	15.0	8.0	0.2	1.1	0.7	2.0	0.4	0.5
(" $-FX)^+$	1.1	1.0	0.6	0.7	0.2	0.1	0.4	0.7	9.1	12.0
$M(C_6F_4X)^+$			0.4	1.2	0.6	3.0	1.0	0.7	32.5	
(" $-X)^+$	4.2	4.0	4.4	2.7	3.0	2.9	0.6	1.0	0.5	
(" $+F)^+$	0.6	0.5	1.9	1.7	2.3	3.3			5.1	
(" $+X)^+$	1.1	0.7	9.0	0.9	15.3	6.8				
MF^+	-	-	0.1	-	0.7	1.7	-	-	0.3	
MF_2^+	-	-	1.0	1.3	2.0		3.0	-	2.6	3.3
MX^+	1.0	0.1	0.4	0.8	2.3	2.0	1.3	2.3	0.3	
MX_2^+	2.0	0.3	3.7	0.8	10.0	2.5	0.5	0.9		
MFX^+	1.9	0.4	2.2		7.5	2.6	1.4	1.8		
M^+	-	-		-	0.6	0.1	-	-	0.4	

Table 10b. Partial Positive Ion FAB and EI Mass Spectra of $M(C_6F_4X)_3$ Complexes

M/X=	Relative Intensity									
	P/Br		As/Br		Sb/Br		CH_3Si/Br		As/H	
	EI	FAB	EI	FAB	EI	FAB	EI	FAB	EI	FAB
non-metal containing ions										
$(C_6F_4)_3^+$	10.4	1.8	0.7	0.6	0.1					
$(C_6F_4)_2^+$	0.6	0.3	0.9	0.3	0.5		0.1			
$(C_6F_3Br)_2^+$	0.1	0.2	0.1						2.5	2.6
$(C_6F_4)(C_6F_3Br)_2$	1.5	0.1	1.4	0.4	0.6	0.3	2.3	3.9		
$(C_6F_4)^+$	1.6		0.7		1.3		0.3		0.2	
other ions										
$(P\text{-}CH_3)^+$							22.0	6.0		
$(P\text{-}CH_3Br)^+$							5.9	2.4		

Scheme 4. Fragmentation of $M(C_6F_4X)_3$ Complexes

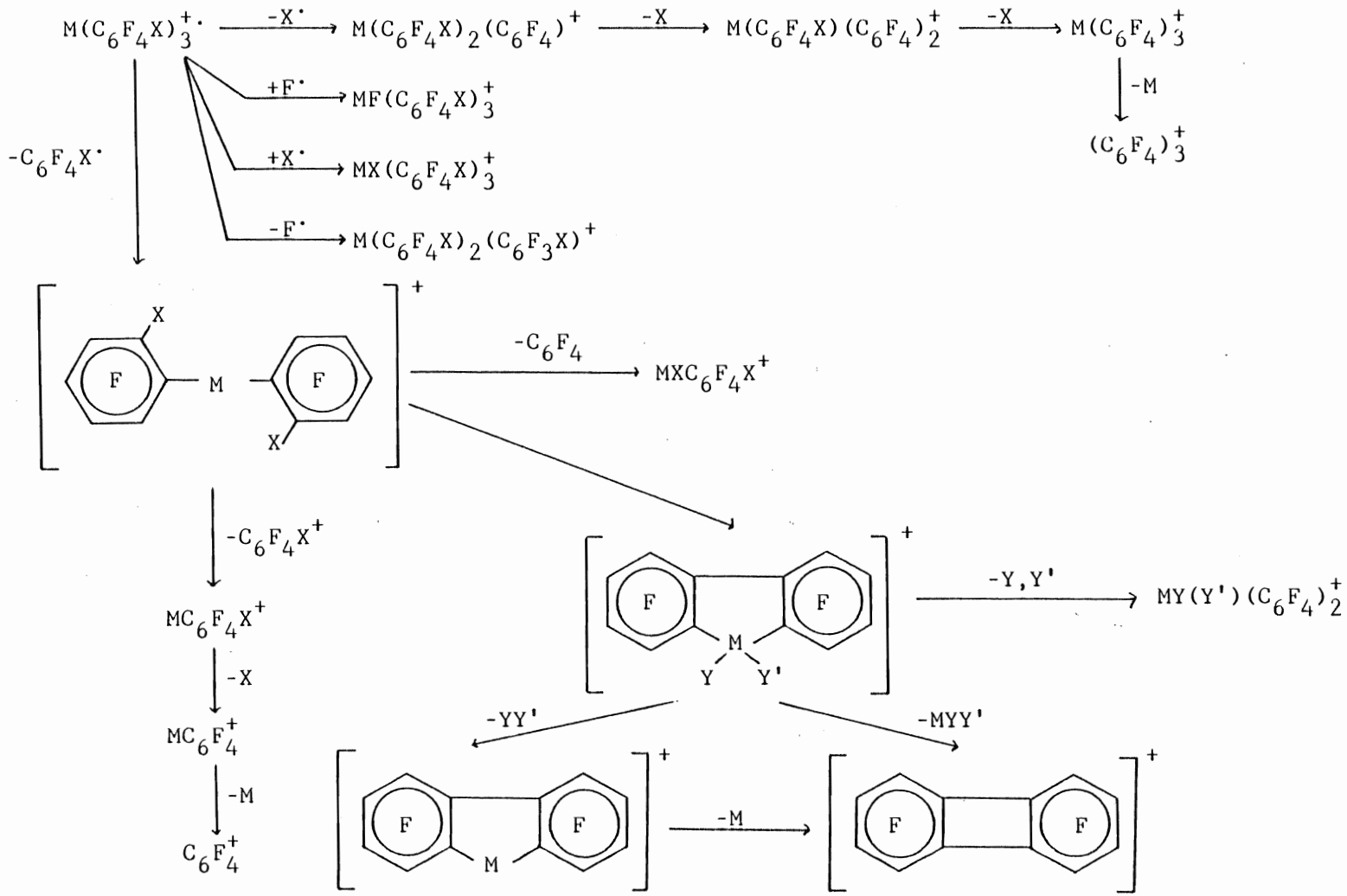

Tables 10a and 10b. Scheme 4 shows the fragmentation processes observed.

The molecular ion, ($[P]^{+\cdot}$), was observed for all complexes (m/z 806 in Figure 23). The relative intensity of this ion was always found to be greater in FAB then in EI. This confirms that FAB is a softer ionizing technique than EI.

Halogen addition to the molecular ion occurs again for these complexes and again only in FAB indicating that it is a solution process involving free radicals that are known to be formed under atom bombardment [25]. Fluorine addition occurs for all complexes except when M=CH_3Si. This is probably simply due to steric crowding around the Si metal center. Bromine addition occurs only when M=Sb. This is best explained by considering that Sb is larger than either P or As, therefore a bromine atom can better fit in among the ring systems. Therefore it is found that for the M=Sb complex, fluorine addition occurs more readily than bromine since fluorine is smaller. Relative intensity of $(P+F)^+$ is 1.6% while for $(P+Br)^+$ it is 1.2%.

Fragmentations of the molecular ion consist principally of radical losses. The radicals that can be lost are: $F^\cdot$ and $Br^\cdot$ (also $CH_3^\cdot$ when M=CH_3Si and $H^\cdot$ for $As(C_6F_4H)_3$) as well as loss of an intact ring system. For the lone complex containing hydrogen as a ring substituent, it was found that hydrogen radical loss did not occur. From

Table 10a it can be seen that bromine radical loss is more favourable than fluorine radical loss. In fact, one, two or all three bromine atoms may be lost. Multiple bromine loss is less favoured for the heavier metal complexes. Only two bromines were observed to be lost from the antimony complex and in only the EI spectrum.

Methyl radical loss when $M=CH_3Si$ is very facile considering the intensity of the $(P-CH_3)^+$ ion, however, in FAB it is stabilized with respect to the molecular ion, providing further evidence of the "softness" of the FAB technique.

The principal fragmentation of the molecular ion is, as for the preceding series of complexes, loss of an intact ring system which, in this case, is $C_6F_4X^{\bullet}$. Again, the resulting ion can be thought of as having one of two structures as in (III) or (IV):

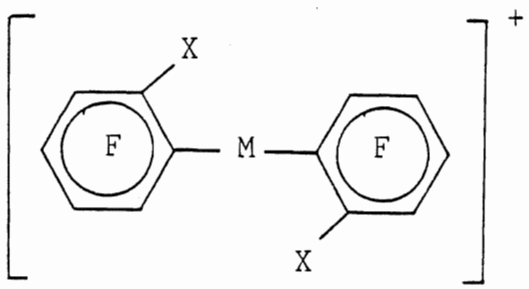

(III)

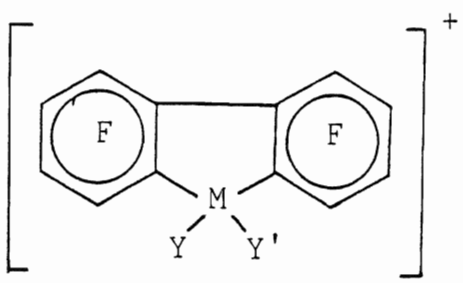

(IV)

The notations Y and Y' are used so as not to confuse these groups with the X substituents in (III).

Structure (III) best explains the appearance of the ion $MC_6F_4X^+$ as well as the possibility of the formation of the species $MXC_6F_4X^+$ and $MFC_6F_4X^+$ via halogen migration.

The second form (IV) is formed by rearrangement and halogen transfer to the central metal atom. This type of rearrangement has been well studied for the EI mass spectra of organometallic complexes [79-83]. The halogen migrations are made possible by the interaction of filled p-orbitals of the halogen atom with empty d-orbitals of the central metal atom. Therefore, halogen migrations to lighter elements such as carbon and nitrogen are not observed since they do not have available empty d-orbitals.

As for the tris(2-chlorophenyl) complexes, the identities of Y and Y', in structure (IV), might be expected to be different for the same reasons of steric hindrance as found in the preceding series. This was found to be true only for the complex $As(C_6F_4H)_3$. For this complex, the most abundant loss from (IV) was the neutral HF. Therefore the precursor ion must be of the form:

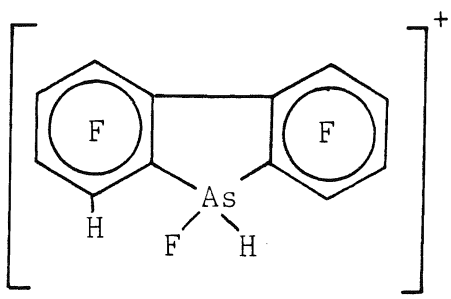

All other complexes showed that loss of FBr (i.e. Y=Y') is a minor process as is loss of F_2 (i.e. Y=Y'=F). Therefore the structure of (IV) must be:

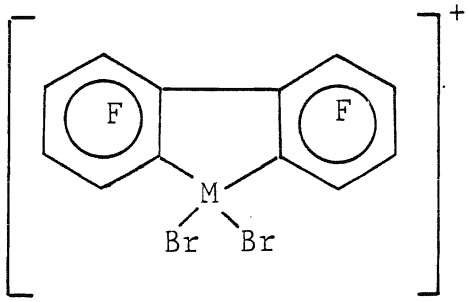

(VI)

The data in Table 10 show that the ease of losing Br, as either $Br^{\cdot}$ or Br_2, from (VI) decreases in the order:

P > As > Sb

(This relationship was established by comparing the ratios of the relative intensities of the ions $[M(C_6F_4Br)_2]^+$ and $[M(C_6F_4Br)_2\text{-}Br]^+$ or $[M(C_6F_4Br)_2\text{-}Br_2]^+$.) This can be explained, in part, using the ideas of hard and soft acid and base theory. If the halogens can be considered to be bases, then based on their sizes, fluorine is a hard base and bromine is a soft base. Similarly, the "hardness" of the metal atoms decreases in the order:

P > As > Sb

Since, using HSAB theory, soft bases prefer to combine with soft acids, then the soft base bromine should prefer to combine with Sb and therefore, the ease of losing Br_2 should decrease in the same order as shown for the hardness of the

metal atoms. This was found to be true. HSAB theory can also be used to explain the increase in intensity of the metal halide ions:

$$MBr\ (MBr_2) > MF\ (MF_2)$$

HSAB ideas can also be used to explain the order of preference for halogen addition to $MC_6F_4X^+$. Recall that this ion is most likely formed by fragmentation of (IV) by losing C_6F_4Br. However, this loss, accompanied by halogen migration yields an ion of the form $MFC_6F_4X^+$ or $MXC_6F_4X^+$. Hydrogen transfer was found not to occur for the complex $As(C_6F_4H)_3$. Both fluorine and bromine migrations were observed when M=P, As and Sb. As expected, migration of bromine was favoured and increases in preference to the central metal atom in the order:

$$Sb > As > P$$

This is in agreement with HSAB theory as explained above.

Halogen migration has been found to occur prior to loss of MX_n (where n=1,2,3) [81]. Depending on the precursor, elimination of MX_n can lead to the ions octafluorobiphenylene or dodecafluorotriphenylene:

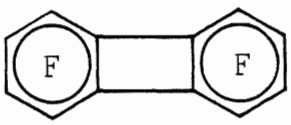

$C_{12}F_8^+$

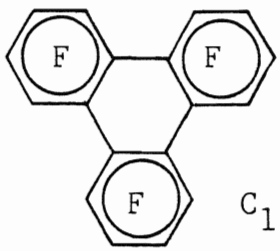

$C_{18}F_{12}^+$

appearing in the mass spectrum at m/z 296 and m/z 444 respectively. In this study, both ions were observed, but only when M=P, As and Sb.

In summary then, fragmentations observed for the complexes of the series $M(C_6F_4X)_3$ are very similar to those observed for the series $M(C_6H_4Cl)_3$. The molecular ion was observed as well as ions resulting from halogen addition to the molecular ion. Radical losses from the molecular ion were also very similar. Rearrangement of the ion formed from loss of an intact ring system radical from the molecular ion produces an ion that is best formulated as in (IV) with Y=Y'=Br (except for $As(C_6F_4H)_3$ where Y=H and Y'=F). Fragmentations of (IV) are similar to those of (II). HSAB theory can be used to explain the order of preference of halogen loss from (IV) as well as the preference of halogen migration to the central metal atom.

v) Perfluoro-1,6-disubstituted Triptycene Derivatives

[$MM'(C_6F_4)_3$, M=M'=P, As, Sb, Bi and CH_3Si and M=P, M'=Sb and M=As, M'=Sb]

Figure 24 shows the positive ion FAB and EI mass spectra of the mixed metal complex $AsSb(C_6F_4)_3$. Peaks that are indicated with an asterisk (*) are due to another complex that was either an impurity in the sample being

Figure 24. Positive Ion FAB and EI Mass Spectra of Perfluoro-1,6-disubstituted Mixed Metal Triptycene of Arsenic and Antimony $AsSb(C_6F_4)_3$.

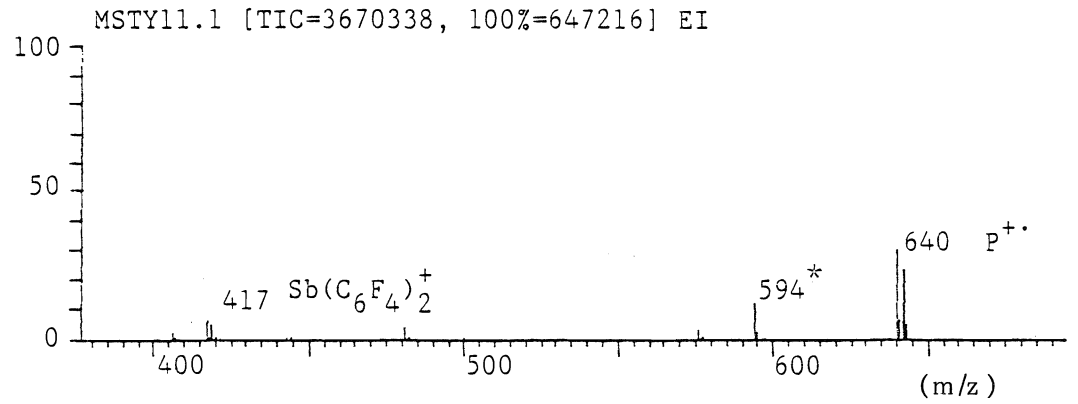
MSTY11.1 [TIC=3670338, 100%=647216] EI
100
50
0
417 $Sb(C_6F_4)_2^+$
594*
640 $P^{+\cdot}$
400
500
600
(m/z)

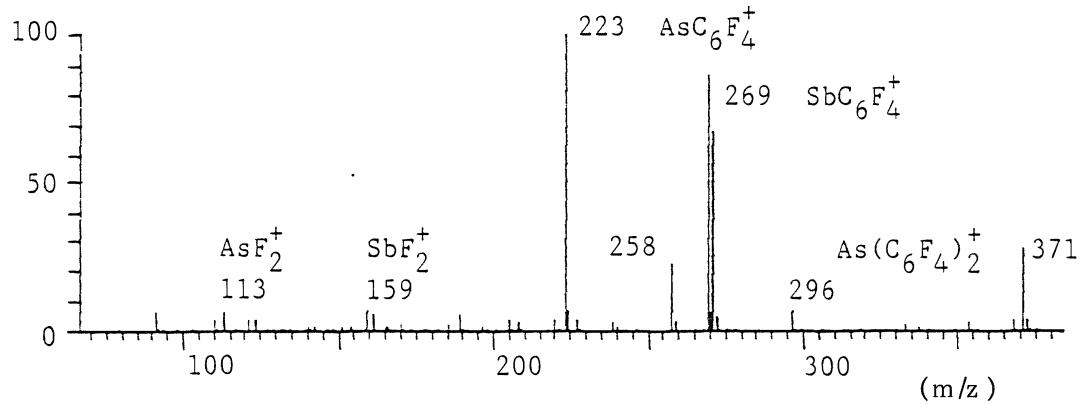
100
50
0
223 $AsC_6F_4^+$
269 $SbC_6F_4^+$
AsF_2^+ 113
SbF_2^+ 159
258
296
$As(C_6F_4)_2^+$ 371
100
200
300
(m/z)

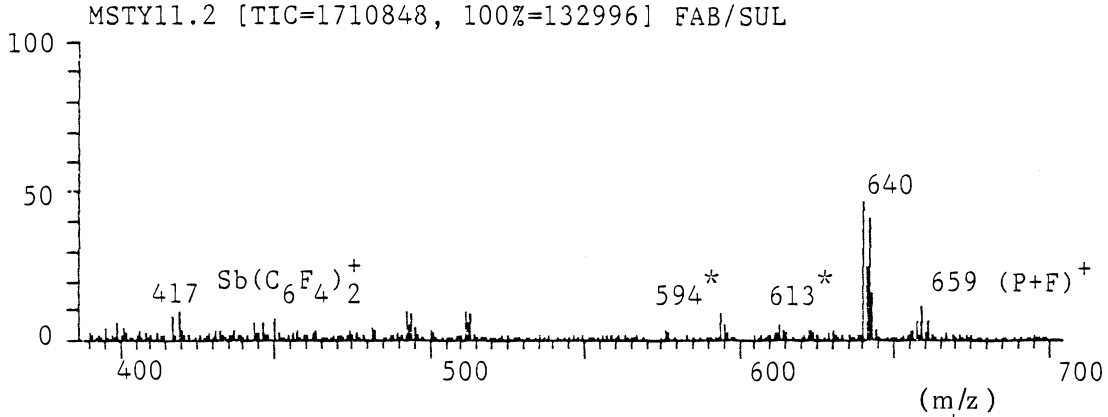
MSTY11.2 [TIC=1710848, 100%=132996] FAB/SUL
100
50
0
417 $Sb(C_6F_4)_2^+$
594*
613*
640
659 $(P+F)^+$
400
500
600
700
(m/z)

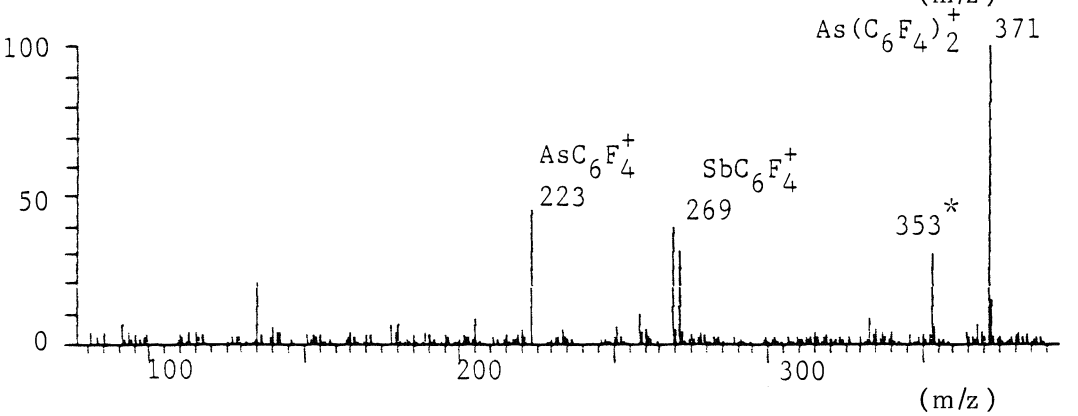
100
50
0
$As(C_6F_4)_2^+$ 371
$AsC_6F_4^+$ 223
$SbC_6F_4^+$ 269
353*
100
200
300
(m/z)

Table 11a. Partial Positive Ion FAB and EI Mass Spectra of $MM'(C_6F_4)_3$ Complexes

	Relative Intensity													
M/M'=	P/P		As/As		Sb/Sb		Bi/Bi		CH3Si/CH3Si		P/Sb		As/Sb	
	EI	FAB	EI	FAB	EI	FAB	EI	FAB	EI	FAB	EI	FAB	EI	FAB
metal containing ions														
$P^{+\cdot}$	19.9		13.3	24.9	9.5	5.3	18.4	3.5	9.7	16.4	21.0	23.8	11.2	9.9
$(P+F)^+$				1.3								1.4		1.6
$(P-F)^+$	1.3		0.1	1.5						1.0	0.6	1.8	0.1	0.8
$(P-MF)^+$	0.8		0.1				0.4		1.4		0.6	0.1	0.1	0.3
$(P-MF_2)^+$	1.1		0.6		0.3		0.4		4.1				0.1	0.2
$(P-M'F)^+$											4.7	0.8	0.1	0.5
$(P-M'F_2)^+$											4.7	1.1	0.8	0.5
$MM'(C_6F_4)_2^+$				6.0			0.1	1.8	0.9	0.8		2.1		2.0
(" $+F)^+$								2.2						1.4
(" $-F)^+$				0.2		1.1			2.5			0.5		0.5
$M(C_6F_4)_2^+$	5.0		8.2	19.8	5.4	4.3	5.3	1.2		1.9	4.7	4.8	5.7	8.9
(" $-F)^+$			0.1	7.8				0.7		0.8	0.2	2.1	0.5	2.6
$M'(C_6F_4)_2^+$											0.6	1.0	2.1	1.7
(" $-F)^+$											0.3	0.4		0.9
$M(C_6F_4)^+$	45.4		54.9	9.9	20.6	18.2	5.3	1.2		0.8	0.3	4.8	18.9	3.5
$M'(C_6F_4)^+$											23.7	3.6	29.1	6.1
MF^+	0.1		0.1	0.7	1.4	1.5	0.6	0.5					0.1	0.3
MF_2^+	4.7		2.2	0.9	2.1	3.0	0.1		4.9		1.7		1.1	0.3
$M'F^+$											2.4	0.9	0.7	1.0
$M'F_2^+$											4.4		2.2	
M^+	-		-	-	2.9	3.3	47.7	20.9	-	-				
M'^+											2.4		1.3	

Table 11b. Partial Positive Ion FAB and EI Mass Spectra of $MM'(C_6F_4)_3$ Complexes

	Relative Intensity													
M/M'=	P/P		As/As		Sb/Sb		Bi/Bi		CH3Si/CH3Si		P/Sb		As/Sb	
	EI	FAB	EI	FAB	EI	FAB	EI	FAB	EI	FAB	EI	FAB	EI	FAB
non-metal containing ions														
$C_{18}F_{12}^+$			0.3	4.9			0.2			1.3		0.1	0.2	0.3
$C_{12}F_8^+$	0.4		1.3		0.9	0.6	0.3		0.3		0.5		1.4	
$C_{12}F_6^+$	2.5		3.9	1.0	3.1	3.1	0.3		0.3		3.6	0.3	4.5	1.1
$C_6F_4^+$	0.2		0.1		0.5	0.5	0.6	1.1			0.1		0.1	
other ions														
$(P\text{-}CH_3)^+$									10.3	2.6				
$(MM'(C_6F_4)_2\text{-}CH_3)^+$									0.4					

Scheme 5. Fragmentation of $MM'(C_6F_4)_3$ Complexes

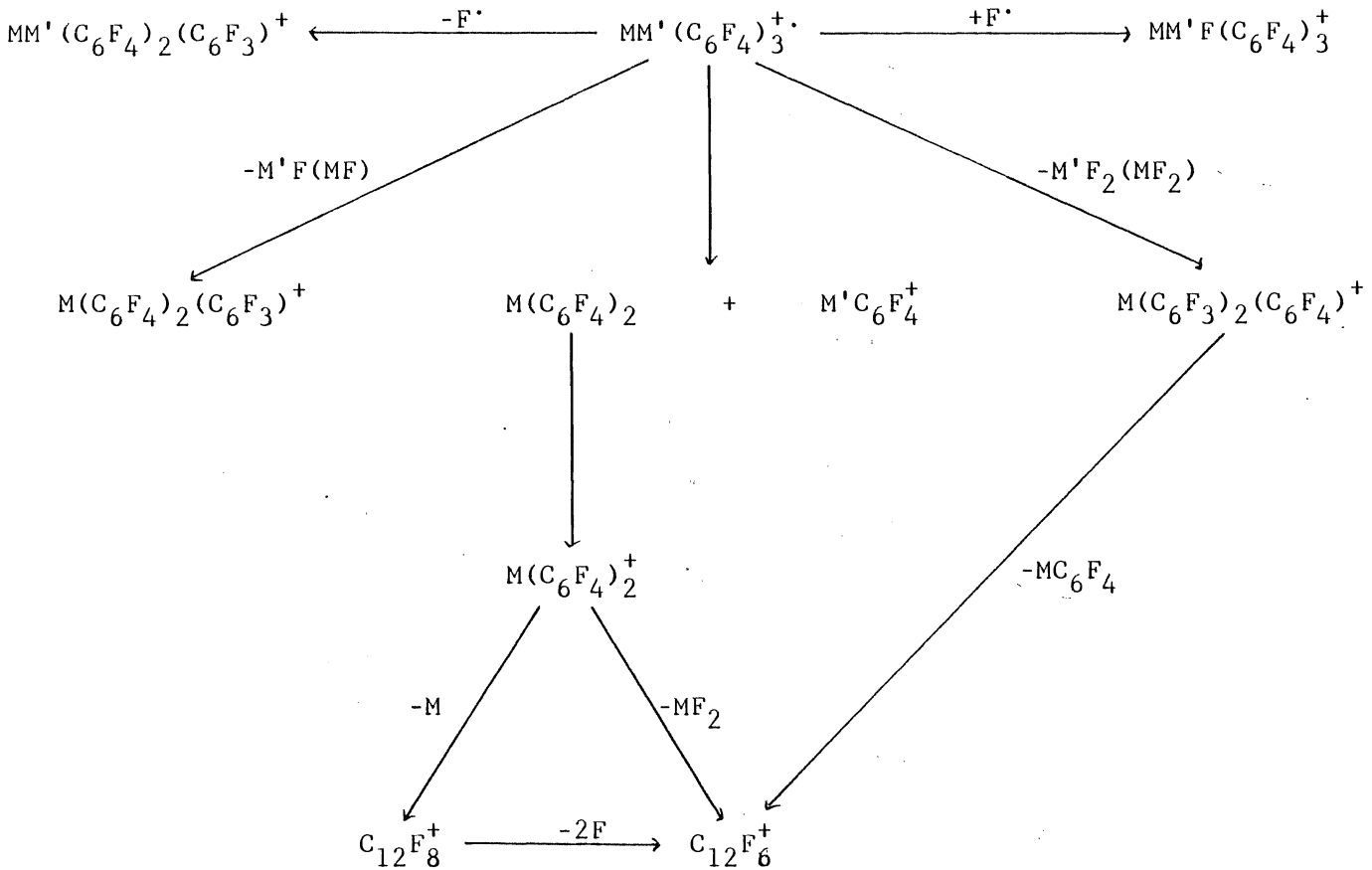

analyzed or that still remained in the spectrometer when this sample was being analyzed. A partial summary of these and the remaining spectra is given in Table 11. No FAB spectrum was obtained for the complex $P_2(C_6F_4)_3$. Scheme 5 shows the fragmentations observed for these complexes. No differentiation was made in the Scheme between identical processes involving different metal atoms, i.e. M=M' in the Scheme.

The fragmentation of these complexes is relatively simple compared to that observed for the preceding two series of complexes. Three main ions appear in the spectra corresponding to: $P^{+\cdot}$, $M(C_6F_4)_2^+$ and $MC_6F_4^+$.

The molecular ion, $P^{+\cdot}$, was observed in good abundance (m/z 640 in Figure 24). No preference was shown with respect to the more favourable ionization technique. Fluorine addition to the molecular ion is almost completely absent and, as expected, is only observed in some FAB spectra. These were for the complexes where M=M'=As and M=P or As and M'=Sb.

Fluorine radical loss from the molecular ion is unimportant as shown by the low intensities for the $(P-F)^+$ ions. A more important mechanism for fluorine loss appears to be via migration to a metal atom followed by loss of MF or MF_2. The mixed metal complexes show that these losses occur more readily for M=Sb than for either M=P or As.

The parent ion can lose one ring system to give

(VI):

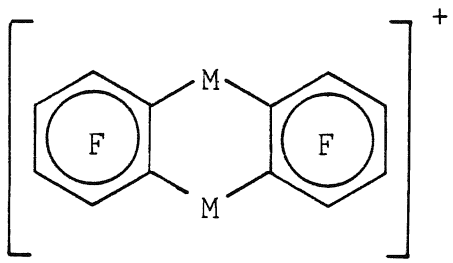

(VI)

However, loss of the ring with one metal atom attached is more likely, yielding (VII):

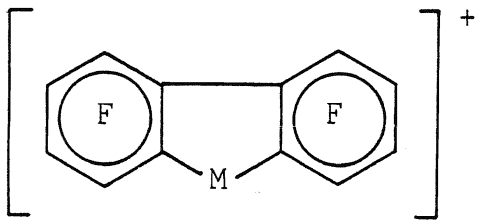

(VII)

This preference is shown by the relatively larger abundance of the ions $M(C_6F_4)_2^+$ and $MC_6F_4^+$ as compared to the abundance of the ion $M_2(C_6F_4)_2^+$. Formation of (VII) actually occurs in two steps [51b]:

$$M_2(C_6F_4)_3^{+\cdot} \longrightarrow M(C_6F_4)^+ + M(C_6F_4)_2$$

$$M(C_6F_4)_2 \longrightarrow M(C_6F_4)_2^+$$

The complex (VII) will then fragment:

$$M(C_6F_4)_2^+ \longrightarrow MF_2 + (C_6F_3)_2^+$$

$$\text{or} \longrightarrow M + (C_6F_4)_2^+$$

Therefore products of the fragmentations include $C_{12}F_6^+$ and $C_{12}F_8^+$. The former requires a halogen migration to the

central metal atom therefore the intensities of these ions should reflect the ease of fluorine migration to the metal center. However, since $C_{12}F_6^+$ is a normal decomposition product of $C_{12}F_8^+$ then this effect is masked and cannot be used.

The mixed metal complexes show that there is a preference in the first step shown above, i.e.:

$$MM'(C_6F_4)_3^{+\cdot} \longrightarrow M'(C_6F_4)^+ + M(C_6F_4)_2$$

in that the single ring is retained by the Sb atom. Therefore:

$$MSb(C_6F_4)_3^{+\cdot} \longrightarrow Sb(C_6F_4)^+ + M(C_6F_4)_2$$

where M=P and As. This is in agreement with the general tendency for increasingly weaker metal-carbon bonds as one goes down the periodic Group V. Previously published results for the phosphorus-arsenic mixed complex [51b] are also in agreement in that, in the EI spectrum, relative abundances of the ions decrease in the order:

$$AsC_6F_4^+ > PC_6F_4^+$$

and

$$P(C_6F_4)_2^+ > As(C_6F_4)_2^+$$

Therefore the major fragmentation of the molecular ion is:

$$PAs(C_6F_4)_3^{+\cdot} \longrightarrow AsC_6F_4^+ + P(C_6F_4)_2$$

the heavier element remains with the single ring, having broken two bonds to the other two rings.

vi) Summary

The molecular ion was observed for all the complexes in both FAB and EI. Halogen addition to this ion occurred mostly for fluorine but bromine addition to a larger metal center was found.

Major losses from the molecular ion occured via radical loss but the principal fragmentation involved loss of an intact ring system to form an ion that rearranged to the structure as shown in (II) or (IV). The rearrangement was accompanied by migration of ring substituents to the central metal atom. Which substituents migrated was dependent on their identities.

Fragmentations were consistent with known bond strengths. The metal with the strongest metal-carbon bonding retained the largest number of coordinating groups.

D. Conclusions

1. Ruthenium(II) Polypyridyl Coordination Complexes

A matrix optimization experiment for the polypyridyl complexes showed that based on the general requirements for a matrix material as well as on the quality of the spectra obtained, 3-nitrobenzyl alcohol was the best matrix.

An investigation of the fragmentation mechanism showed that the important factors involved were: initial dissociation of the complex salt, successive losses of intact ligands, cyclometallation of bpy-type ligands and proton loss from ligands having readily removable hydrogens (i.e. dpa).

It was found that the identity of the anion present in the complex salt had an important effect on the spectrum obtained. Additional ions were observed in the mass spectrum having the form $[RuL_2]X^+$ and $[RuL_2]^{2+}$. Some anions, such as $CF_3SO_3^-$ and $CF_3CO_2^-$, were unusually strongly bound to the central Ru(II) atom, possibly by multiple chelation. Small anions such as Cl^- formed these ions since it would have a stronger electrostatic attraction to the $[RuL_2]^{2+}$ ion than would a large anion such as PF_6^-.

An almost complete structural characterization could be made of the intact complex. From the isotope pattern of ions, and the charge of the multiply charged ion, the identity of the metal atom and its oxidation state could be

determined. The number and type of anions could be inferred from observations of the negative ion spectrum and ions such as $[RuL_3]^{2+}$, $[RuL_3]^{+}$ and $[RuL_3]X^{+}$ in the positive ion spectrum. The number, type and stoichiometric ratio of the ligands contained in the complex were determined from ions such as $[RuL_2]^{+}$, $[RuL]^{+}$ and $(L+H)^{+}$. The formula weight of the complex could also be calculated from the ions $[RuL_3]X^{+}$, $[RuL_3]^{2+}$, and $[RuL_3]^{+}$.

By observing relative intensities of the appropriate ions formed from mixed ligand complexes, relative chelating powers of the ligands were estimated. From these, it was concluded that the information contained in the FAB mass spectrum could be correlated with the known solution behaviour of the observed species.

The appearance of multiply charged ions was found to be dependent on the type of matrix used. A mechanism was proposed in which the formation of the doubly charged ion was explained as a result of an oxidative quenching of the excited state of the complex. Such reactions are known from photochemical studies of the Ru(II) polypyridyl complexes.

Analysis of one known mixture and one unknown mixture of complexes showed that no ligand exchange occurred. Therefore the FAB technique was concluded to be a good method for separating and identifying components in a mixture.

2. Group V Triptycenes and Related Complexes

The molecular ion was observed for all the complexes in both FAB and EI suggesting that the ionization mechanism was similar for these complexes using both techniques. This was confirmed by the similarity in the spectra obtained and in a general tendency for a more abundant molecular ion in FAB than in EI. This was expected since FAB is a "softer" ionization technique.

Halogen additions to the molecular ion were observed but only in FAB indicating that this was a solution process involving free radicals formed under particle bombardment. Fluorine addition was found for many complexes but, due to its size, bromine addition was observed only to the larger metal center.

Fragmentation of the molecular ion occurred via loss of radicals. The principal radical loss was of an intact ring system. The resulting ion then underwent a rearrangement accompanied by migration of substituent groups to the central metal atom. The groups to migrate were determined by the complex. For the series $M(C_6H_4Cl)_3$, abundant loss of HCl indicated that one hydrogen and one chlorine migrated. For the $M(C_6F_4Br)_3$ series, however, the major loss was of Br_2 indicating that both bromines migrated to the central metal atom.

Relative metal-carbon bond strengths could be estimated by comparing relative intensities of species

appearing in the mass spectra. These estimates were found to be in agreement with the expected gradual weakening of the metal-carbon bond from P to Bi. Therefore the technique of FAB also has application to structural characterization of these complexes.

References

1. Hunt, D.F., Int. J. Mass Spectrom. Ion Proc., 45 :111(1982).

2. Macfarlane, R.D. and Torgenson, D.F., Science, 191 :920(1976).

3. Becky, H.D., Int. J. Mass Spectrom. Ion Phys., 2 :500(1969).

4. Colby, B.N. and Evans, C.A. Jr., Anal. Chem., 45 :1884(1973).

5. Chan, K.W.S., and Cook, K.D., J. Am. Chem. Soc., 104 :5031(1982).

6. Mumma, R.O., and Vastola, F.J., Org. Mass Spectrom., 6 :1373(1972).

7. Hercules, D.M., Day, R.J., Balasunmagam, K., Dang, T.A., and Li, C.P., Anal. Chem., 54 :280A(1984).

8. Denoyer, E., Van Grieken, R., Adams, F., and Natusch, D.F.S., Anal. Chem., 54 :27A(1984).

9. Benninghoven, A. and Sichtermann, W.K., Anal. Chem., 50 :1180(1978).

10. Barber, M., Bordoli, R.S., Sedgwick, R.D., and Tyler, A.N., Nature, 293 :270(1981).

11. Barber, M., Bordoli, R.S., Sedgwick, R.D. and Tyler, A.N., J. Chem. Soc. Chem. Comm., 1984 :325.

12. a) Mahoney, J.F. Perel, J. and Forrester, A.T., Appl. Phys. Lett., 38 :320(1981).
    b) Franks, J., Int. J. Mass Spectrom. Ion Proc., 46 :343(1983).

13. Benninghoven, A., Appl. Phys., 11 :35(1976).

14. Barber, M., Bordoli, R.S., Elliot, G.J., Sedgwick, R.D., and Tyler, A.N., Anal. Chem., 54 :645A(1982).

15. Ligon, W.V., and Dorn, S.B., Int. J. Mass Spectrom. Ion Proc., 57 :75(1984).

16. Ligon, W.V., and Dorn, S.B., Int. J. Mass Spectrom. Ion Proc., 61 :113(1984).

17. Barber, M., Bordoli, R.S., Elliot, G.J., Sedgwick, R.D., and Tyler, A.N., J. Chem. Soc. Faraday Tran., 79 :1249(1983).

18. Wong, S.S., Rollgen, F.W., Manz, I., and Przybylski, M., Biomed. Mass Spectrom., 12 :43(1985).

19. Caprioli, R.M., Anal. Chem., 55 :2387(1983).

20. Caprioli, R.M., in Desorption Mass Spectrometry, Are SIMS and FAB the Same? , Lyon, P.A., ed., ACS Symposium Series, No. 291, Am. Chem. Soc., Washington, 1985.

21. DePauw, E., Anal. Chem., 55 :2195(1983).

22. Johnstone, R.A.W. and Lewis, I.A.S., Int. J. Mass Spectrom. Ion Proc., 46 :451(1983).

23. Kalinoski, H.T., Hacksell, U., Barofsky, D.F., Barofsky, E. and Daves, G.D., Jr., J. Amer. Chem. Soc., 107 :6476(1985).

24. Pelzer, G., DePauw, E., Dung, D.V., and Marien, J., J. Phys. Chem., 88 :5065(1982).

25. Clayton, E. and Wakefield, A.J.C, J. Chem. Soc. Chem. Comm., 1984 :969.

26. Miller, J.M., J. Organomet. Chem., 249 :299(1983).

27. Miller, J.M., in Advances in Inorganic Chemistry and Radiochemistry , Emeleus, H.J. and Sharp, A.G. eds., Academic Press, New York, 28 :1(1984).

28. Rinehart, K.L., Science, 218 :254(1982).

29. Barber, M., Bordoli, R.S., Sedgwick, R.D., and Tyler, A.N., Biomed. Mass Spectrom., 8 :492(1981).

30. van der Greef, J. and ten Noever de Brauw, Int. J. Mass Spectrom. Ion Proc., 46 :379(1983).

31. Miller, J.M. and Fulcher, A., Can. J. Chem., 63 :2308(1985).

32. Miller, J.M., Mondal, H., Wharf, I. and Onyszchuk, M., J. Organomet. Chem., 306 193(1986).

33. Dalietos, D., Furst, A., Theodoropoulos, D. and Lee, T.D., Int. J. Mass Spectrom. Ion Proc., 61 :141(1984).

34. Davis, R., Groves, I.F., Durrant, J.L.A., Brooks, P., and Lewis, I., J. Organomet. Chem., 241 :C27(1983).

35. Blumenthal, T., Bruce, M.I., Shawkataly, D.B., Green, B.N. and Lewis, I., J. Organomet. Chem., 269 :C10(1984).

36. Tkatchenko, I., Neibecker, D., Fraisse, D., Gomez, F. and Barofsky, D.F., Int. J. Mass Spectrom. Ion Proc., 46 :499(1983).

37. Sharp, T.R., White, M.R., Davis, J.F., and Stang, P.J., Org. Mass Spectrom., 19 :107(1984).

38. Cohen, A.I., Glavan, K.A., and Kronauge, J.F., Biomed. Mass Spectrom., 10 :287(1983).

39. Divisia-Blohorn, B., Kyriakakou, G., and Ulrich, J., Org. Mass Spectrom., 20 :463(1985).

40. Unger, S., Anal. Chem., 56 :363(1984).

41. Bojesen, G., Org. Mass Spectrom., 20 :413(1985).

42. Cerny, R.L., Sullivan, P.B., Bursey, M.M., and Meyer, T.J., Anal. Chem., 55 :1954(1983).

43. Cerny, R.L., Bursey, M.M., Jameson, D.L., Malachowski, M.R. and Sorrell, T.N., Inorg. Chim. Acta, 89 :89(1984).

44. Cerny, R.L., Sullivan, P.B., Bursey, M.M., and Meyer, T.J., Inorg. Chem., 24 :397(1985).

45. Hacksell, U., Kalinoski, H.T., Barofsky, D.F., and Daves, G.D., Jr., Acta Chem. Scand. B, 39 :469(1985).

46. Brandt, W.W., Dwyer, F.P., and Gyarfas, E.C., Chem. Rev., 54 :959(1954).

47. Kalyanasundaram, K., Coord. Chem. Rev., 46 :159(1982).

48. McBryde, W.A.E., A Critical Review of Equilibrium Data for Proton and Metal Complexes of 1,10-Phenanthroline, 2,2'-Bipyridine and Related Compounds , IUPAC, Chem. Data Ser. No. 17, Pergammon Press, Oxford, 1978.

49. Schilt, A.A., Analytical Applications of 1,10-Phenanthroline and Related Compounds , Pergamon Press, Oxford, 1969.

50. a) Thomas, N.C., PhD thesis, Monash University, Australia, 1985.
b) Black, D. St. C., Deacon. G.B. and Thomas, N.C., Inorg. Chim. Acta, 65 :L75(1982).

51. a) Al-Jabar, N.A.A., and Massey, A.G., J. Organomet. Chem., 288 :145(1985).
b) Al-Jabar, N.A.A. and Massey, A.G., J. Organomet. Chem., 287 :57(1985).
c) Al-Jabar, N.A.A. and Massey, A.G., J. Organomet. Chem., 276 :331(1984).

52. Gower, J.L., Biomed. Mass Spectrom., 12 :191(1985).

53. De Pauw, E., Mass Spectrom. Rev., 5 :191(1986).

54. Meili, J., and Seibl, J., Int. J. Mass Spectrom. Ion Proc., 46 :367(1983).

55. Meili, J., and Seibl, J. Org. Mass Spectrom., 19 :581(1984).

56. Tolun, E., Proctor, C.J., Todd, J.F.J., Walshe, J.M.A., and Connor, J.A., Org. Mass Spectrom., 19 :294(1984).

57. Morris, D.E., Ohsawa, Y., Segers, D.P., DeArmond, M.K. and Hanck, K.W., Inorg. Chem., 23 :3010(1984).

58. Collman, J.P., and Hegedus, L.S., Principles and Applications of Organotransition Metal Chemistry , University Science Books, California, 1980.

59. Wickramasinghe, W.A., Bird., P.H. and Serpone, N., J. Chem. Soc. Chem. Comm., 1981 :1284.

61. Williams, D.H., Bradley, C., Bojesen, G., Santikarn, S. and Taylor, L.C.E., J. Am. Chem. Soc., 103 :5700(1981).

62. Cook, K.D., and Chan, K.W.S., Int. J. Mass Spectrom. and Ion Proc., 54 :135(1983).

63. Barofsky, D.F., and Giessman U., Int. J. Mass Spectrom. and Ion Proc., 46 :359(1983).

64. Ryan, T.M., Day, R.J. and Cooks, R.G., Anal. Chem., 52 :2054(1984).

65. Wood, G.W., McIntosh, J.H. and Lau, P.Y., J. Org. Chem., 40 :636(1975).

66. Cotter, R.J., Breeman, R.V., Yergey, J. and Heller, D.N., Int. J. Mass Spectrom. Ion Proc., 46 :395(1985).

67. Heller, D.N., Yergey, J. and Cotter, R.J., Anal. Chem., 55 :1310(1983).

68. Schmelzeisen-Redeker, G., McDowall, M.A., Geissmann, U., Levsen, K. and Rollgen, F.W., J. Chromatog., 323 :127(1985).

69. Schmelzeisen-Redeker, G., Rollgen, F.W., Wirtz, H. and Vogtle, F., Org. Mass Spectrom., 20 :752(1985).

70. Murawski, S.L. and Cook, K.D., Anal. Chem., 56 :1015(1984).

71. Cook, K.D. and Chan, K.W.S., Anal. Chem., 55 :1306(1983).

72. Juris, A., Balzani, V., Belser, P. and von Zelewsky, A., Helv. Chim. Acta, 64 :2175(1981).

73. Balasanmugan, K., Day, R.J., and Hercules, D.M., Inorg. Chem., 24 :4477(1985).

74. Bojesen, G. and Moller, J., Int. J. Mass Spectrom. Ion Proc., 68 :239(1986).

75. Huang, Q., Wu., G. and Tang., H., Int. J. Mass Spectrom. Ion Proc., 70 :145(1986).

76. Moon. D.W., and Winograd, N., Int. J. Mass Spectrom. Ion Proc., 52 :217(1983).

77. Magee., C.W., Int. J. Mass Spectrom. Ion Proc., 49 :211(1983).

78. Dube, G., Org. Mass Spectrom., 19 :242(1984).

79. Rake, A.T. and Miller, J.M., J. Chem. Soc., (A) 1970 :1881.

80. Miller, J.M., J. Chem. Soc., (A) 1967 :828.

81. Jones, T.R.B., Miller, J.M. and Fild, M., Org. Mass Spectrom., 12 :317(1977).

82. Miller, J.M., Jones, T.R.B. and Deacon, G., Inorg. Chim. Acta, 32 :L75(1979).

83. Miller, J.M., Can. J. Chem., 47 :1613(1969).

Appendix A

Positive Ion FAB Mass Spectra of
Ruthenium (II) Polypyridyl Coordination Complexes

1. [Ru (bpy)$_3$](PF$_6$)$_2$
2. [Ru (bpy)$_3$](CF$_3$SO$_3$)$_2$
3. [Ru (bpy)$_3$]Cl$_2$
4. [Ru (phen)$_3$](PF$_6$)$_2$
5. [Ru (phen)$_3$](CF$_3$CO$_2$)$_2$
6. [Ru (dpa)$_3$](PF$_6$)$_2$
7. [Ru (dmb)$_3$](PF$_6$)$_2$
8. [Ru (bpy)$_2$ (phen)](PF$_6$)$_2$
9. [Ru (phen)$_2$ (bpy)](PF$_6$)$_2$
10. [Ru (dmb)$_2$ (bpy)](PF$_6$)$_2$
11. [Ru (dmb)$_2$ (phen)](PF$_6$)$_2$
12. [Ru (bpy)$_2$ (dpa)](PF$_6$)$_2$
13. [Ru (phen) (dmb) (bqy)](PF$_6$)$_2$
14. [Ru (bpy) (dmb) (bqy)](PF$_6$)$_2$
15. [Ru (bpy) (phen) (bqy)](PF$_6$)$_2$
16. [Ru (bpy) (phen) (dmb)](PF$_6$)$_2$
17. [Ru (bpy) (phen) (dpk)](PF$_6$)$_2$
18. [Ru (bpy) (phen) (tmp)](PF$_6$)$_2$
19. [Ru (bpy) (dmb) (dib)](PF$_6$)$_2$
20. [Ru (bpy) (phen) (dzf)](PF$_6$)$_2$
21. [Ru (bpy) (phen) (dpa)](PF$_6$)$_2$
22. [Ru (dmb) (phen) (dpa)](PF$_6$)$_2$
23. [Ru (bpy) (phen) (CO) Cl](PF$_6$)
24. [Ru (bpy) (dmb) (CO) Cl](PF$_6$)
25. [Ru (bpy) (Bq) (CO)]Cl
26. [Ru (bpy) (tpy) Cl](PF$_6$)

Figure A.1

$[Rubpy_3](PF_6)_2$

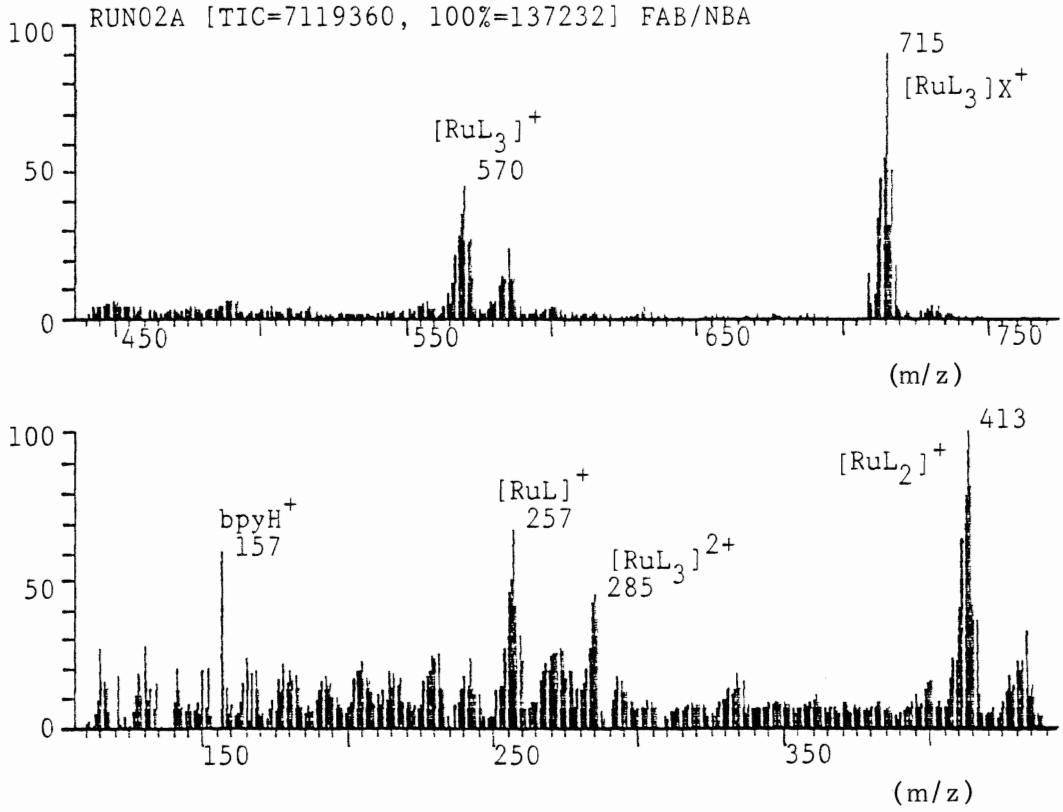

Figure A.2

$[Rubpy_3](CF_3SO_3)_2$

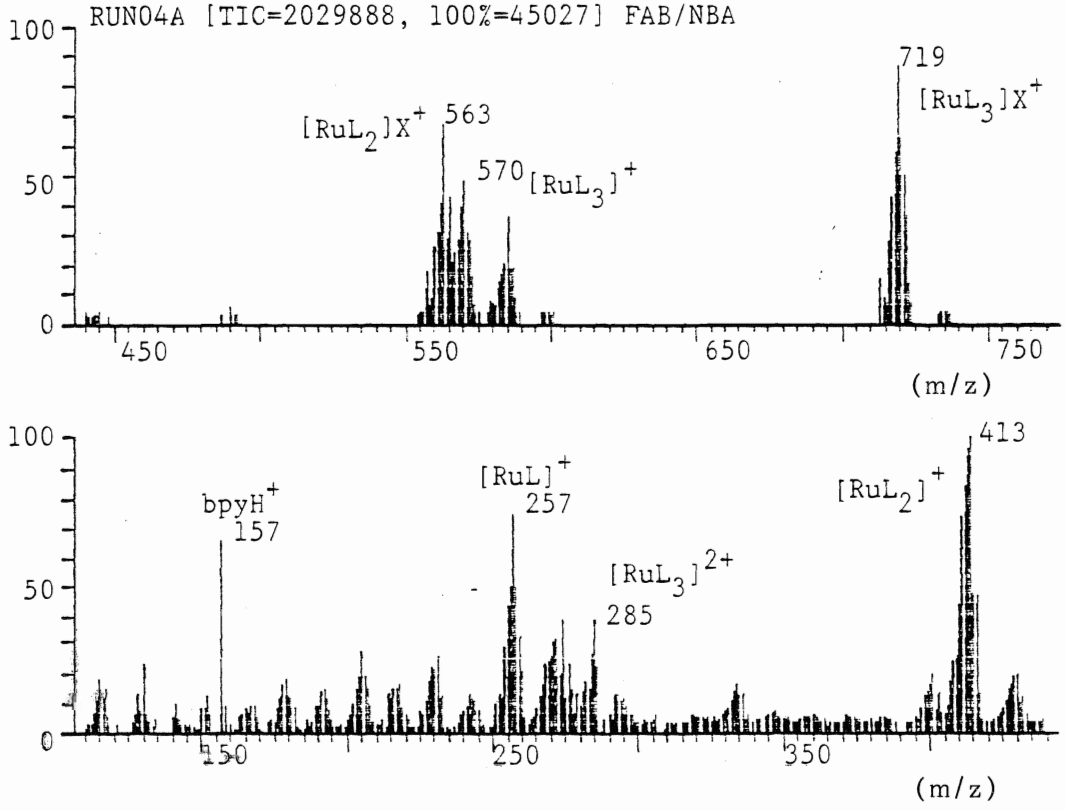

Figure A.3

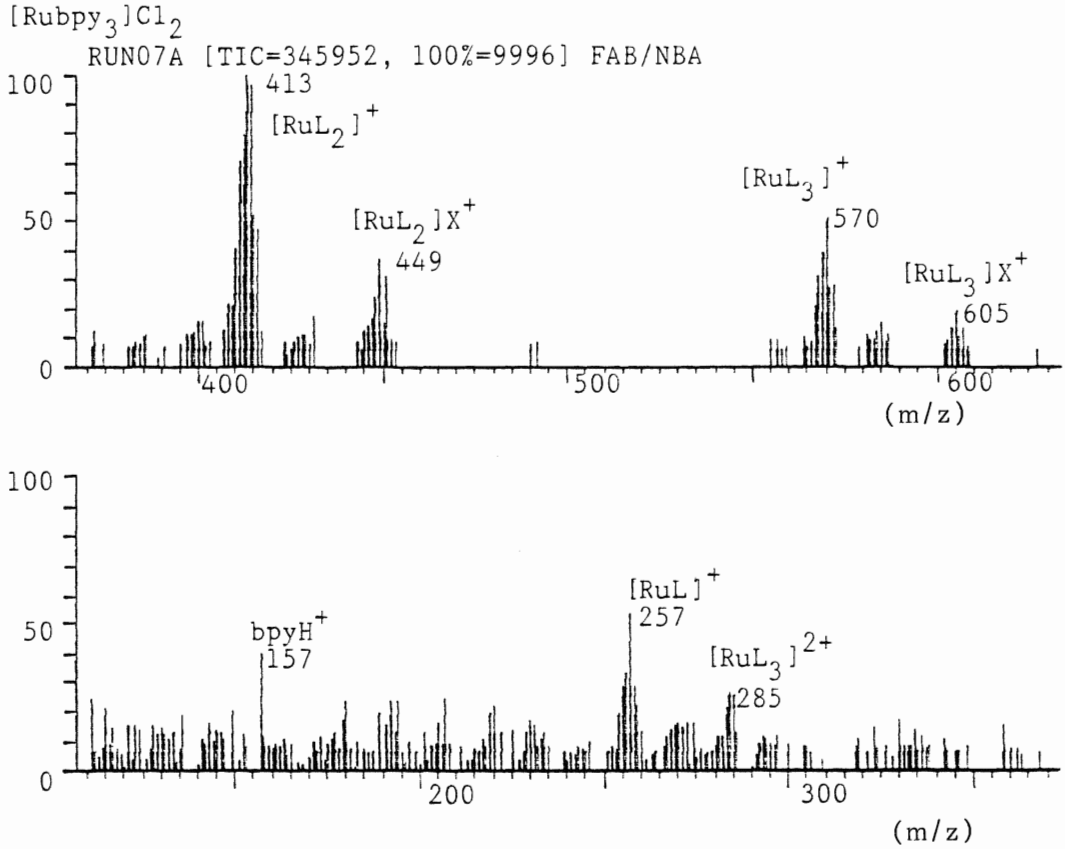
[Rubpy3]Cl2
RUN07A [TIC=345952, 100%=9996] FAB/NBA
100
50
0
413
[RuL2]+
[RuL2]X+
449
[RuL3]+
570
[RuL3]X+
605
400
500
600
(m/z)
100
50
0
bpyH+
157
[RuL]+
257
[RuL3]2+
285
200
300
(m/z)

Figure A.4

$[Ruphen_3](PF_6)_2$

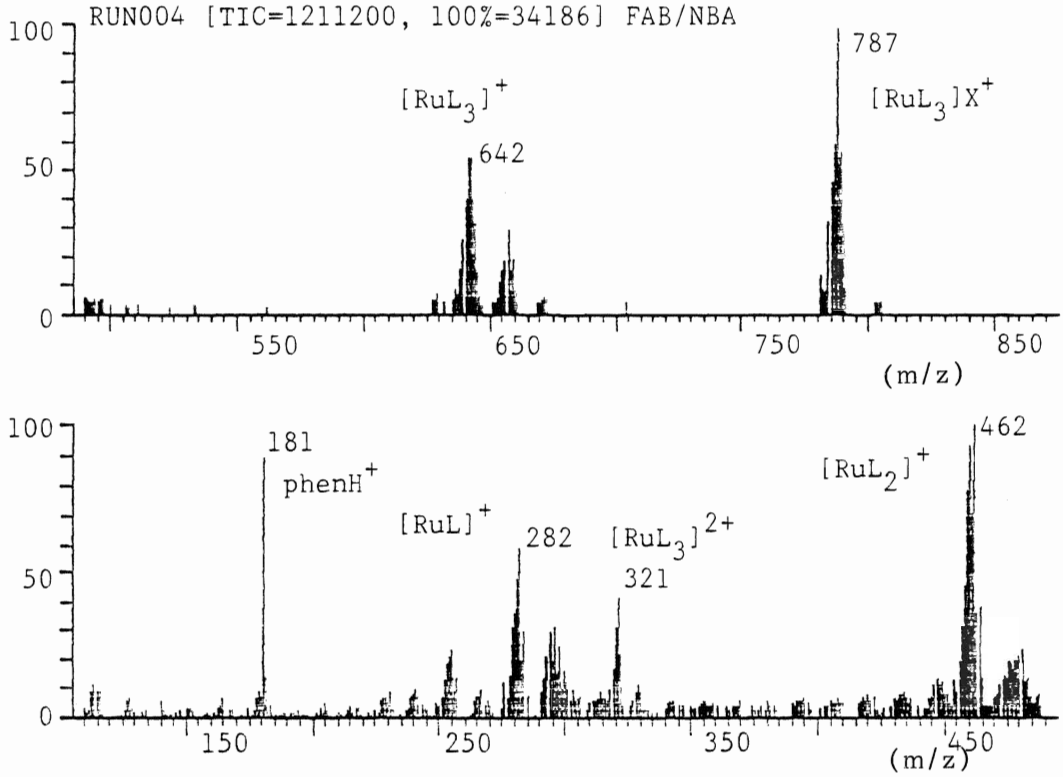

Figure A.5

$[Ruphen_3](CF_3CO_2)_2$

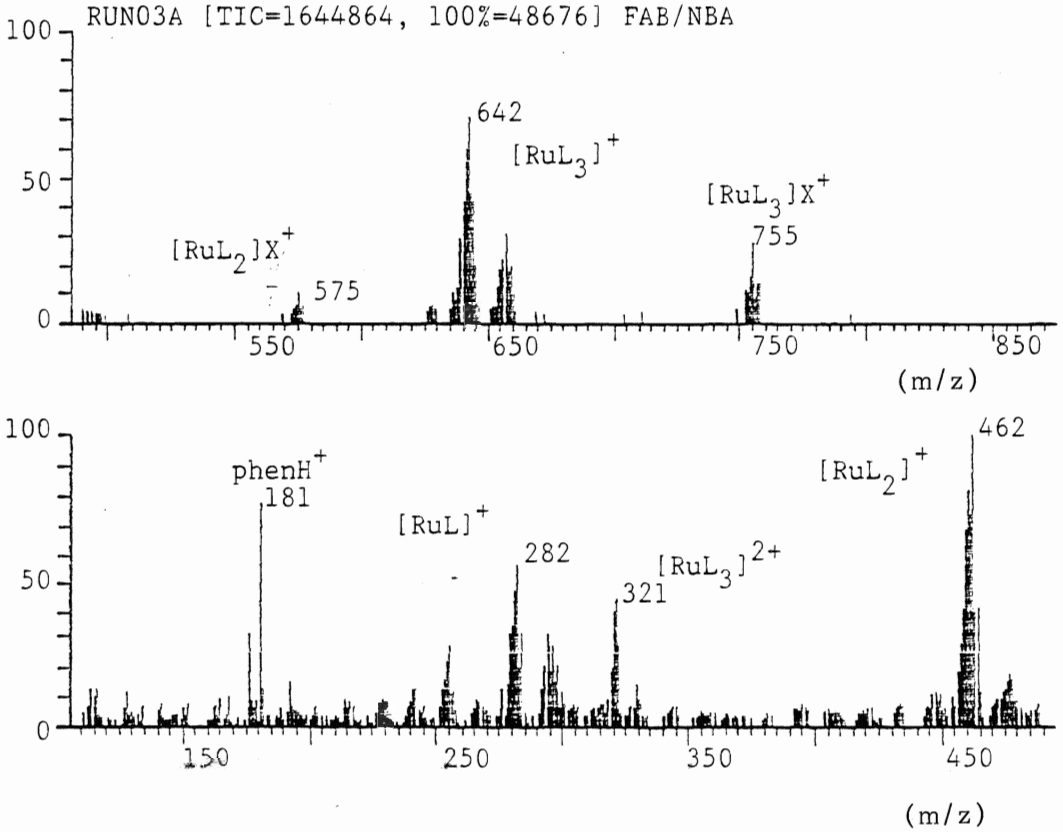

Figure A.6

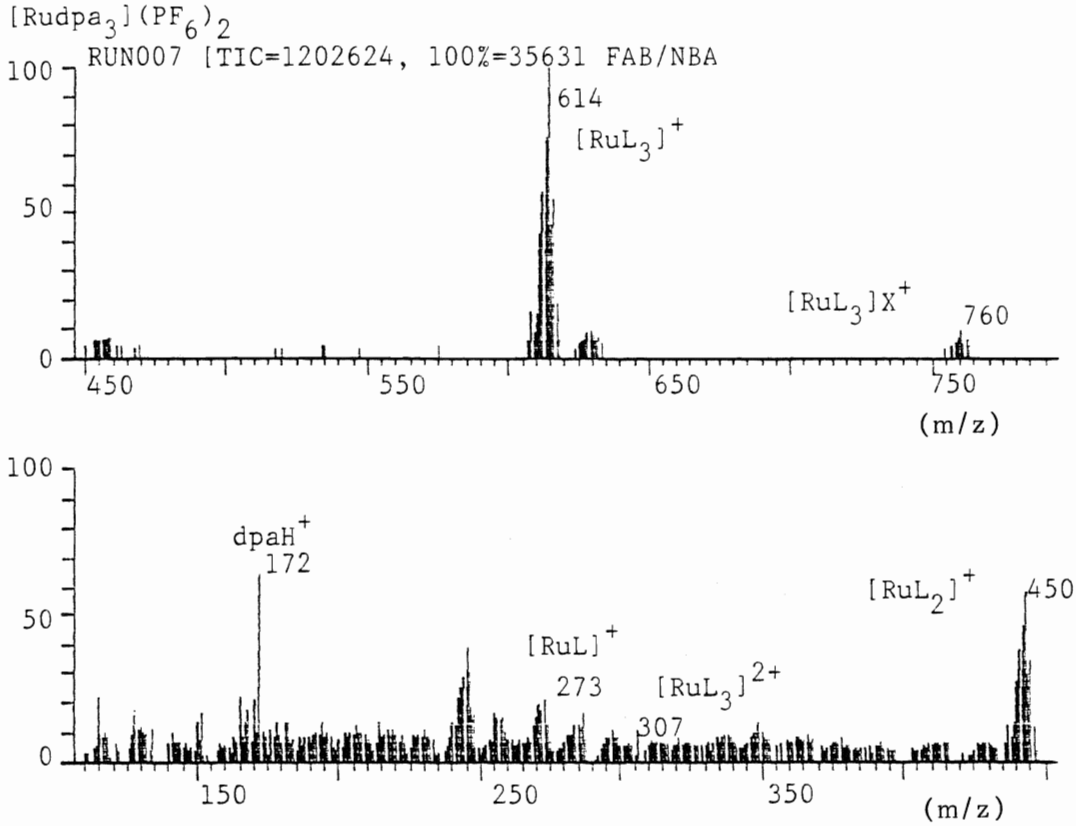

Figure A.7

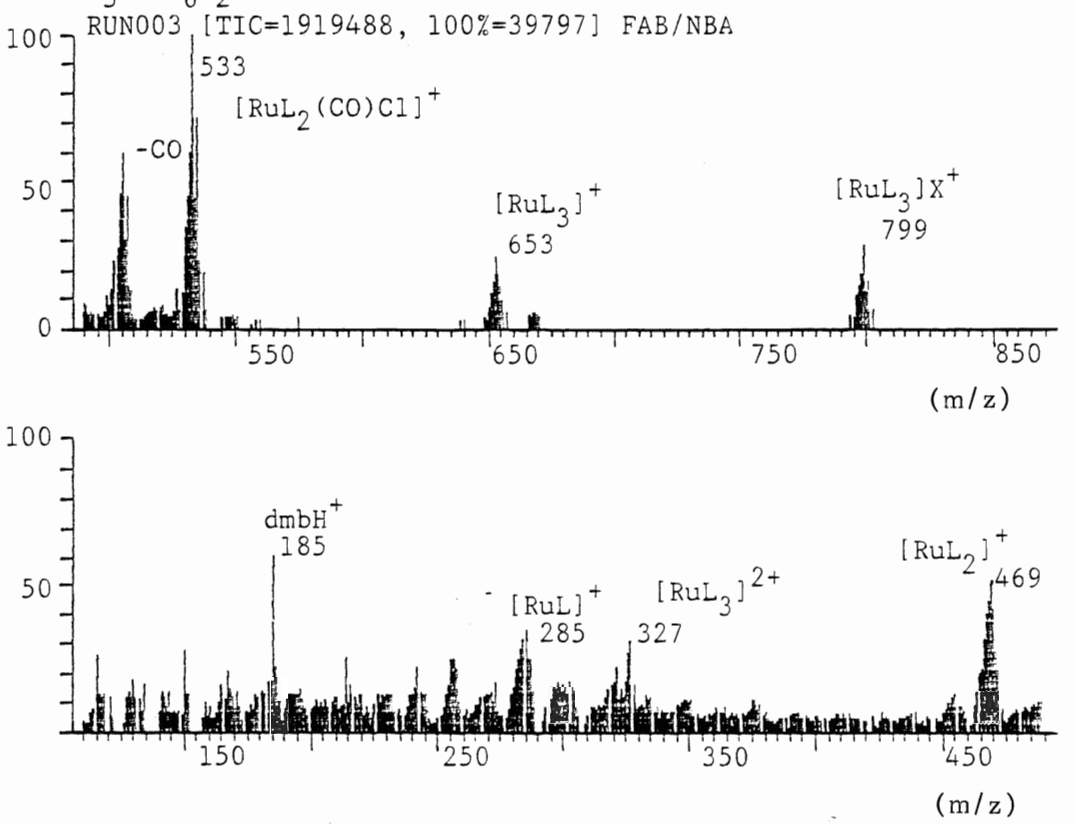

Figure A.8

[Rubpy$_2$phen](PF$_6$)$_2$

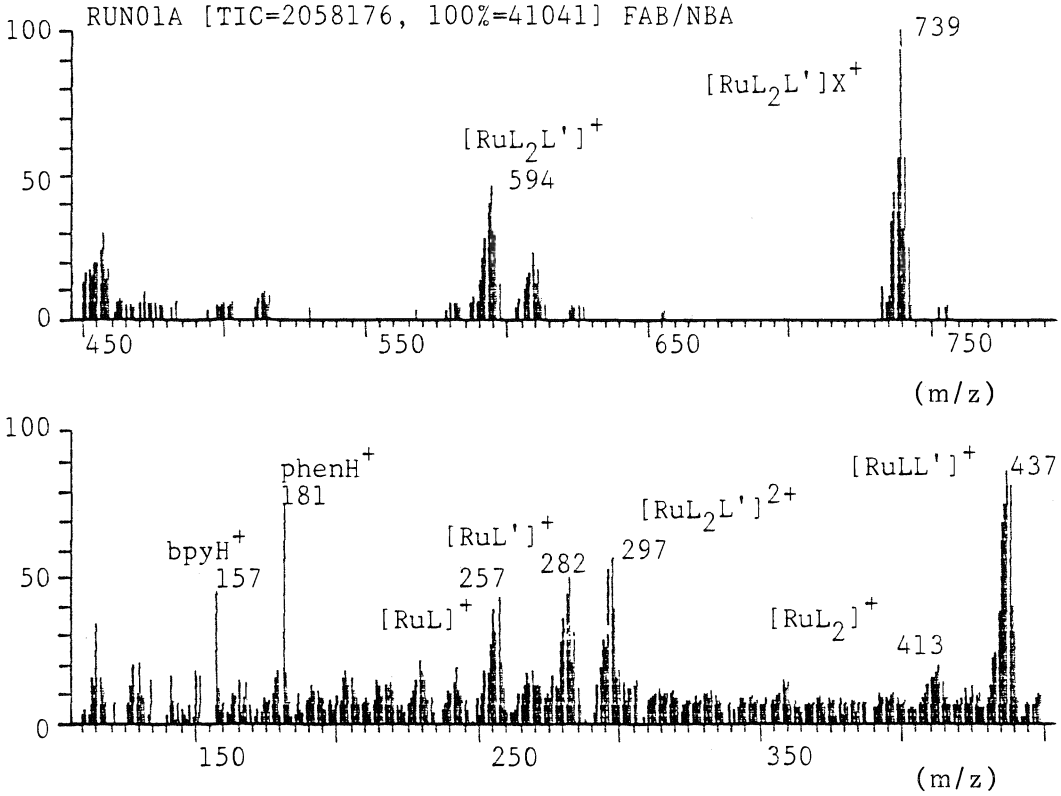

Figure A.9

[Ruphen$_2$bpy](PF$_6$)$_2$

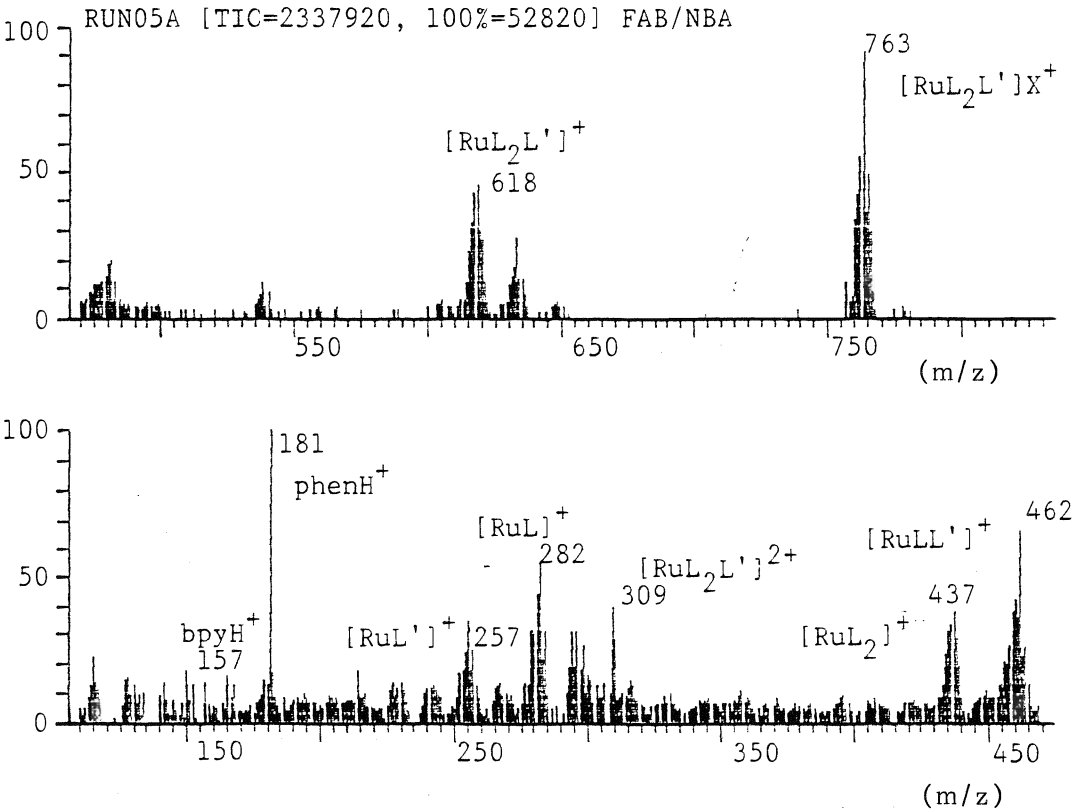

Figure A.10

[Rudmb$_2$bpy](PF$_6$)$_2$

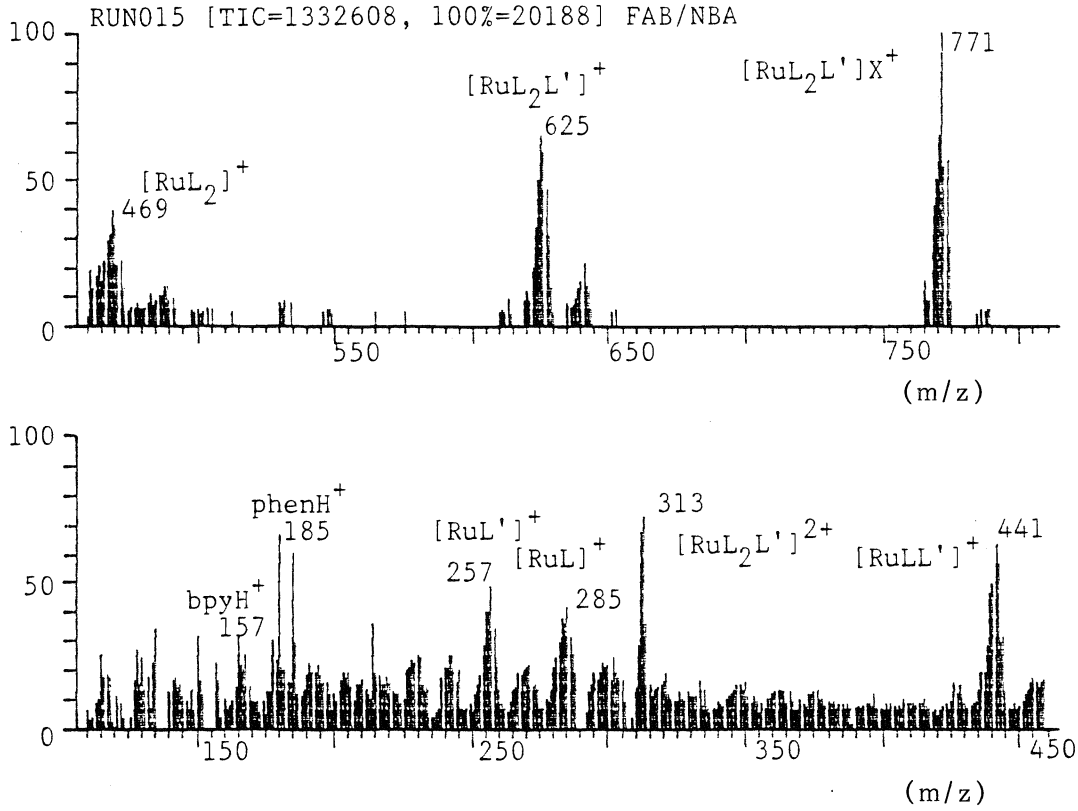

Figure A.11

[Rudmb$_2$phen](PF$_6$)$_2$

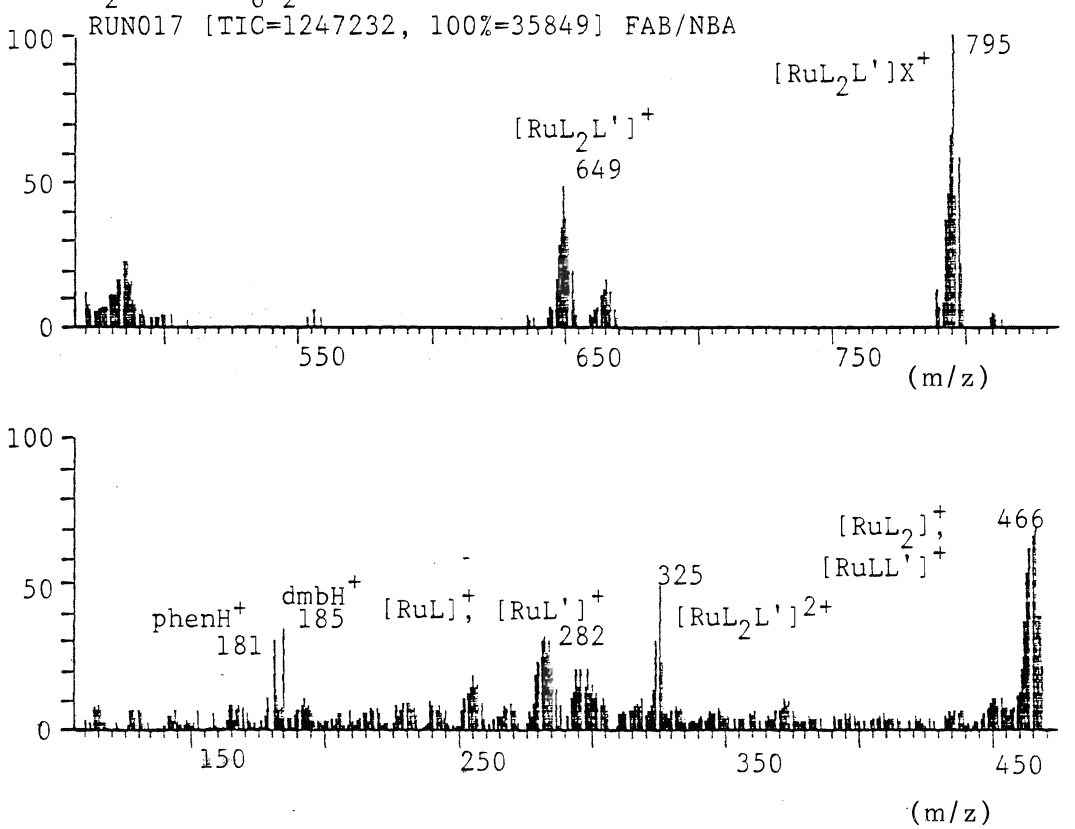

Figure A.12

[Rubpy$_2$dpa](PF$_6$)$_2$

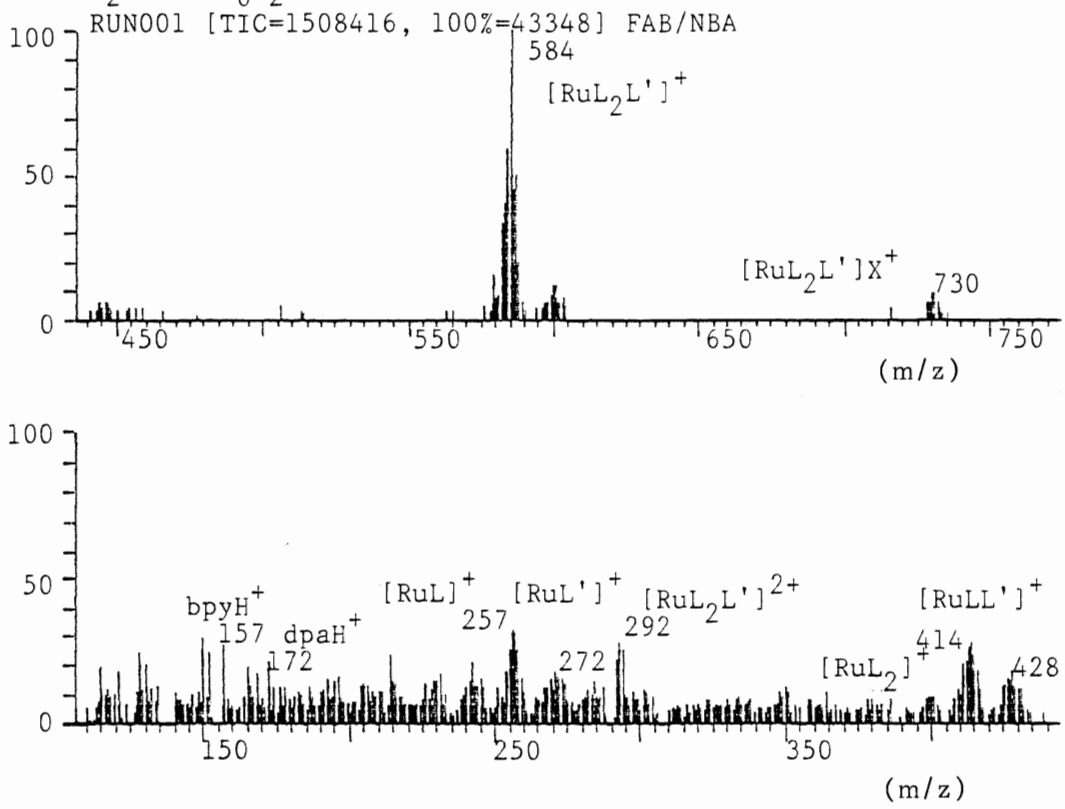

Figure A.13

[Ruphendmbbqy](PF$_6$)$_2$

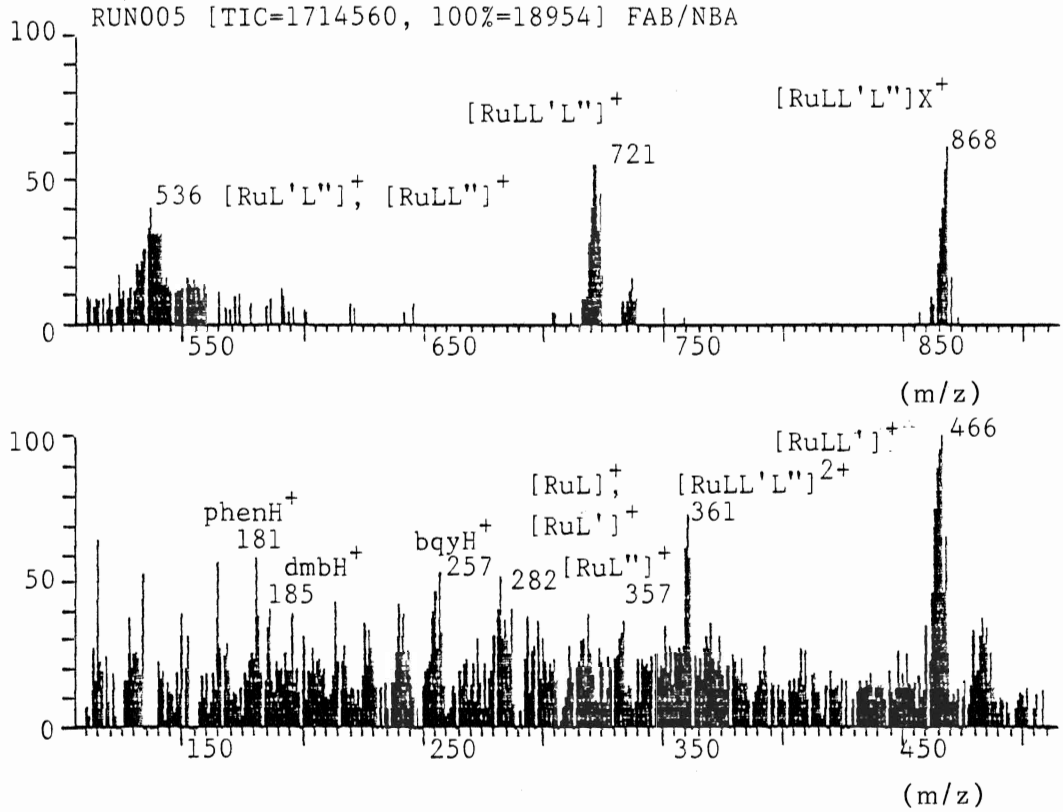

Figure A.14

[Rubpydmbbqy](PF$_6$)$_2$

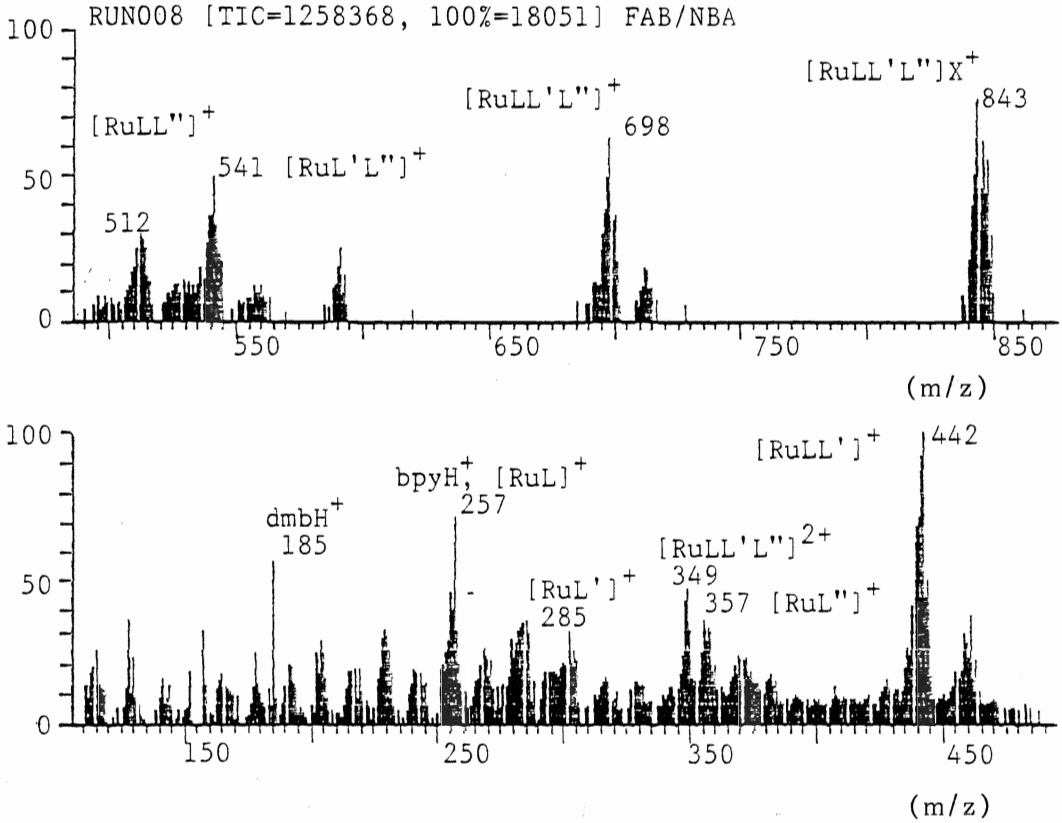

Figure A.15

[Rubpyphenbqy]$(PF_6)_2$

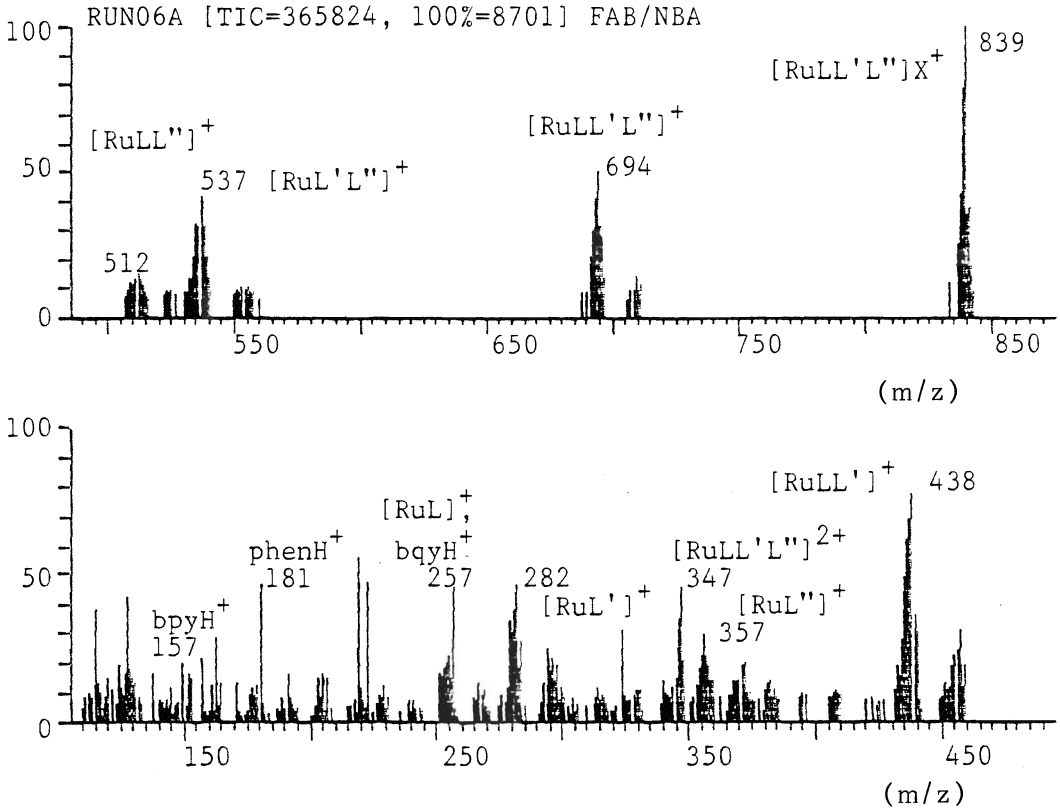

Figure A.16
[Rubpyphendmb]$(PF_6)_2$

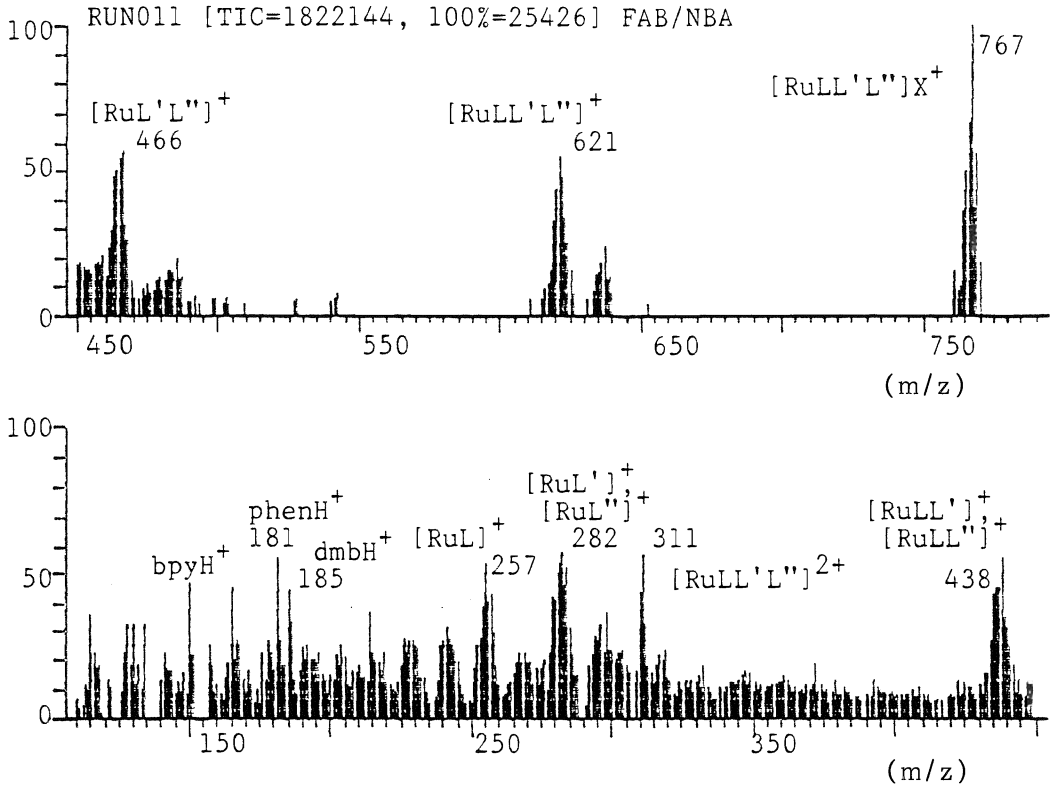

Figure A.17
[Rubpyphendpk]$(PF_6)_2$

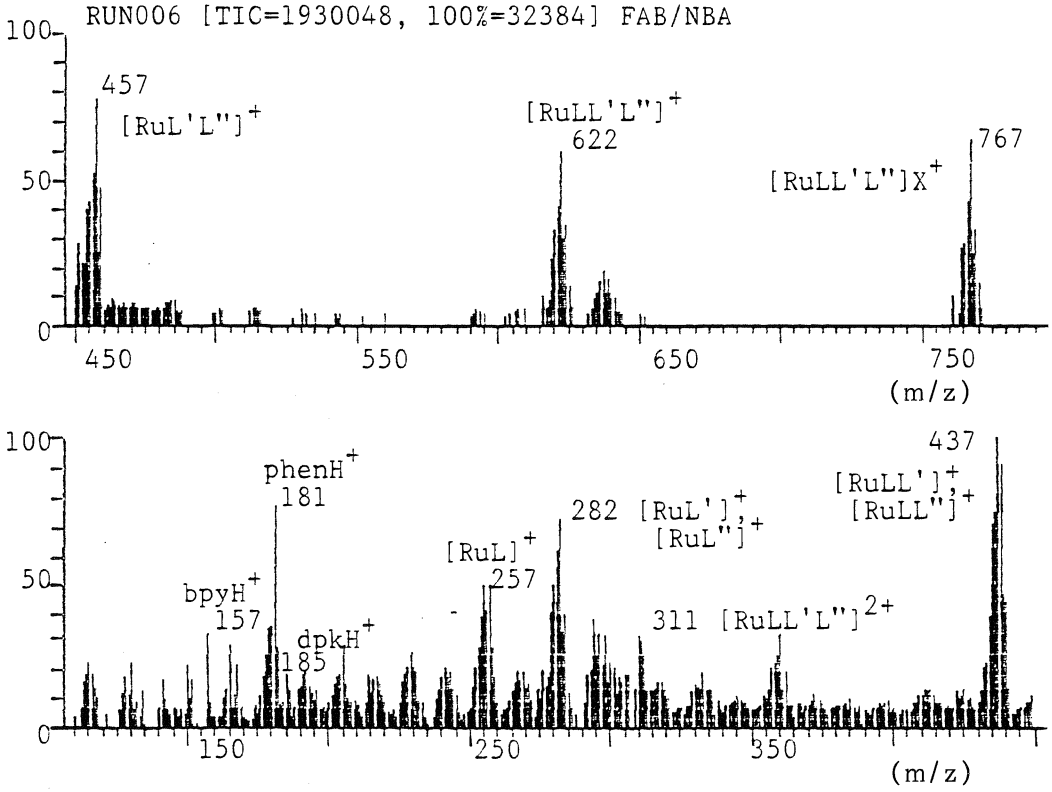

Figure A.18
[Rubpyphentmp]$(PF_6)_2$

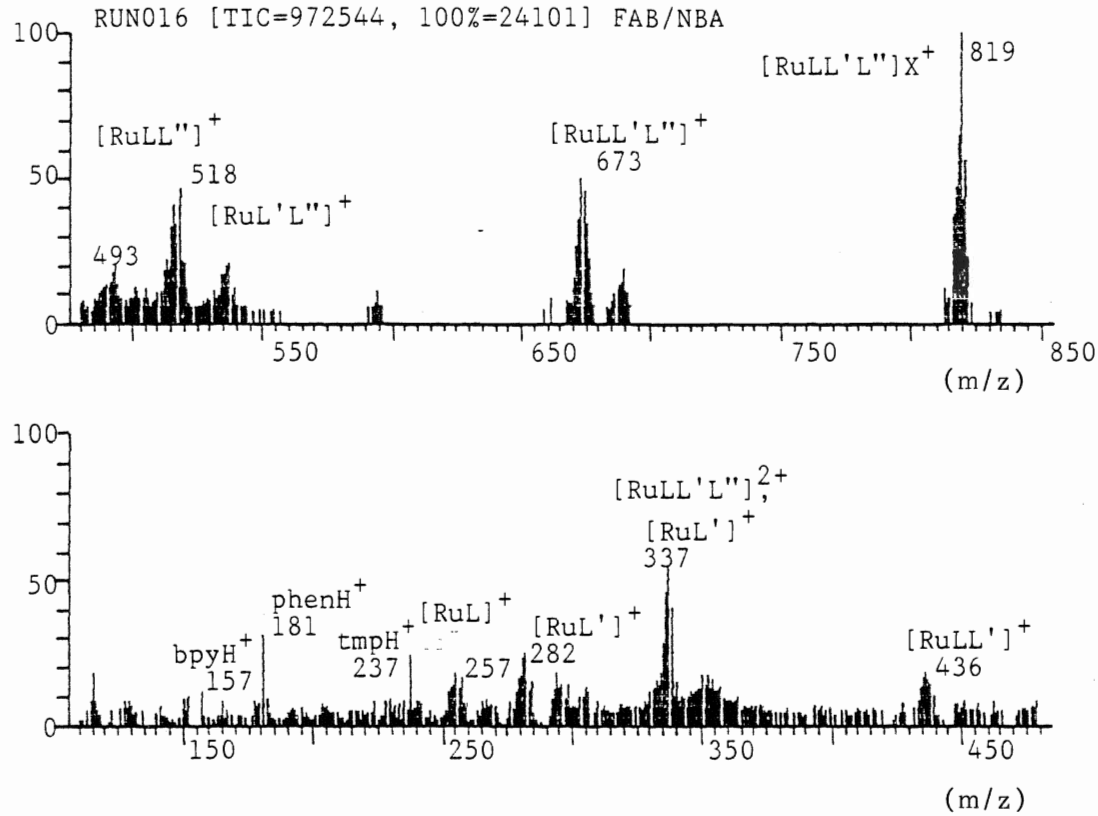

Figure A.19
[Rubpydmbdib]$(PF_6)_2$

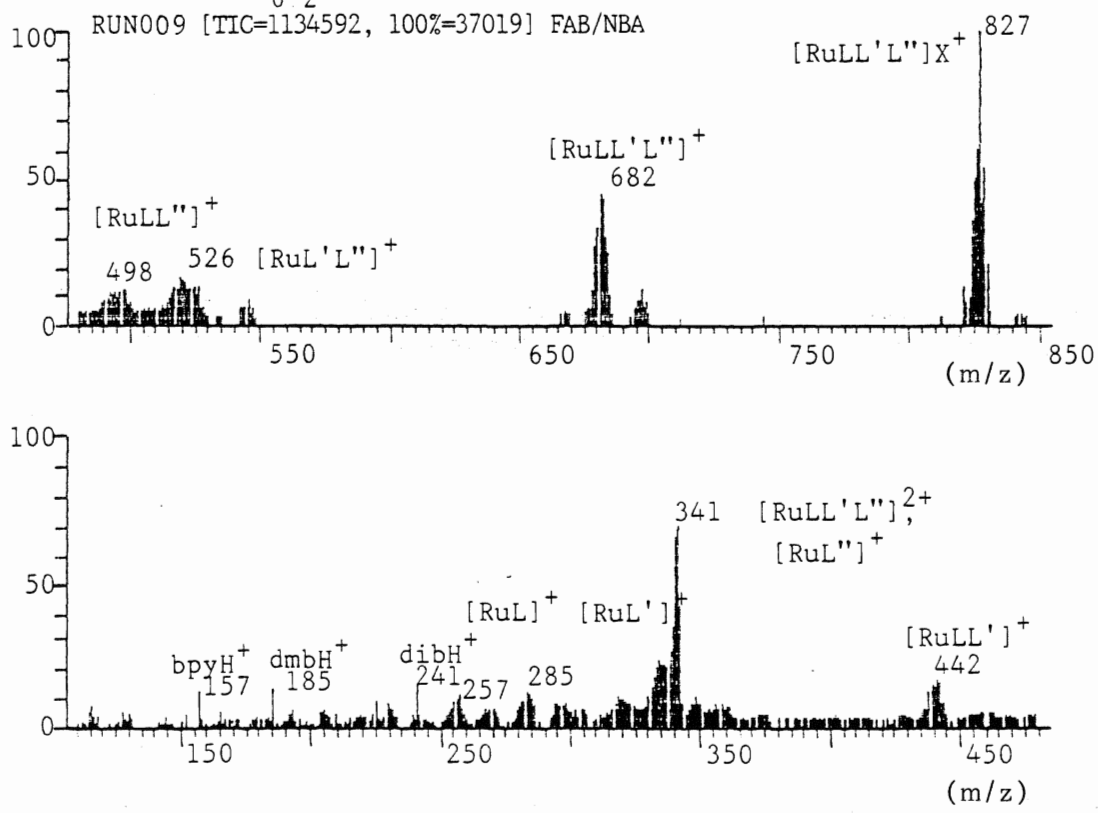

Figure A.20
[Rubpyphendzf]$(PF_6)_2$

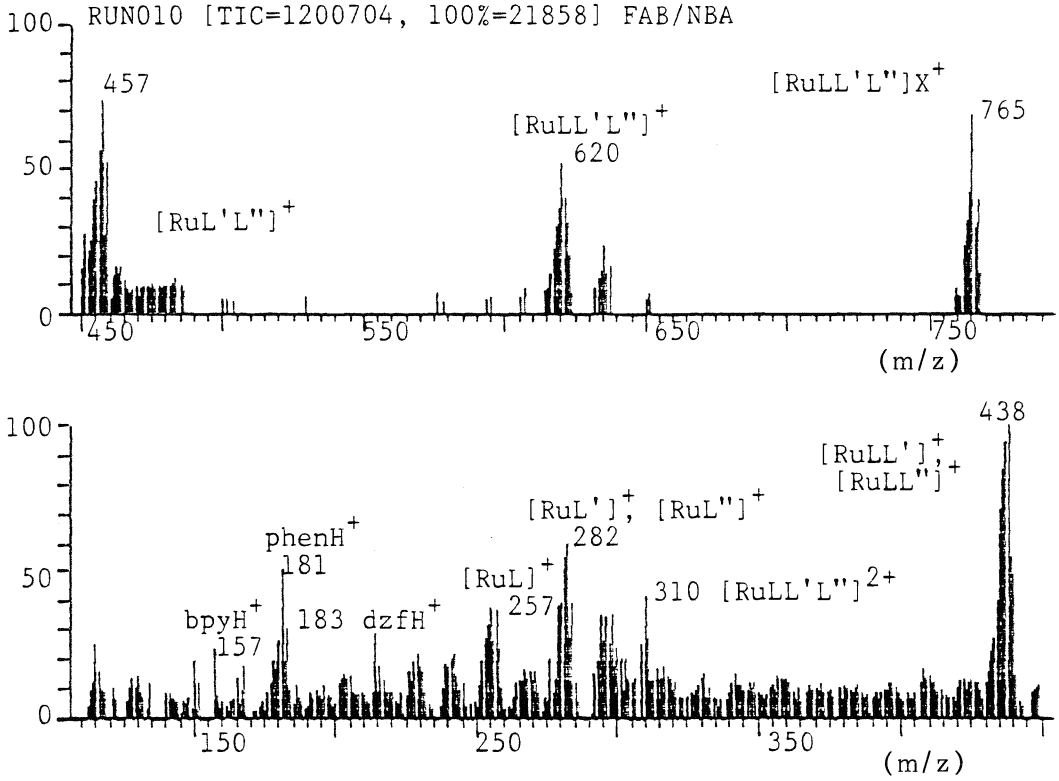

Figure A.21

[Rubpyphendpa]$(PF_6)_2$

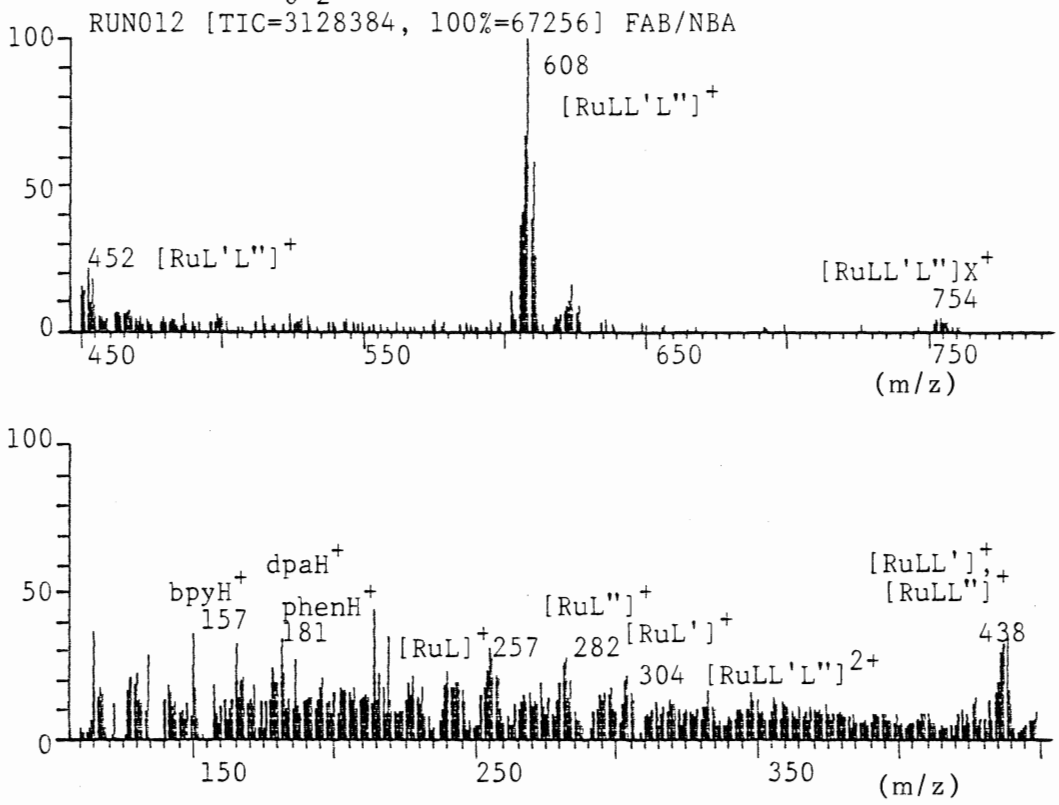

Figure A.22

[Rudmbphendpa]$(PF_6)_2$

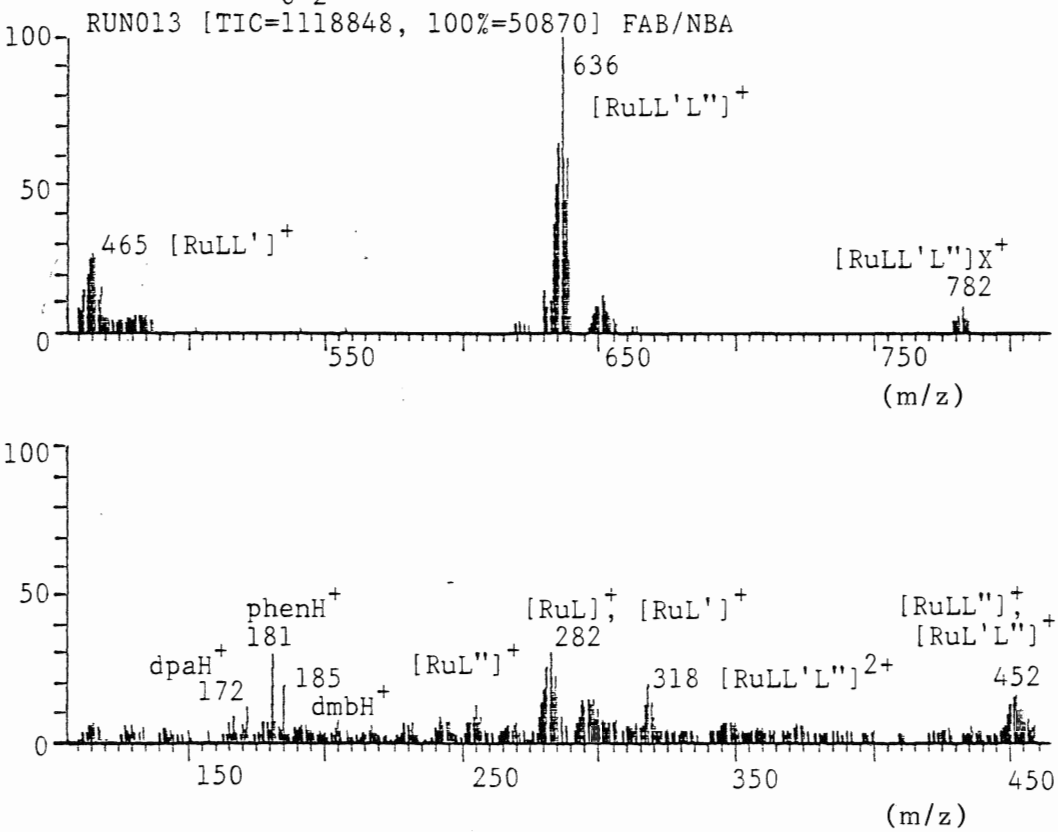

Figure A.23
[Rubpyphen(CO)Cl](PF$_6$)

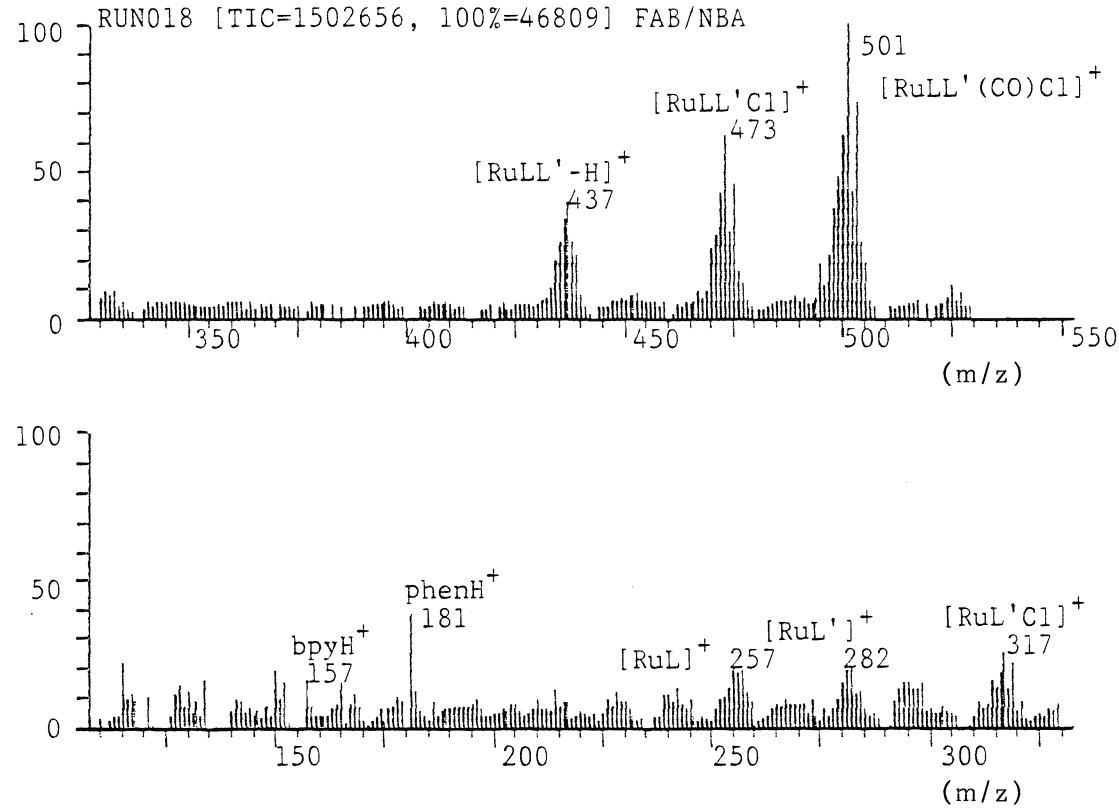

Figure A.24
[Rubpydmb(CO)Cl](PF$_6$)

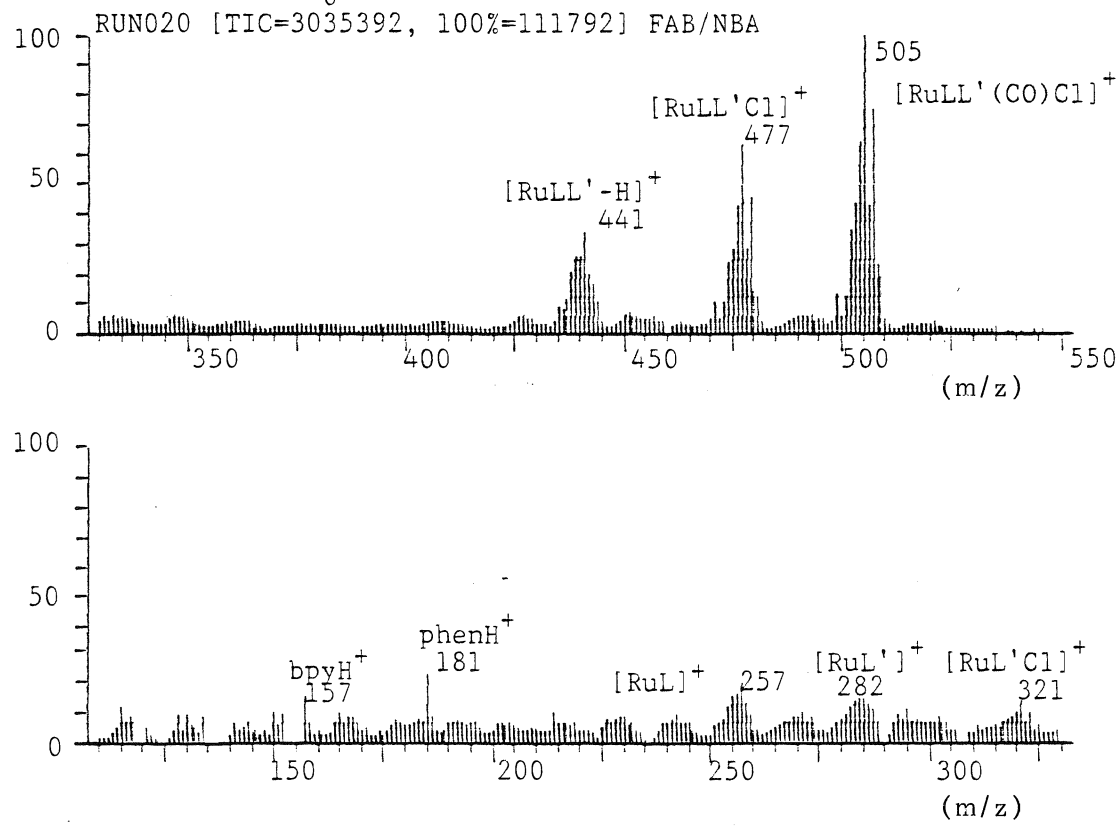

Figure A.25
[RubpyBq(CO)]Cl

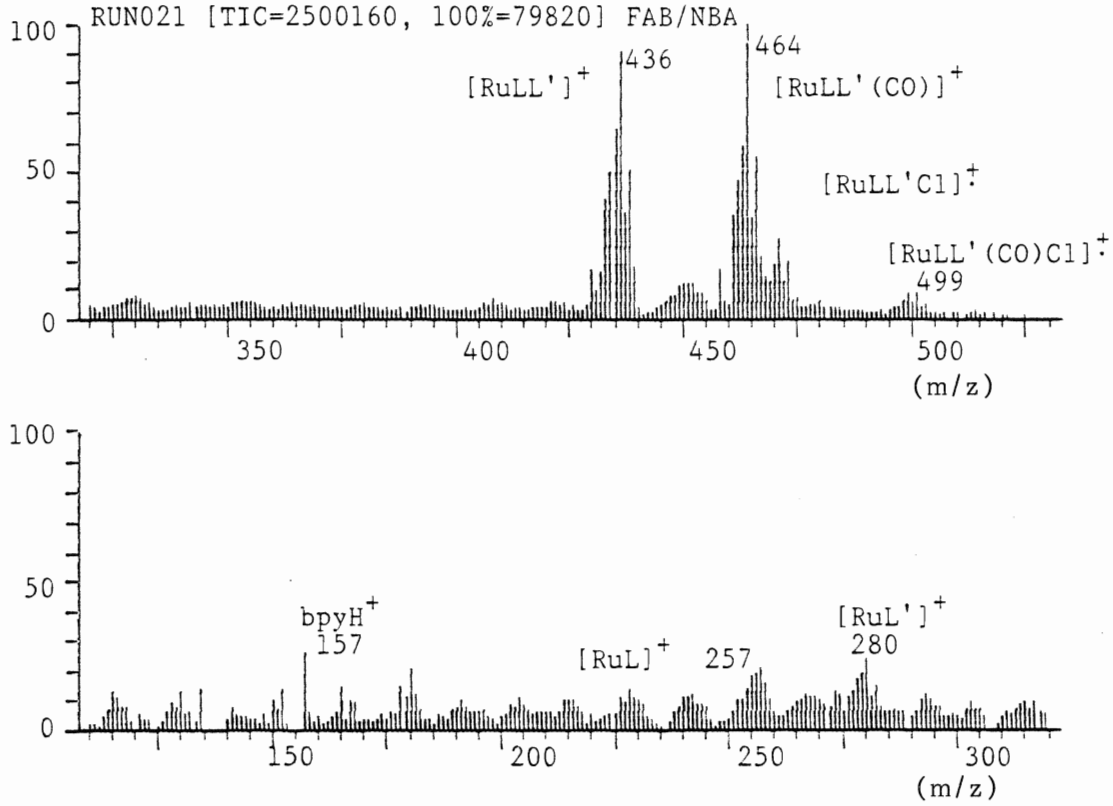

Figure A.26
[RubpytpyCl](PF$_6$)

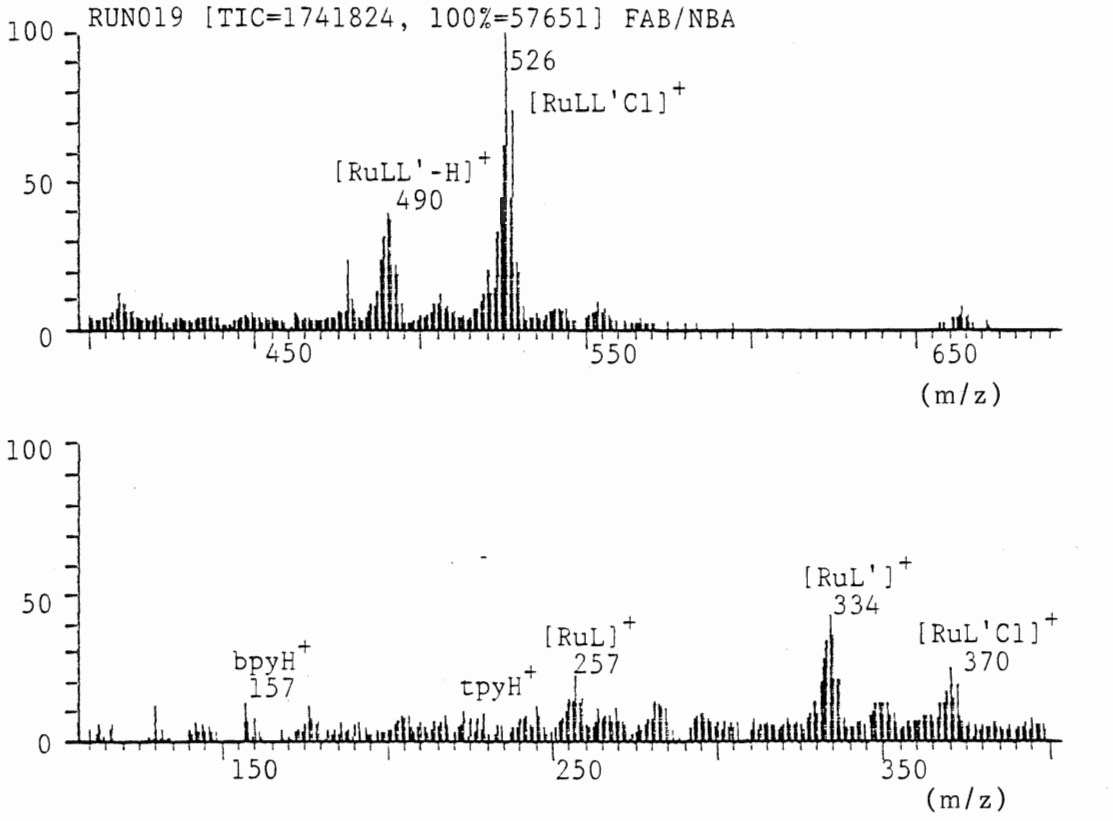

Appendix B

Positive Ion FAB and EI Mass Spectra of Group (V) Triptycenes and Related Complexes

Figure 1. $P(C_6H_4Cl)_3$

Figure 2. $As(C_6H_4Cl)_3$

Figure 3. $Sb(C_6H_4Cl)_3$

Figure 4. $Bi(C_6H_4Cl)_3$

Figure 5. $P(C_6F_4Br)_3$

Figure 6. $As(C_6F_4Br)_3$

Figure 7. $Sb(C_6F_4Br)_3$

Figure 8. $CH_3Si(C_6F_4Br)_3$

Figure 9. $As(C_6F_4H)_3$

Figure 10. $P_2(C_6F_4)_3$

Figure 11. $As_2(C_6F_4)_3$

Figure 12. $Sb_2(C_6F_4)_3$

Figure 13. $Bi_2(C_6F_4)_3$

Figure 14. $(CH_3Si)_2(C_6F_4)_3$

Figure 15. $PSb(C_6F_4)_3$

Figure 16. $AsSb(C_6F_4)_3$

Figure B.1a P= $P(C_6H_4Cl)_3$

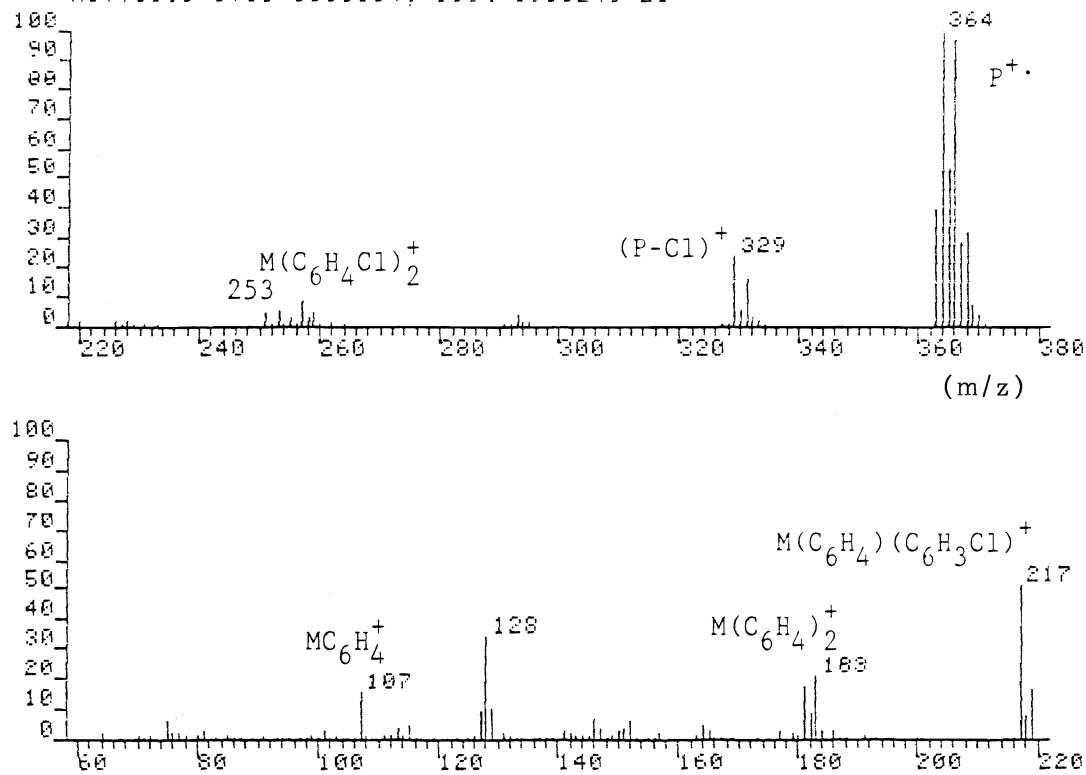

Figure B.1b

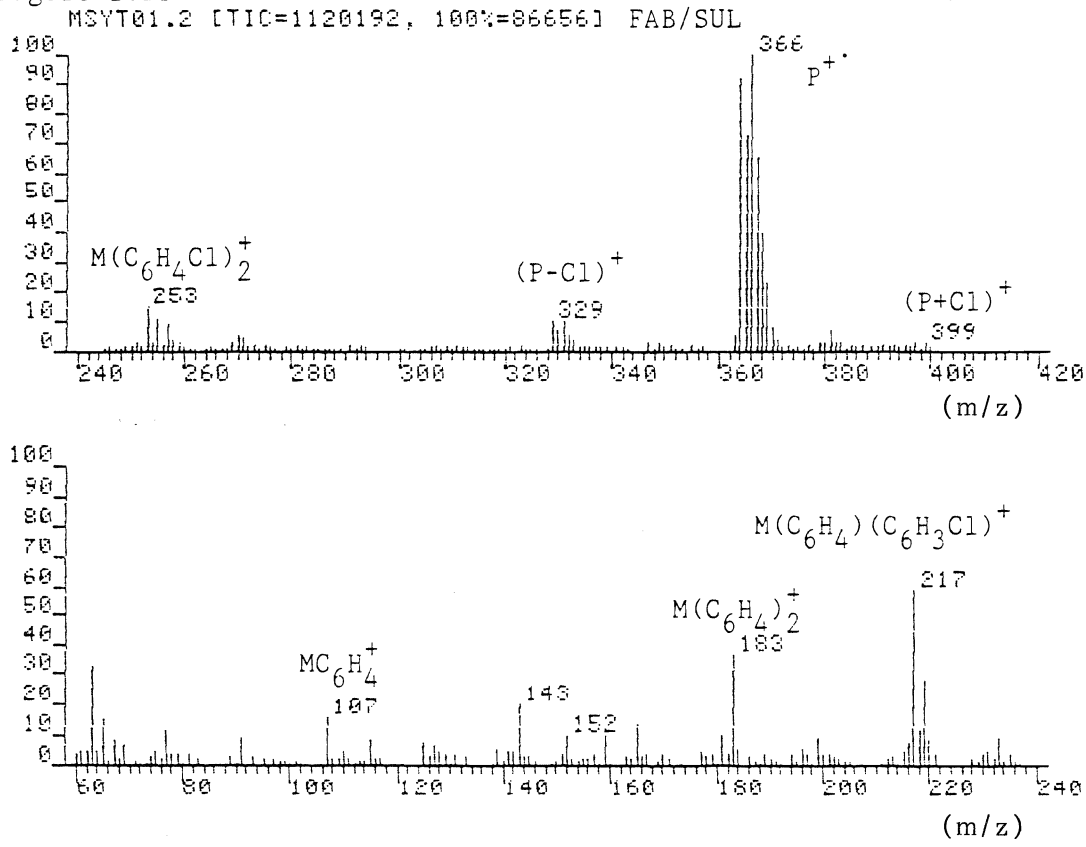

Figure B.2a $P=As(C_6H_4Cl)_3$

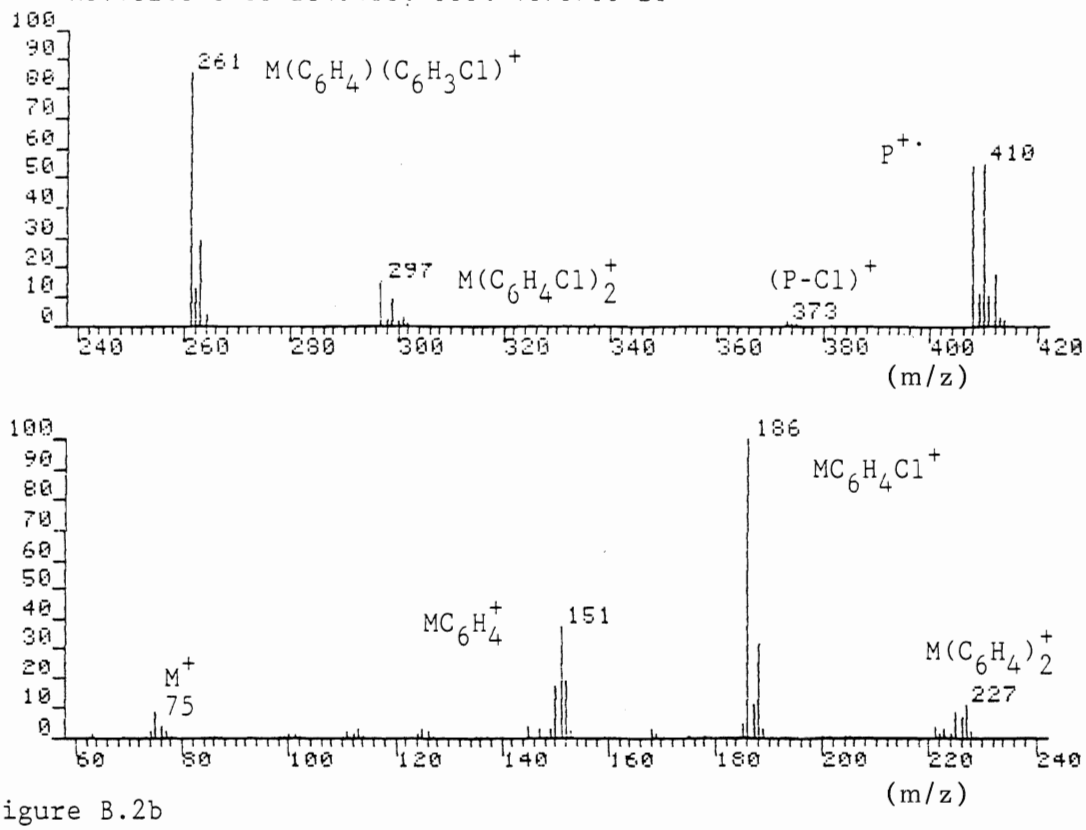

Figure B.2b

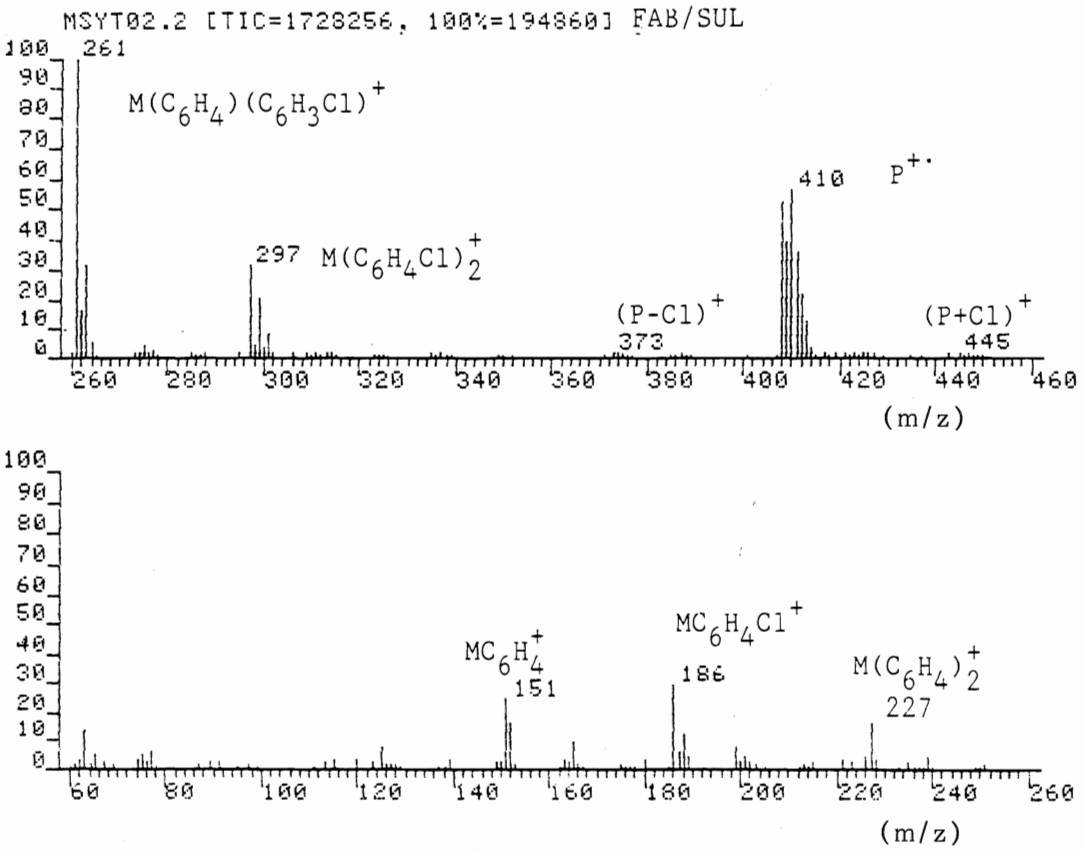

Figure B.3a P= $Sb(C_6H_4Cl)_3$

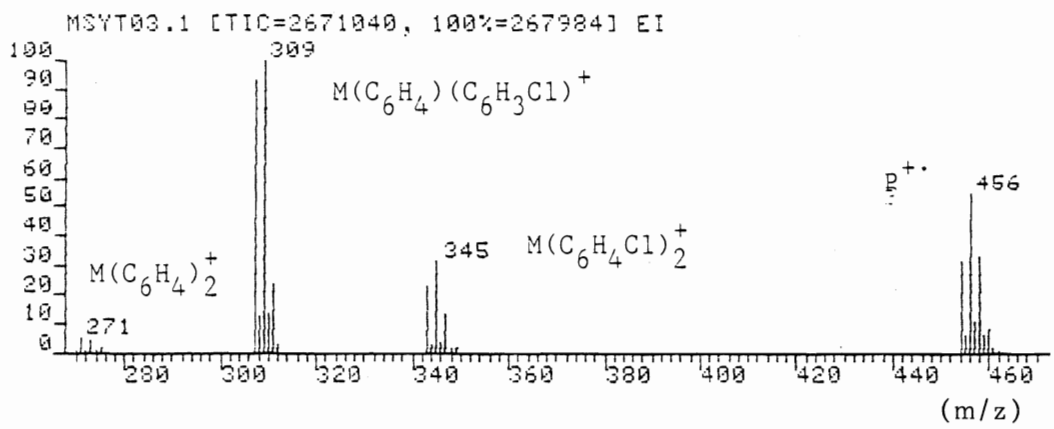

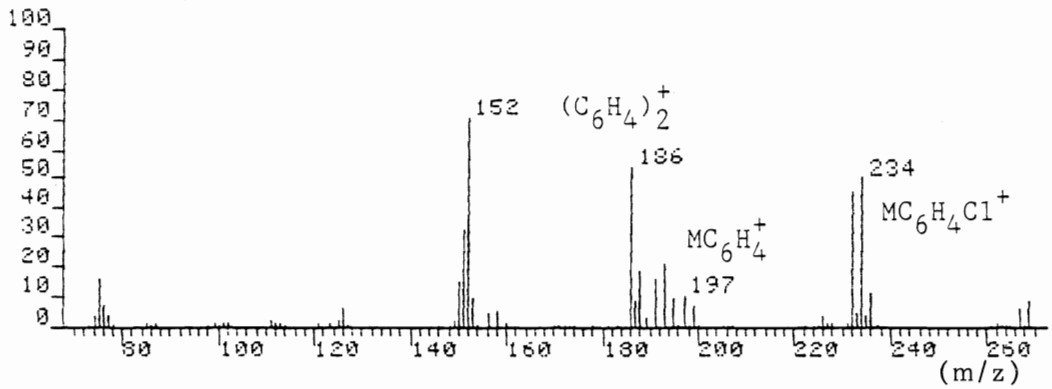

Figure B.3b

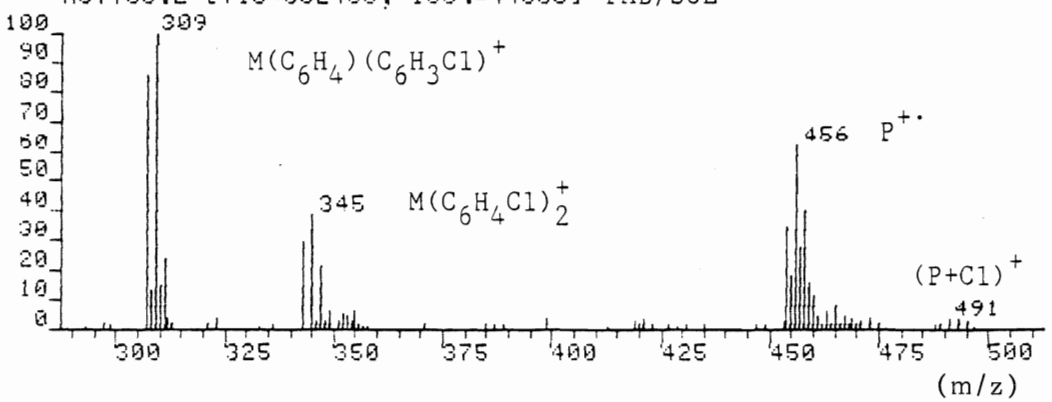

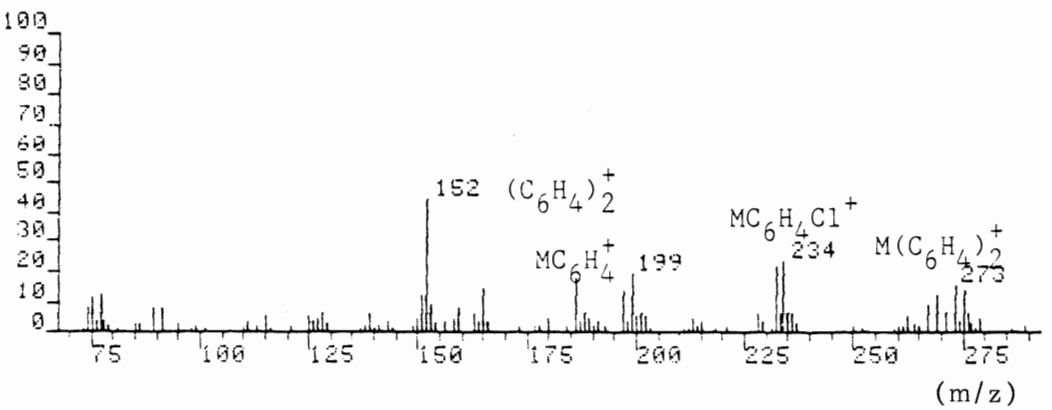

Figure B.4a P= $Bi(C_6H_4Cl)_3$

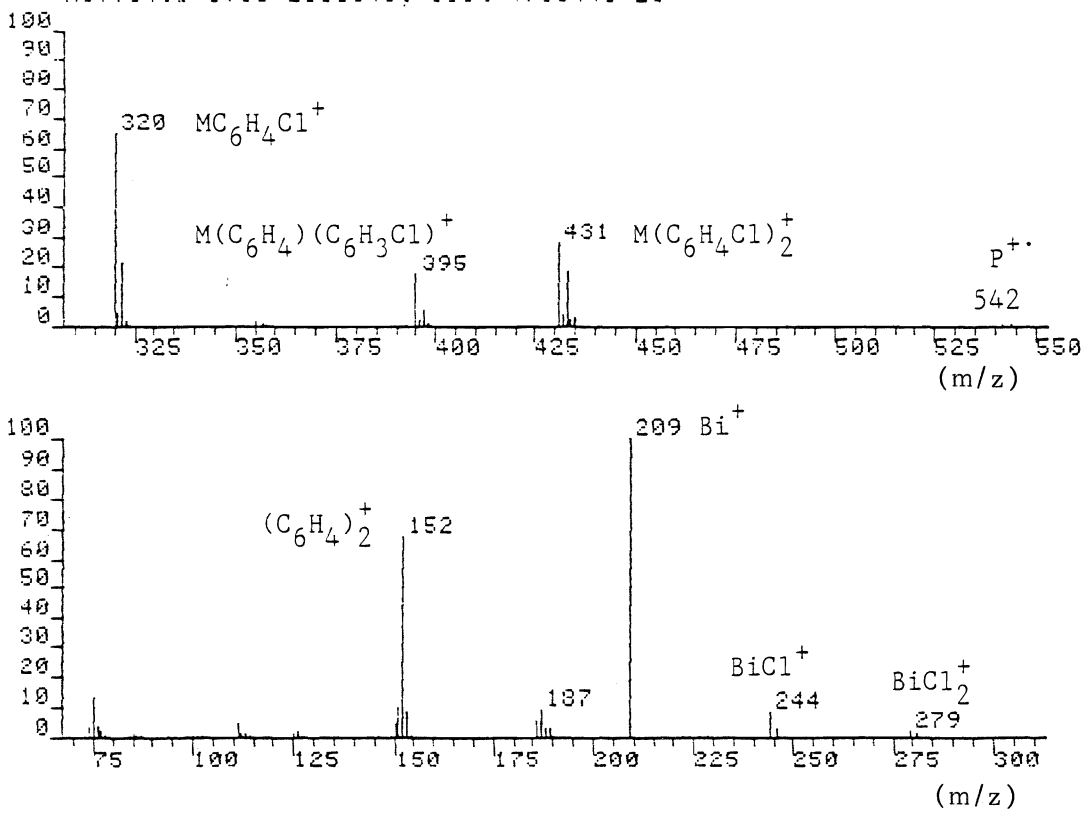

Figure B.4b

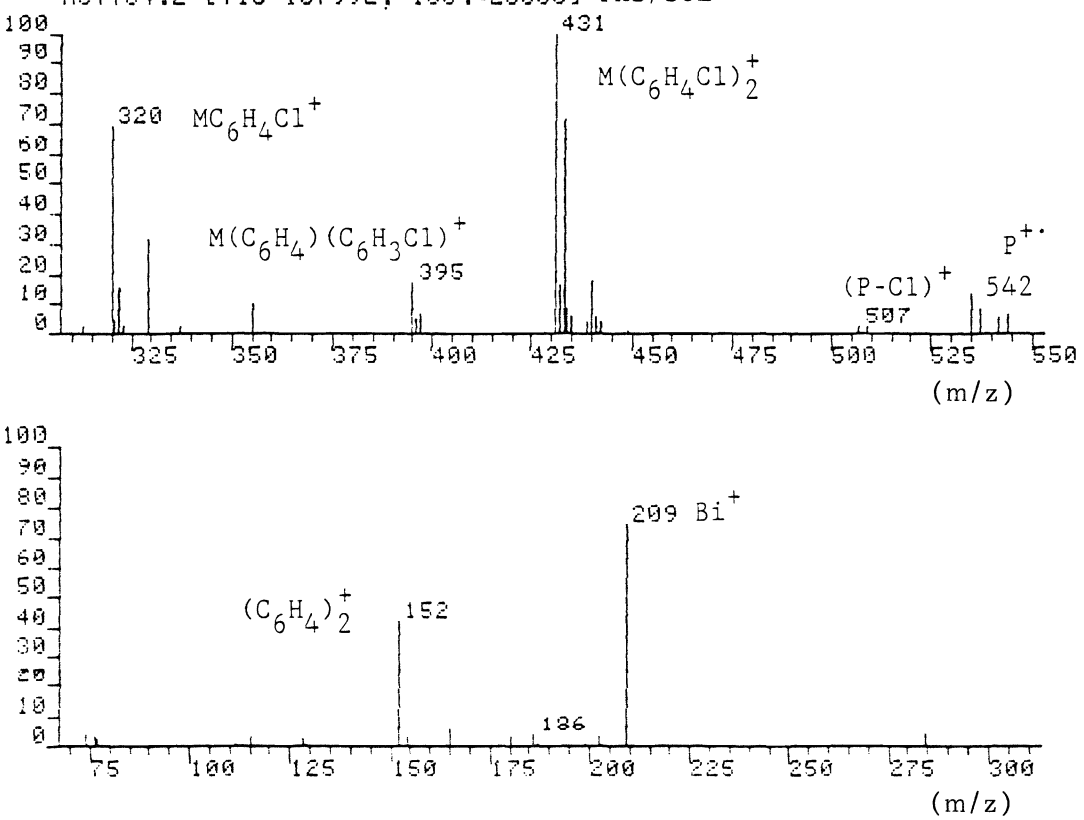

Figure B.5a P= $P(C_6F_4Br)_3$

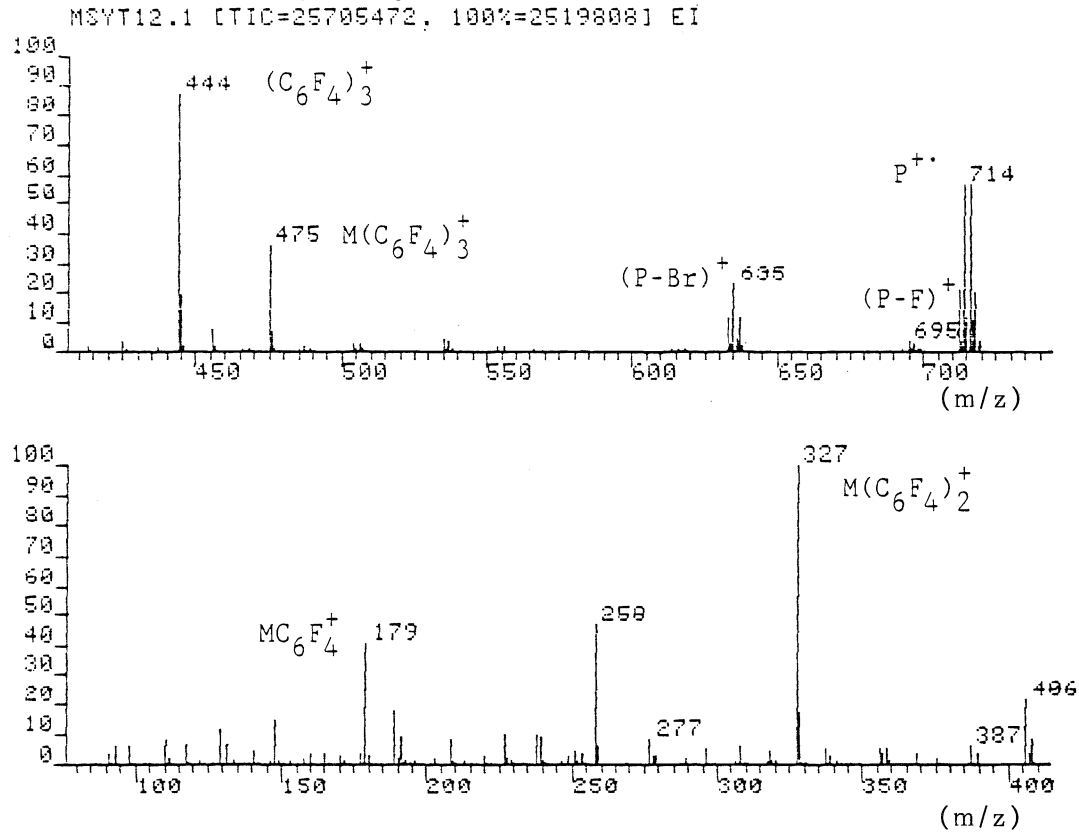

Figure B.5b

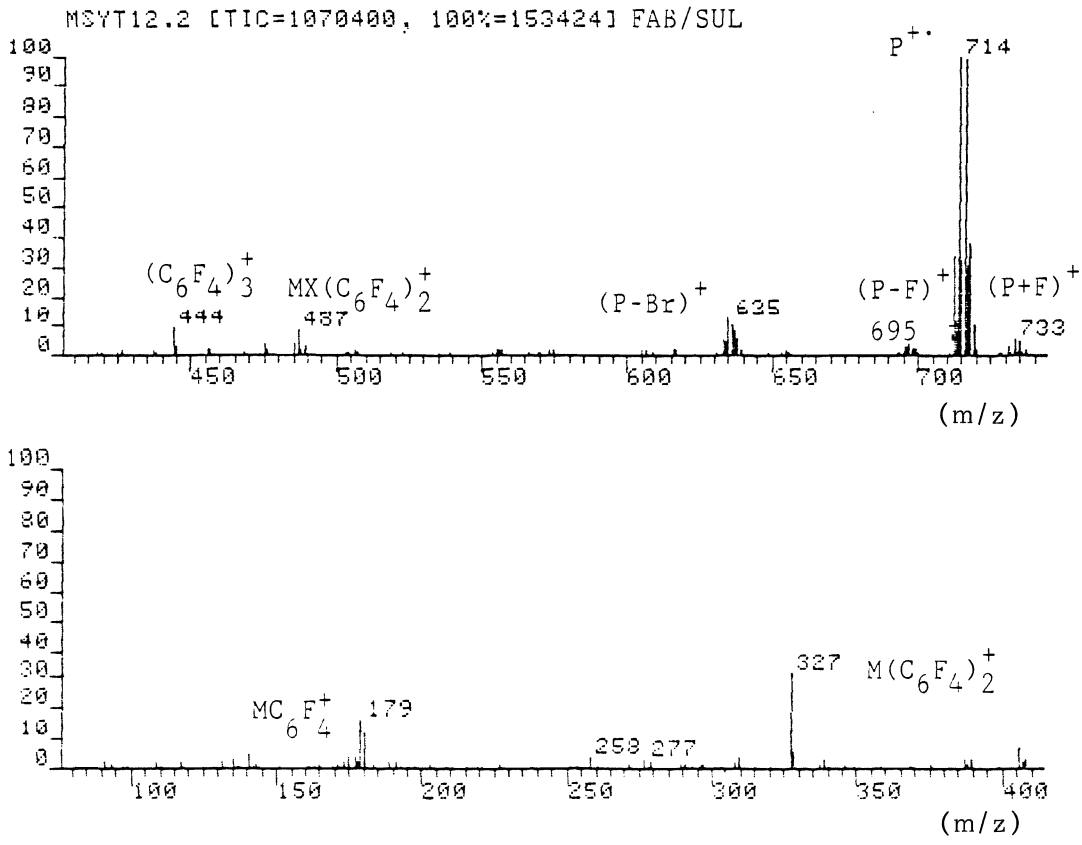

Figure B.6a P= $As(C_6F_4Br)_3$

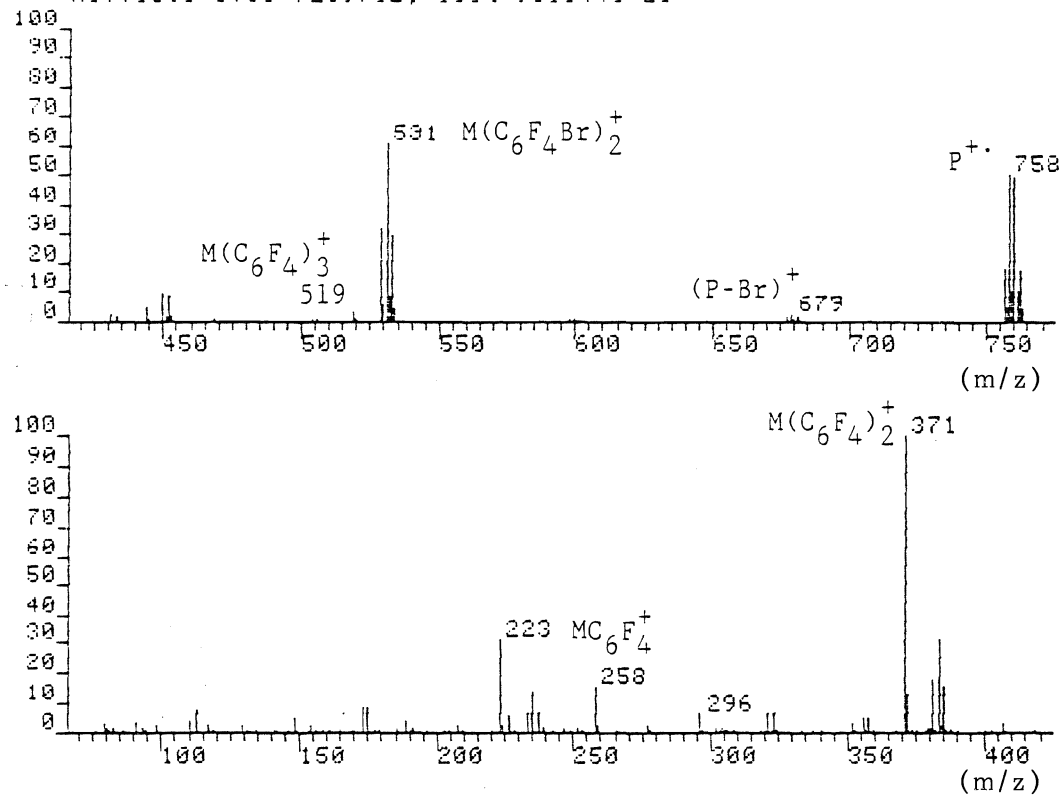

Figure B.6b

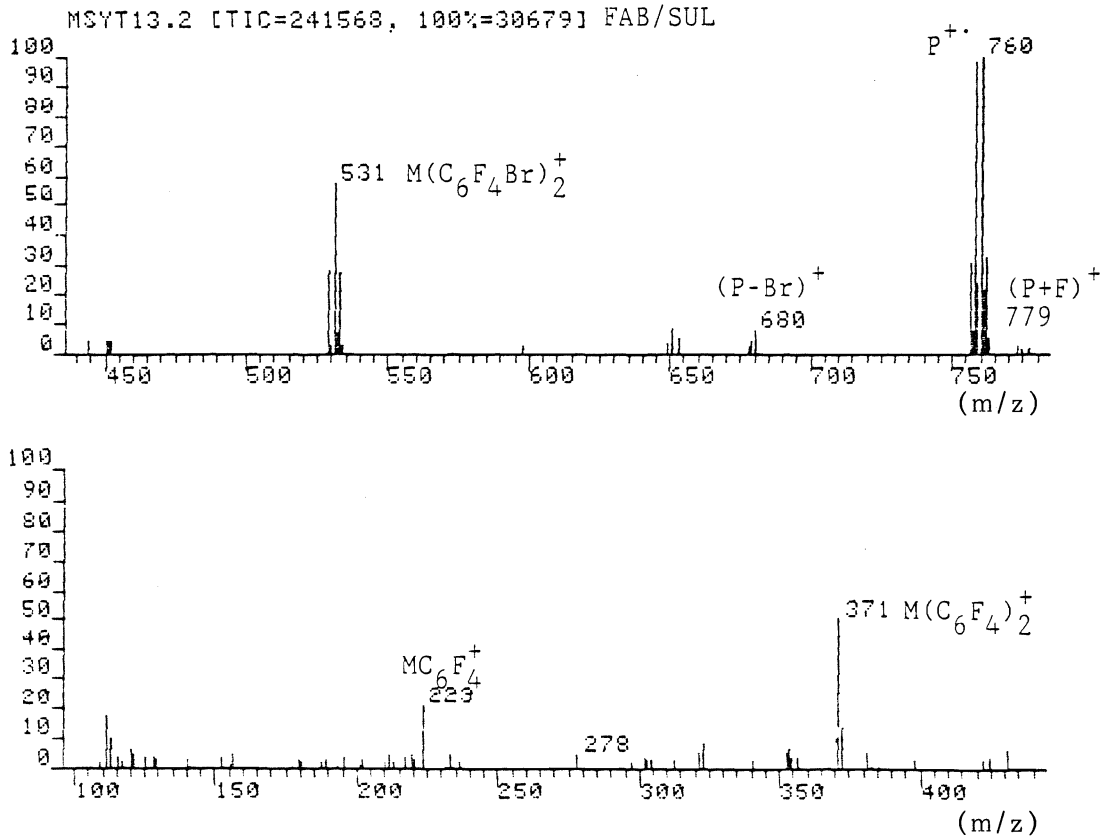

Figure B.7a P= $Sb(C_6F_4Br)_3$

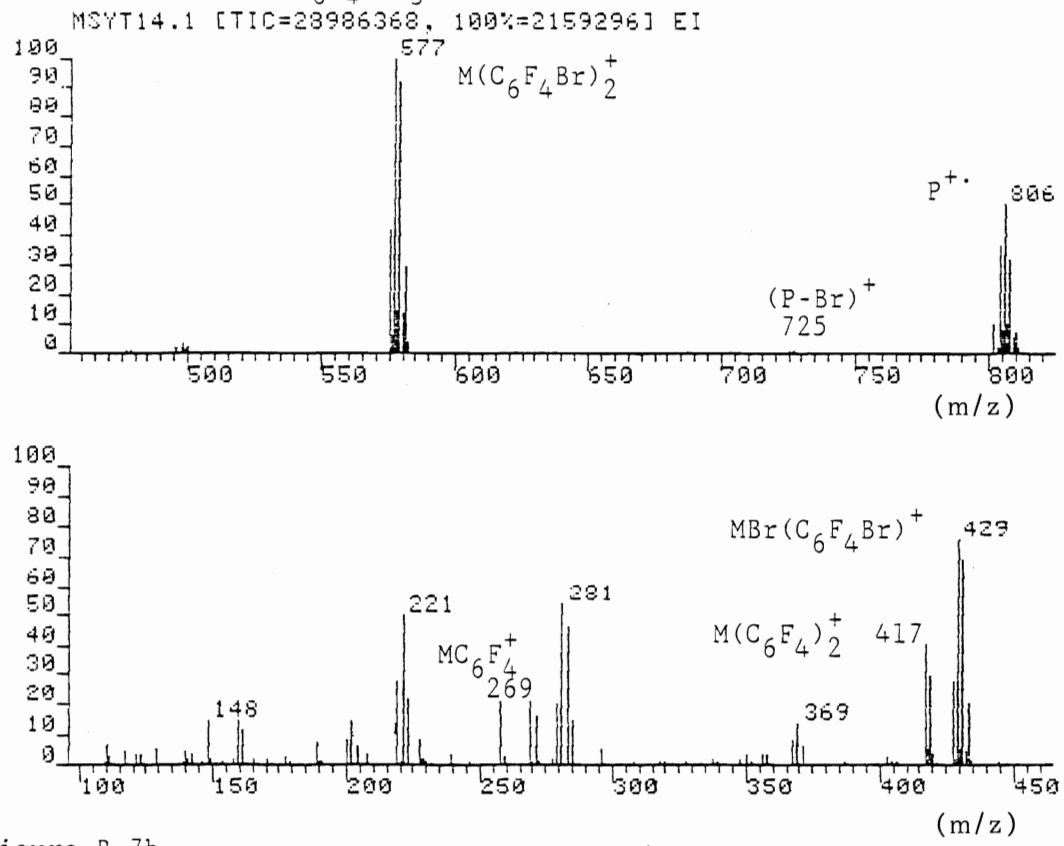

Figure B.7b

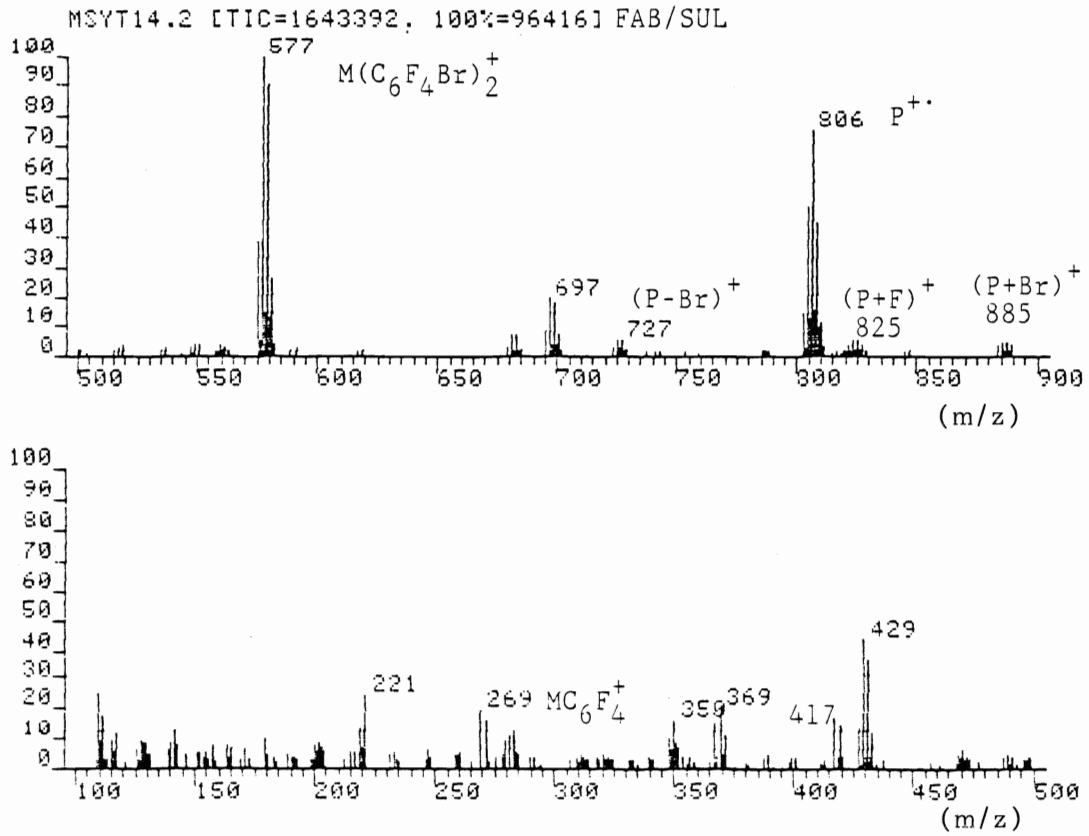

Figure B 8.a P= $CH_3Si(C_6F_4Br)_3$

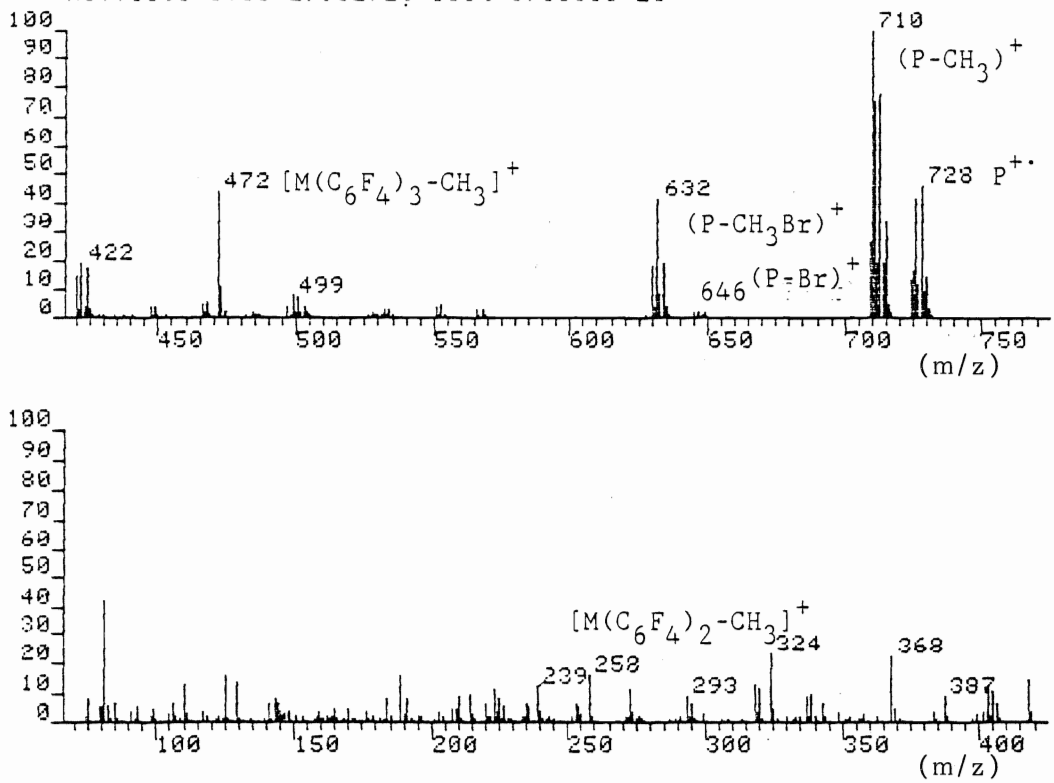

Figure B8.b

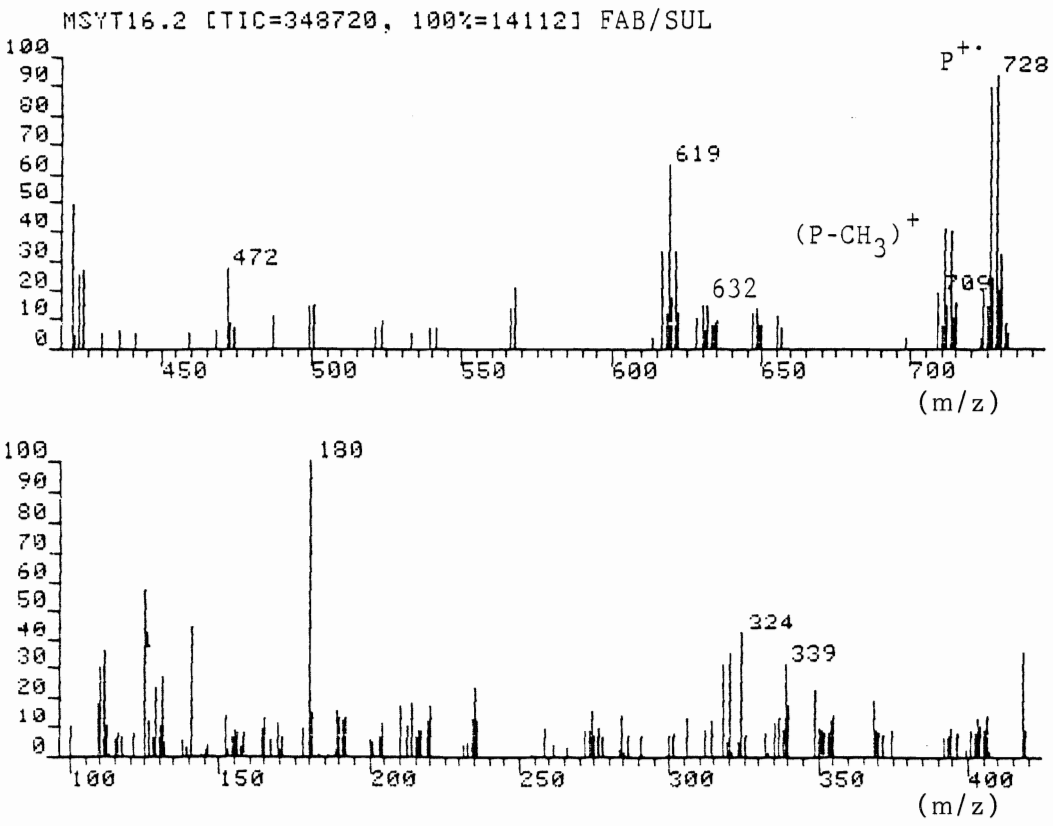

Figure B9.a P= $As(C_6F_4H)_3$

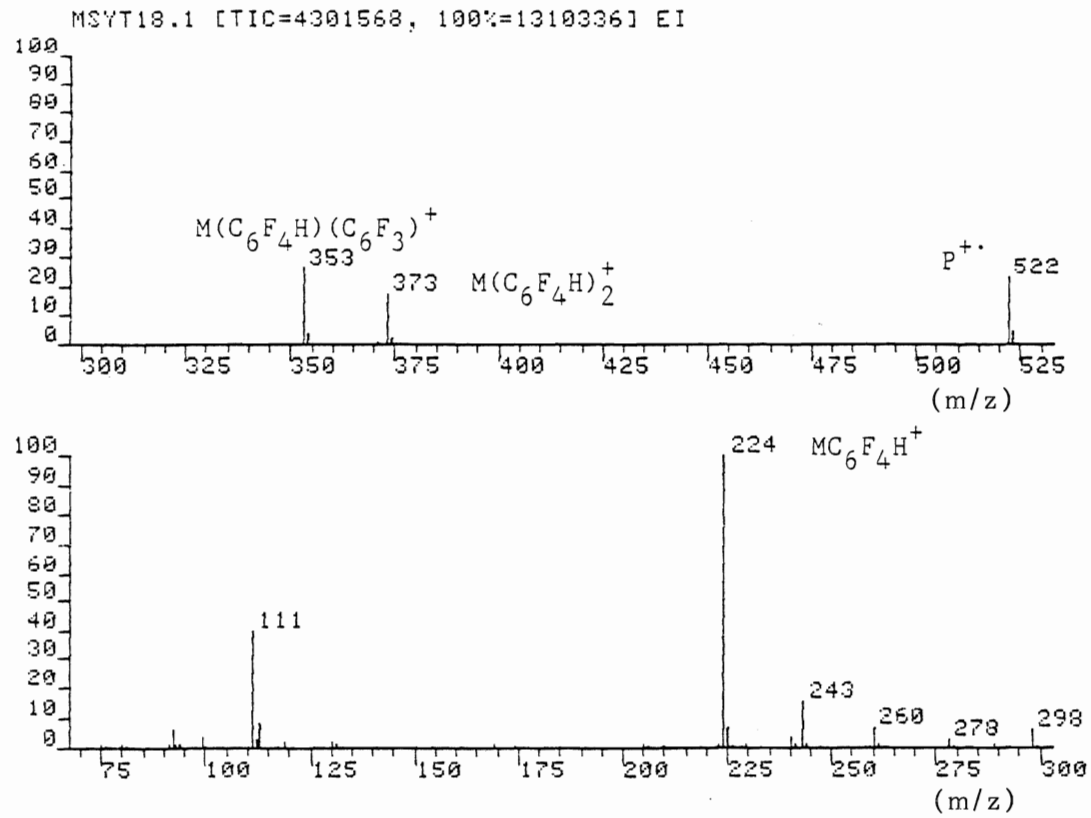

Figure B9.b

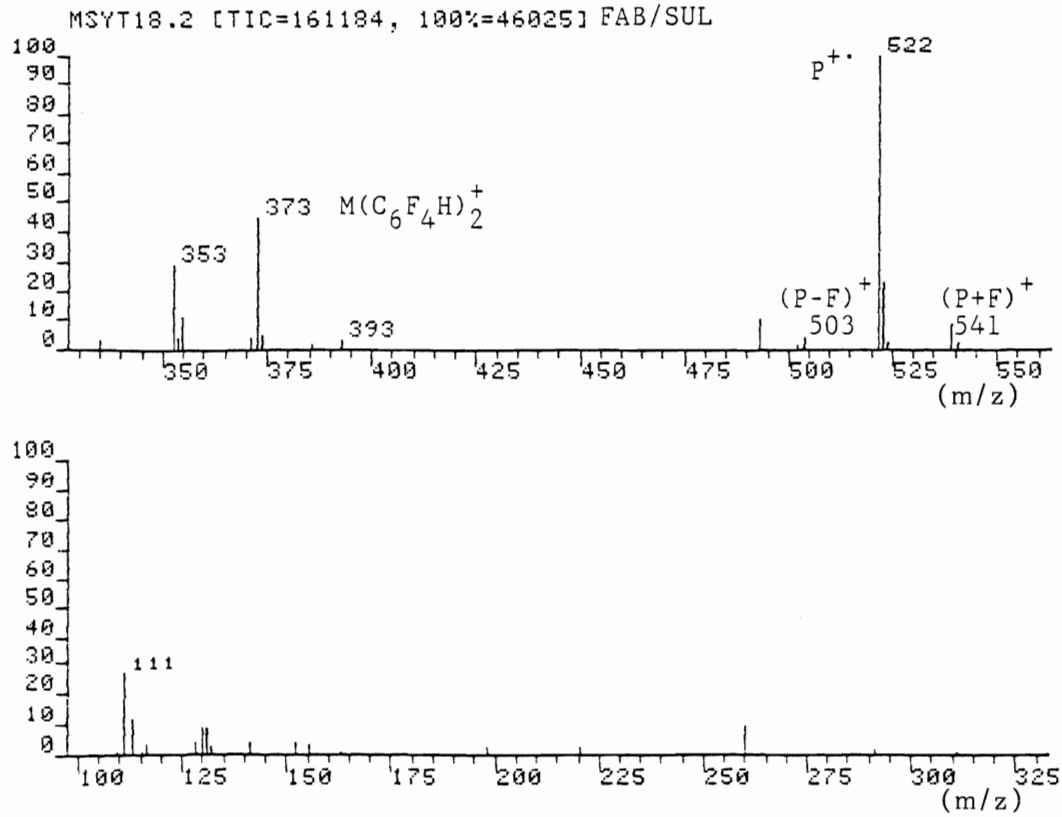

Figure B.10a P= $P_2(C_6F_4)_3$

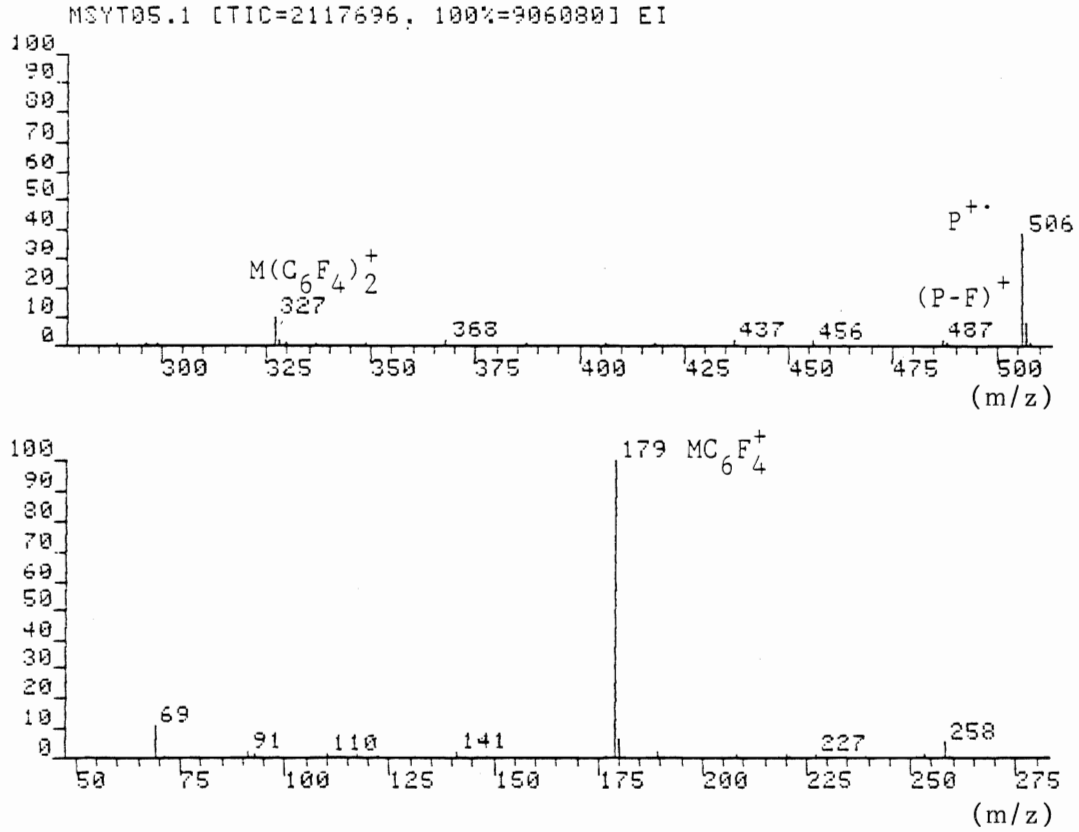

Figure B.11a P= $As_2(C_6F_4)_3$

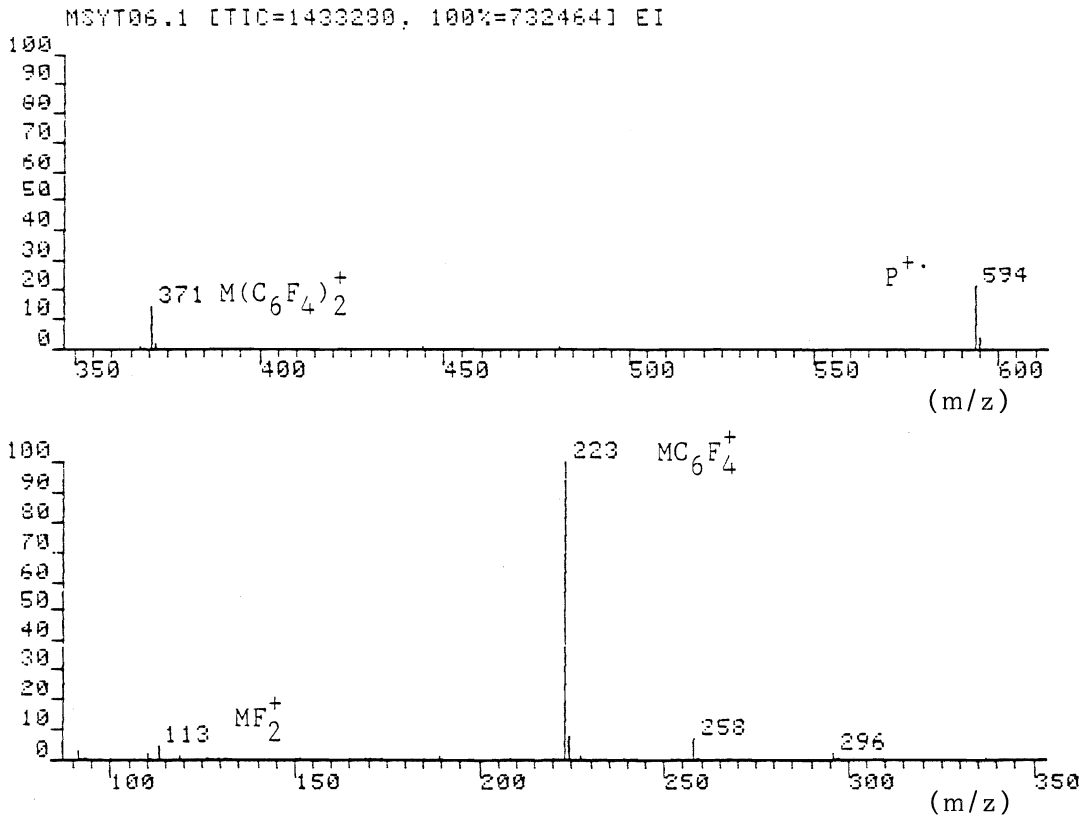

Figure B.11b

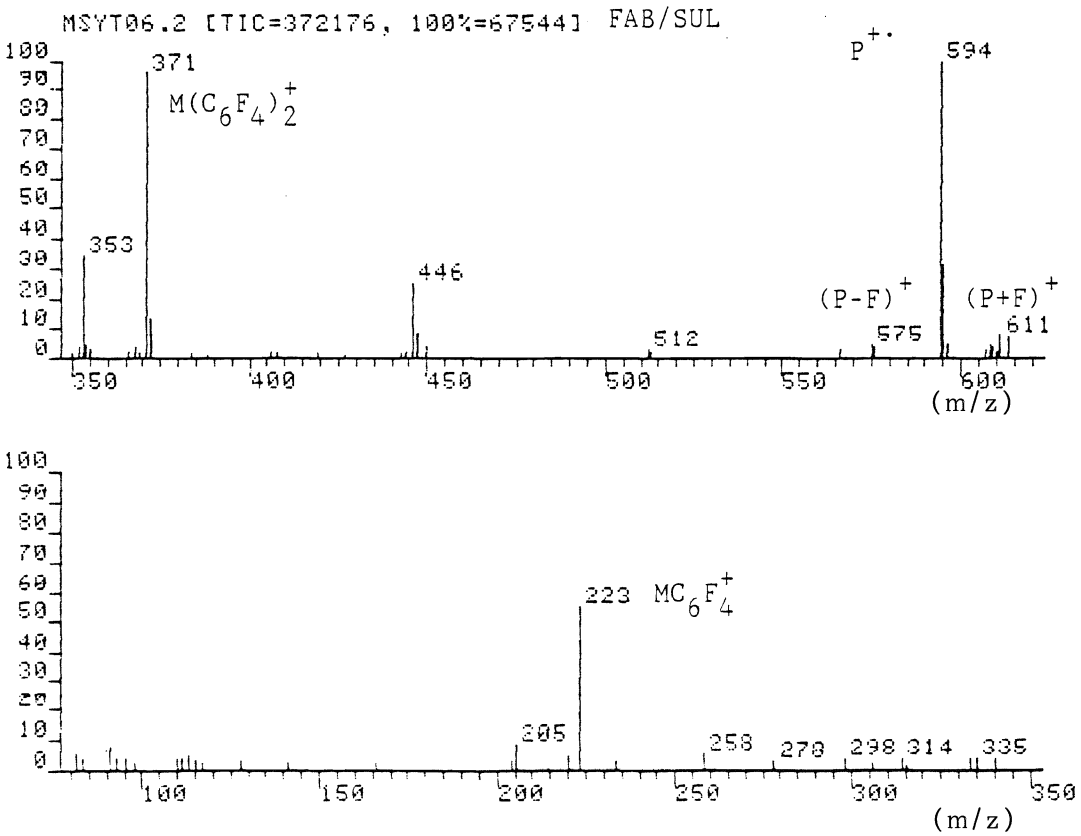

Figure B.12a $P=Sb_2(C_6F_4)_3$

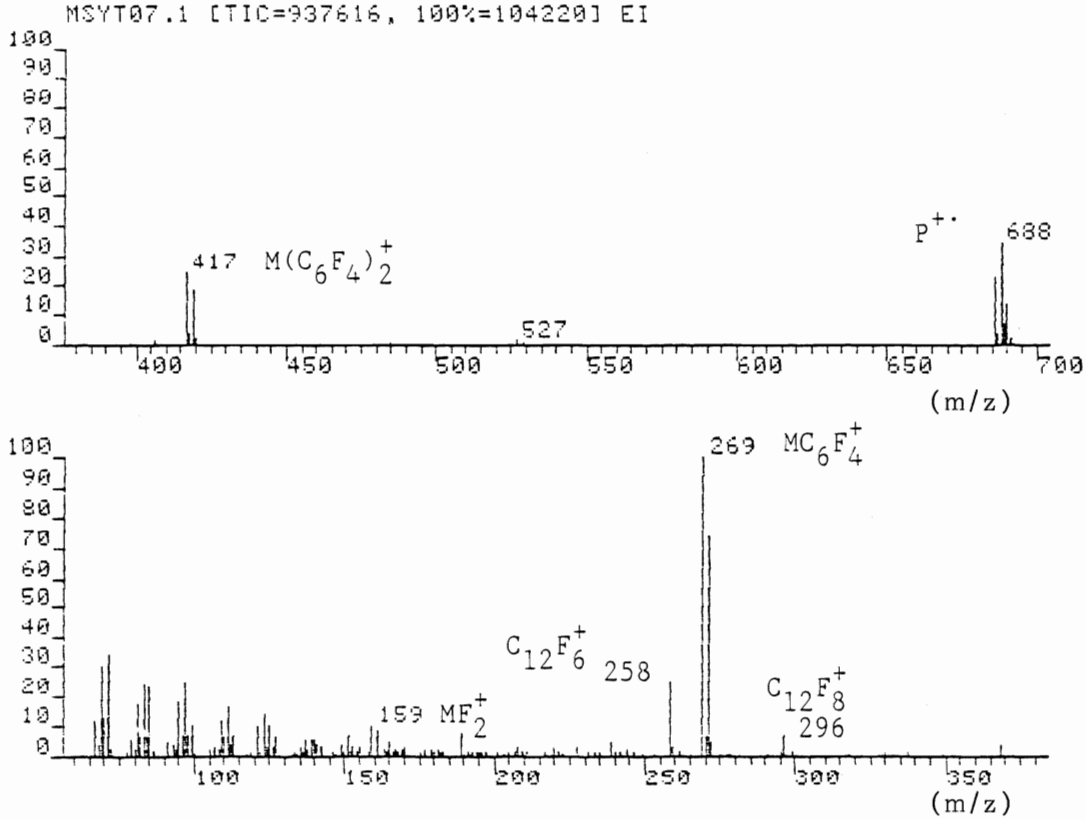

Figure B.12b

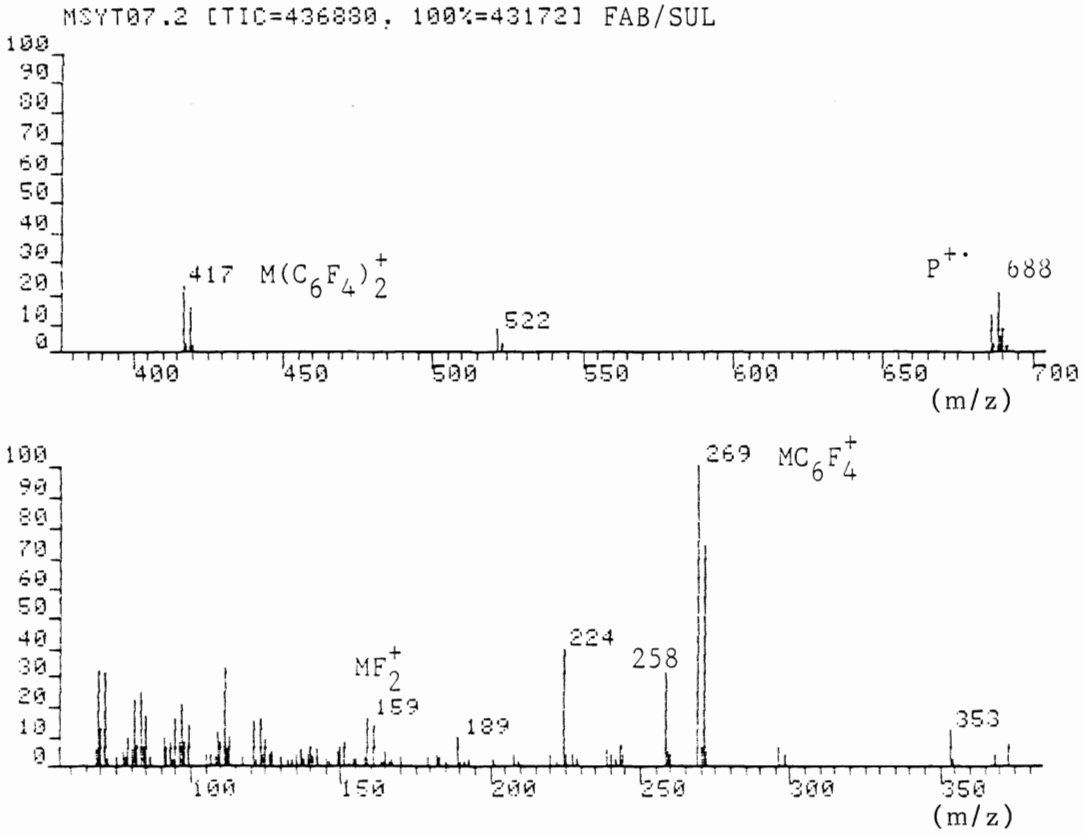

Figure B.13a P= $Bi_2(C_6F_4)_3$

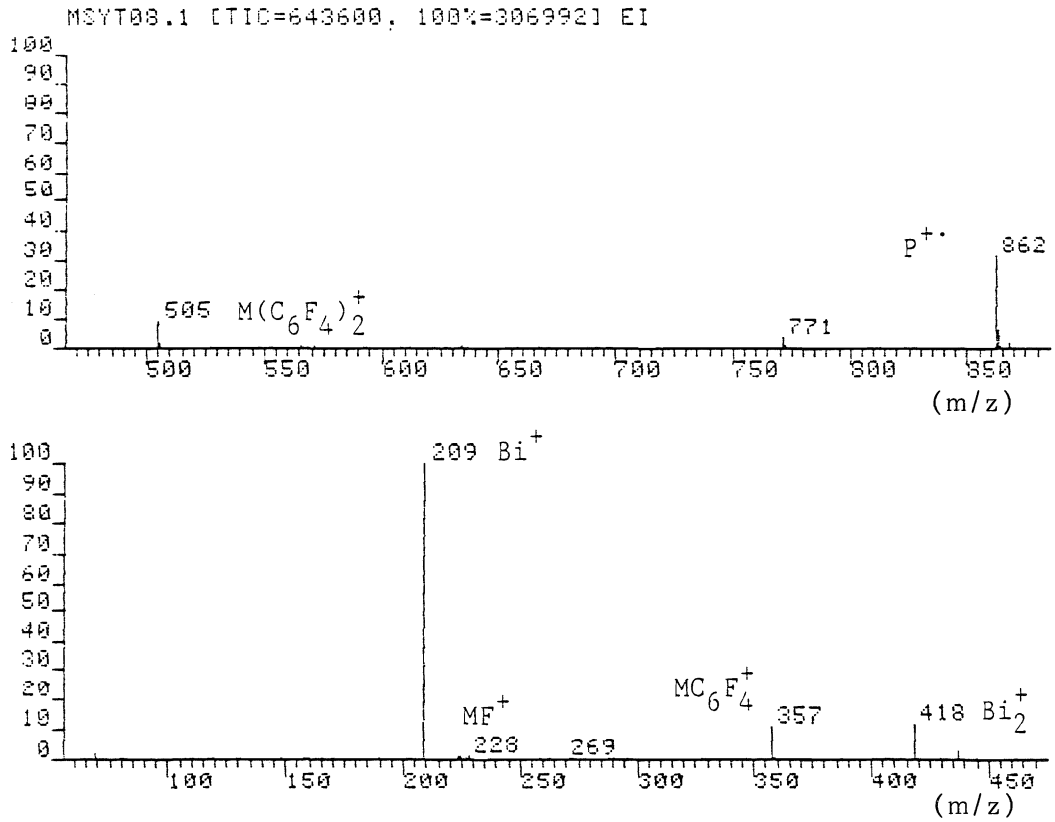

Figure B.13b

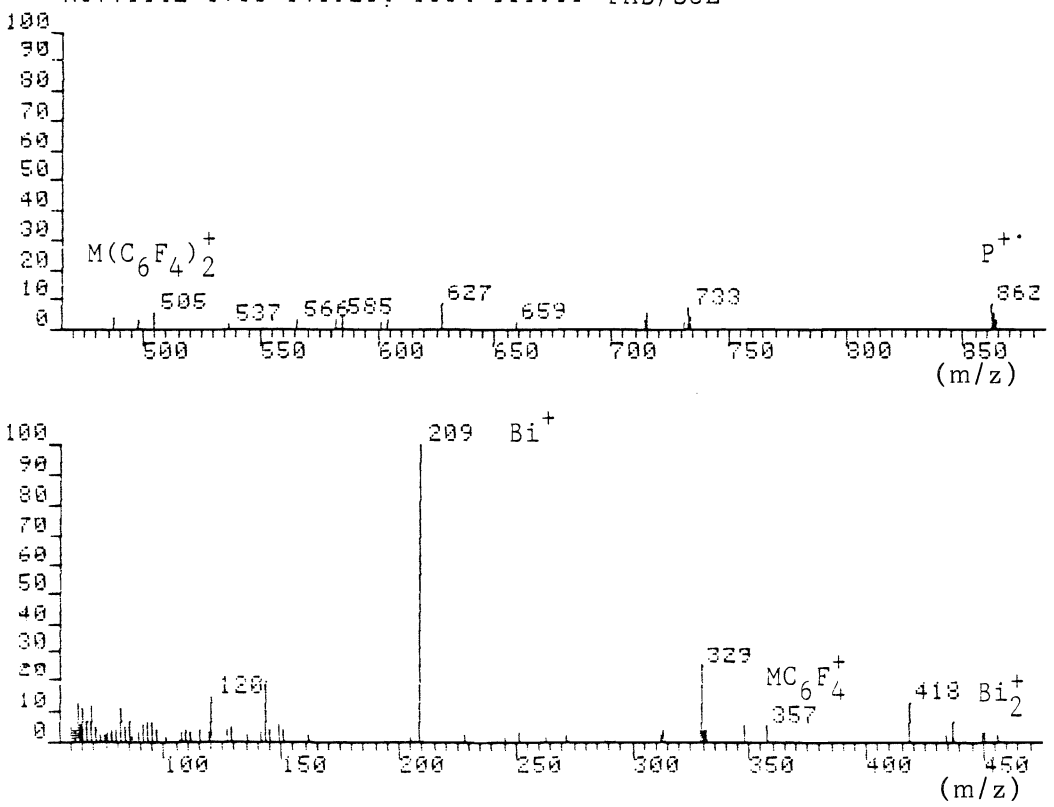

Figure B.14a P= $(CH_3Si)_2(C_6F_4)_3$

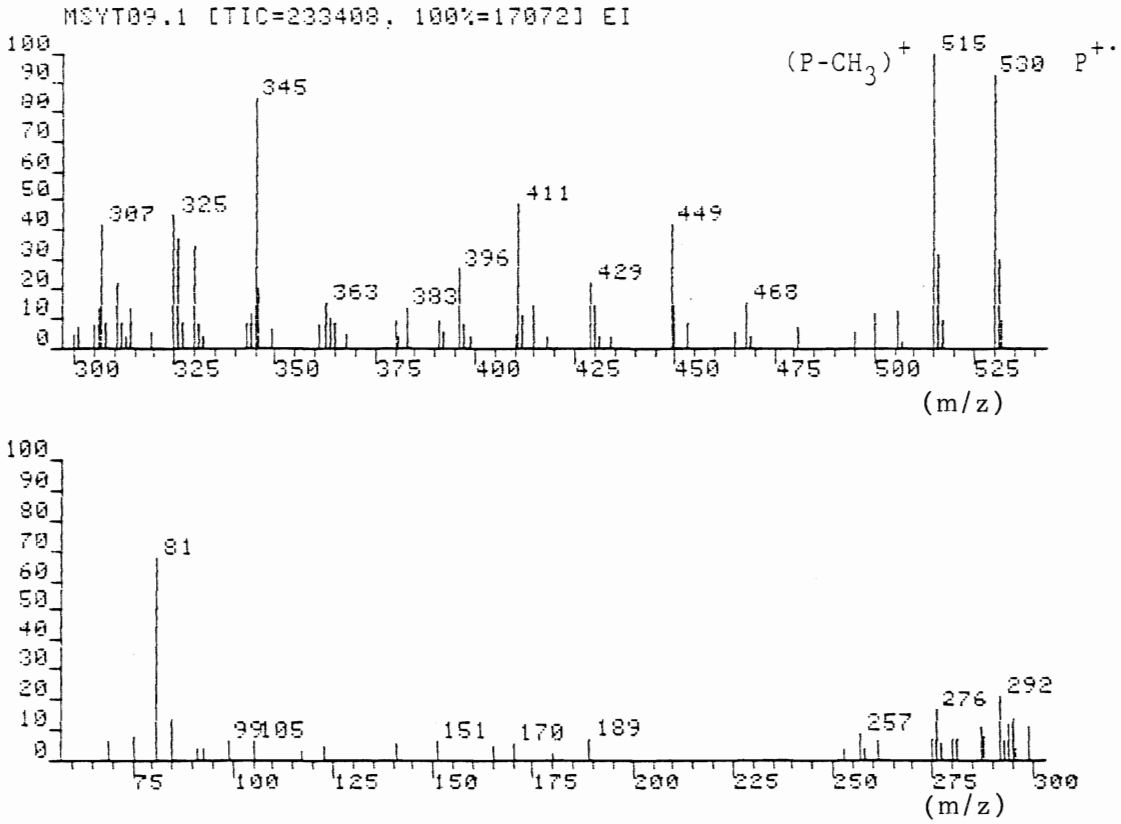

Figure B.14b

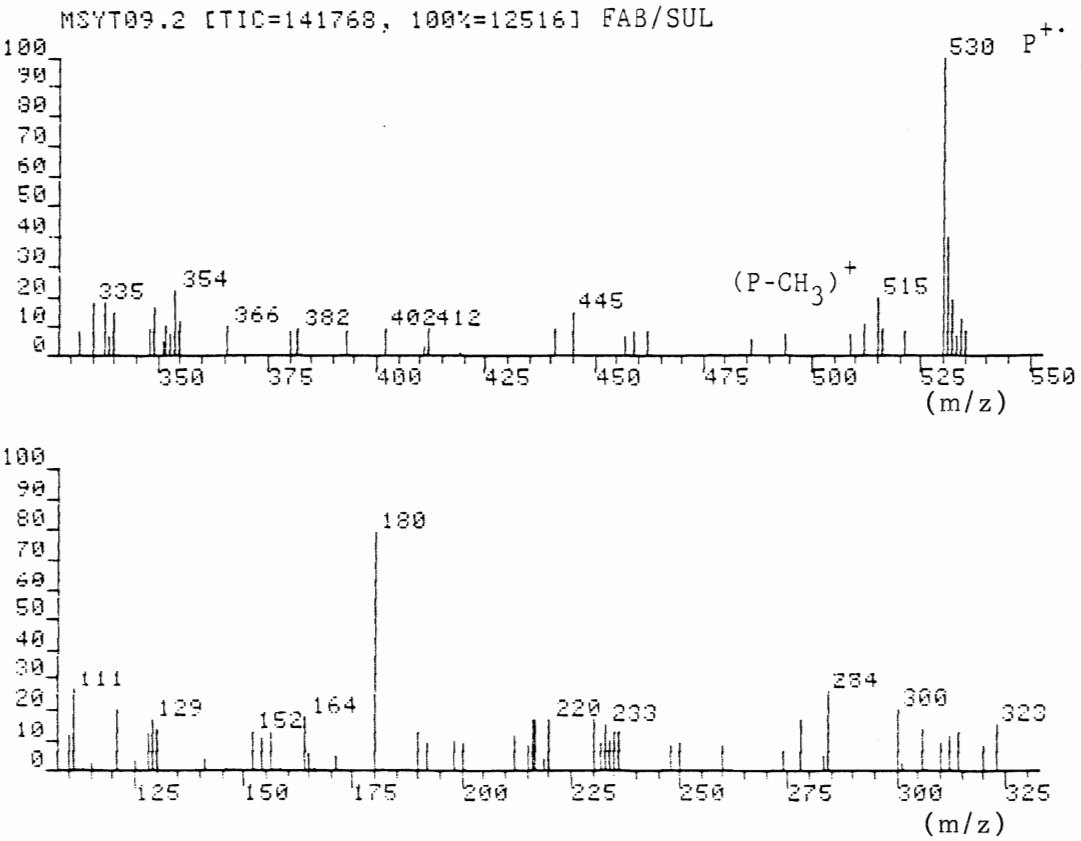

Figure B.15a P= $PSb(C_6F_4)_3$

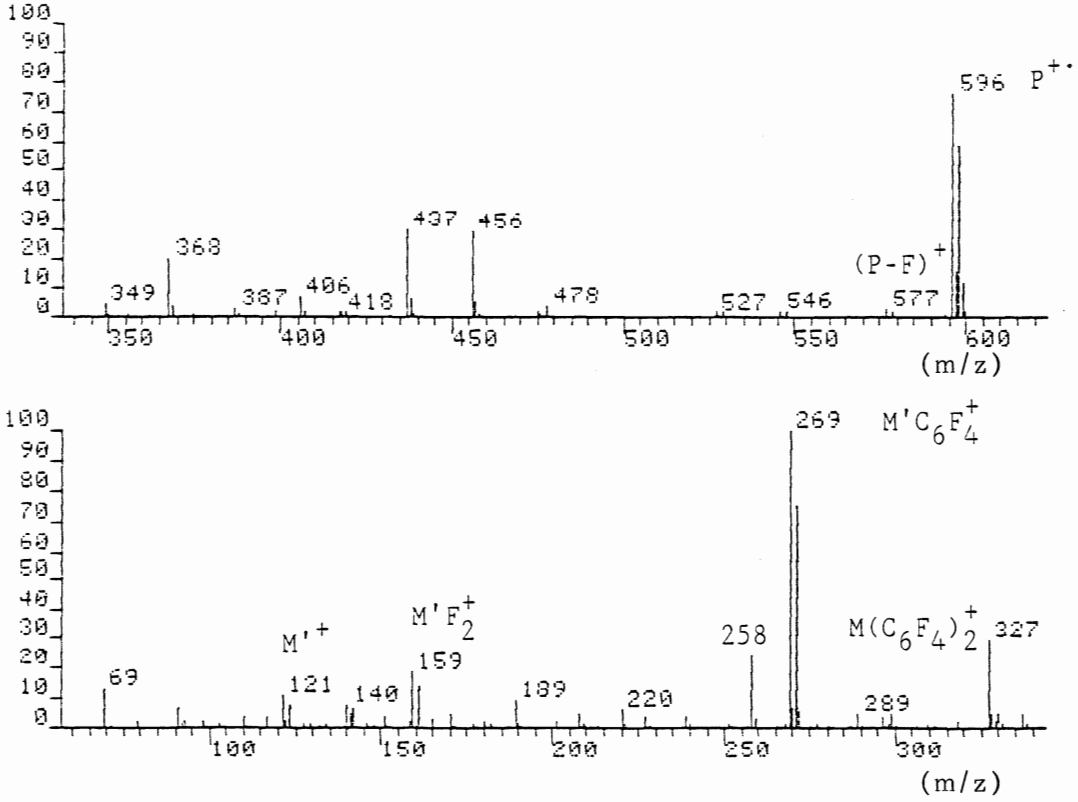

Figure B.15b

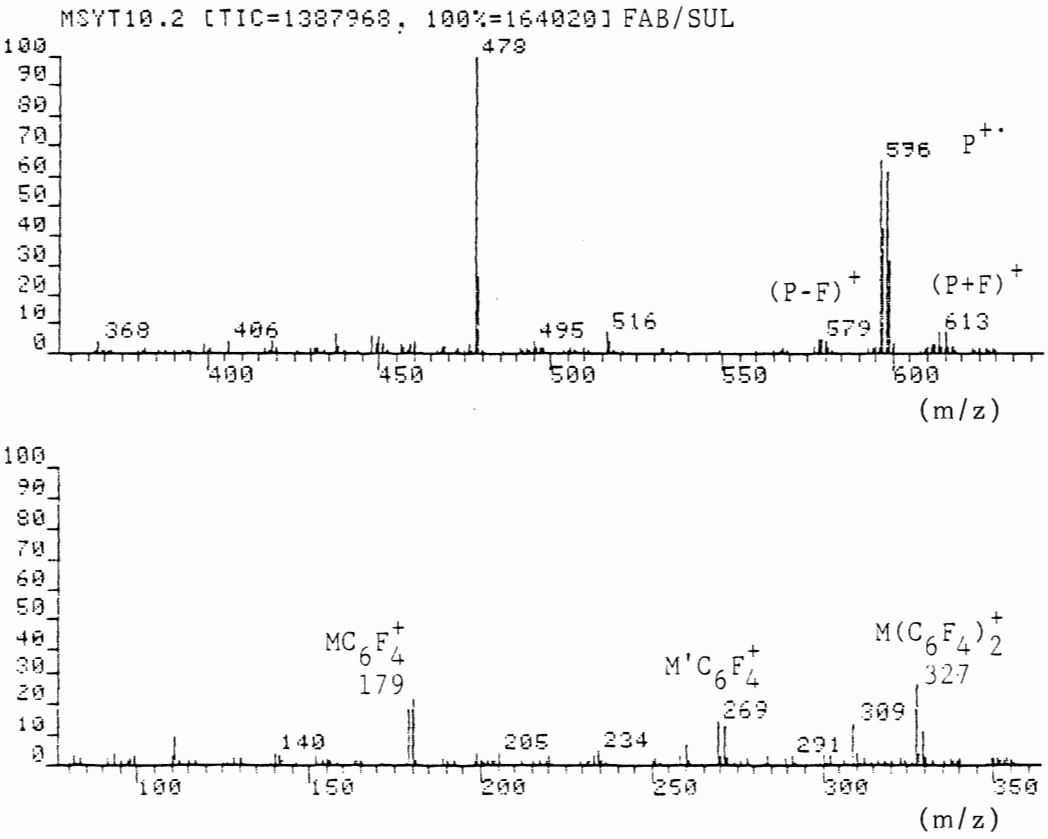

Figure B.16a P= $AsSb(C_6F_4)_3$

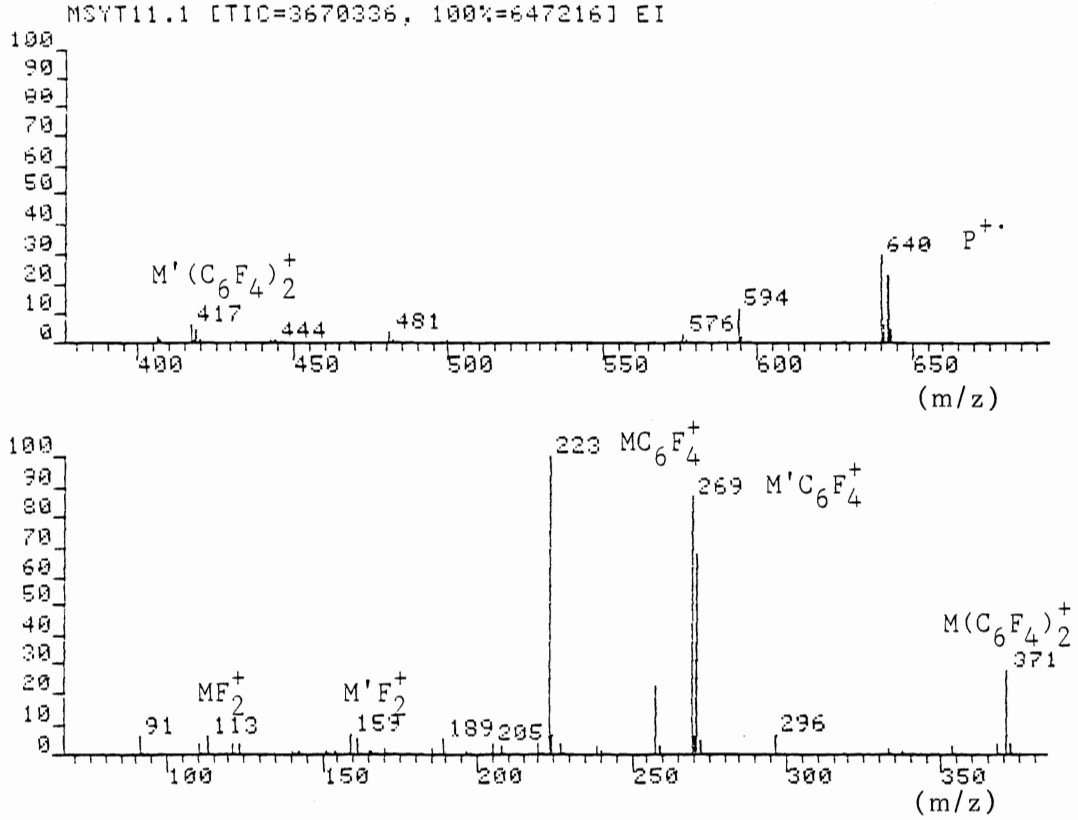

Figure B.16b